

FOSSE ENERGY

DOE/BC/15111-2
(OSTI ID: 775021)

RESPONSIVE COPOLYMERS FOR ENHANCED PETROLEUM RECOVERY

Annual Report
September 30, 1999-September 29, 2000

By
Charles McCormick
Roger Hester

Date Published: February 2001

Work Performed Under Contract No. DE-AC26-98BC15111

University of Southern Mississippi
Hattiesburg, Mississippi



**National Energy Technology Laboratory
National Petroleum Technology Office
U.S. DEPARTMENT OF ENERGY
Tulsa, Oklahoma**

DISCLAIMER

This report was prepared as an account of work sponsored by an agency of the United States Government. Neither the United States Government nor any agency thereof, nor any of their employees, makes any warranty, expressed or implied, or assumes any legal liability or responsibility for the accuracy, completeness, or usefulness of any information, apparatus, product, or process disclosed, or represents that its use would not infringe privately owned rights. Reference herein to any specific commercial product, process, or service by trade name, trademark, manufacturer, or otherwise does not necessarily constitute or imply its endorsement, recommendation, or favoring by the United States Government or any agency thereof. The views and opinions of authors expressed herein do not necessarily state or reflect those of the United States Government.

This report has been reproduced directly from the best available copy.

DOE/BC/15111-2
Distribution Category UC-122

Responsive Copolymers for Enhanced Petroleum Recovery

By
Charles McCormick
Roger Hester

February 2001

Work Performed Under Contract DE-AC26-98BC15111

Prepared for
U.S. Department of Energy
Assistant Secretary for Fossil Energy

Jerry Casteel, Technology Manager
National Petroleum Technology Office
P.O. Box 3628
Tulsa, OK 74101

Prepared by
University of Southern Mississippi
Department of Polymer Science
Hattiesburg, MS 39406

TABLE OF CONTENTS

CHAPTER ONE:

Introduction	1-1
Research Objectives	1-1
Responsive Polymer synthesis, Characterization, and Behavior in Aqueous Media	1-1
A. Polyelectrolytes of NVF with NaAMBA, NaAMPS, and NaA	1-1
B. pH and Electrolyte Responsive Copolymers of Acrylamide and Zwitterionic Betaine Monomers	1-2
C. Rheology of Dilute Aqueous Polymer Solutions	1-3

CHAPTER TWO:

Synopsis	2-1
Introduction	2-1
Experimental	2-2
Results and Discussion	2-3
Conclusions	2-13
References	2-14

CHAPTER THREE:

Synopsis	3-1
Introduction	3-1
Experimental	3-1
Results and Discussion	3-2
Conclusions	3-16
References	3-17

CHAPTER FOUR:

Synopsis	4-1
Introduction	4-1
Experimental	4-2
Results and Discussion	4-5
Conclusions	4-15
References	4-16

CHAPTER FIVE.

Synopsis	5-1
Introduction	5-1
Experimental	5-1
Results and Discussion	5-4
Conclusions	5-6
References	5-7

CHAPTER SIX.

Synopsis	6-1
Introduction	6-1
Experimental	6-2
Results and Discussion	6-3
Conclusions	6-6
References	6-7
Nomenclature	6-7

CHAPTER SEVEN.

Synopsis	7-1
Introduction	7-1
Experimental	7-2
Results and Discussion	7-6
Conclusions	7-8
References	7-8
Appendix	7-8
Nomenclature	7-8

LIST OF TABLES

Table 2.1	Reaction Parameters for the Copolymerization of N-Vinylformamide (M_1) and Sodium 3-Acrylamido-3-methylbutanoate (M_2)	2-4
Table 2.2	Reaction Parameters for the Copolymerization of N-Vinylformamide (M_1) and Sodium 2-Acrylamido-2-methylpropanesulfonate (M_2)	2-5
Table 2.3	Reaction Parameters for the Copolymerization of N-Vinylformamide (M_1) and Sodium Acrylate(M_2)	2-5
Table 2.4	Reactivity Ratios for N-Vinylformamide(M_1) and Acrylamide(M_1) with various Anionic Comonomers(M_2)	2-8
Table 2.5	Structural Data for the Copolymers of N-Vinylformamide (M_1) with Sodium-3-Acrylamido-3-Methylbutanoate (M_2)	2-10
Table 2.6	Structural Data for the Copolymers of N-Vinylformamide (M_1) with Sodium 2-Acrylamido-2-methylpropanesulfonate (M_2)	2-10
Table 3.1	Molecular Weight and Second Virial Coefficient Data for Copolymers of NVF with NaAMBA, NaAMPS, and Na	3-8
Table 4.1	Reaction Parameters for the Copolymerization of Acrylamide (M_1) with 4-(2-Acrylamido-2-Methylpropyltrimethylammonio) Butanoate(M_2)	4-6
Table 4.2	Structural Data for the Copolymers of Acrylamide (M_1) with 4-(2-Acrylamido-2-Methylpropyltrimethylammonio) Butanoate (M_2)	4-7
Table 4.3	Classical Light Scattering Data for the Copolymers of Acrylamide (M_1) with 4-(2-Acrylamido-2-Methylpropyltrimethylammonio) Butanoate(M_2)	4-8
Table 5.1	Reaction parameters for the copolymerization of acrylamide (M_1) with 4-(2-acrylamido-2-methylpropyltrimethylammonio) ethanoate (M_2)	5-5
Table 5.2	Structural data for the copolymers of acrylamide (M_1) with 4-(2-acrylamido-2-methylpropyltrimethylammonio) ethanoate (M_2)	5-6
Table 5.3	Classical light scattering data for the copolymers of acrylamide (M_1) with 4-(2-acrylamido-2-methylpropyltrimethylammonio) ethanoate (M_2)	5-7
Table 6.1	Polymer and Solution Properties	6-5

LIST OF FIGURES AND SCHEMES

Figure 2.1	Structures for the monomers N-vinylformamide (NVF), acrylamide (AM), sodium acrylate (NaA), sodium-3-acrylamido-3-methylbutanoate (NaAMBA), and sodium 2-acrylamido-2-methylpropanesulfonate (NaAMPS)	2-4
Figure 2.2	Mole percent NVF (0 or AM 0) incorporated into copolymers with NaAMBA as a function of comonomer feed ratio. The short dashed line represents ideal random incorporation	2-6
Figure 2.3	Mole percent NVF (0 or AM 0) incorporated into copolymers with NaAMPS as a function of comonomer feed ratio. The short dashed line represents ideal random incorporation	2-7
Figure 2.4	Mole percent NVF (0 or AM 0) incorporated into copolymers with NaA as a function of comonomer feed ratio. The short dashed line represents ideal random incorporation	2-7
Figure 2.5	Mol% Alternation (M1-M2) versus mol% NVF or AM incorporated into copolymers	2-9
Figure 3.1	Copolymers of N-vinylformamide with Sodium-3-Acrylamido-3-Methyl-butanoate (BAVF series), Sodium-2-Acrylamido-2-Methylpropane sulfonate (PSVF series), and Sodium Acrylate (AAVF series)	3-3
Figure 3.2	Effect of polymer concentration on the apparent viscosity for the BAVF copolymer series	3-4
Figure 3.3	Effect of polymer concentration on the apparent viscosity for the PSVF copolymer series.	3-5
Figure 3.4	Effect of polymer concentration on the apparent viscosity for the AAVF copolymer Series	3-5
Figure 3.5	The reduced viscosity as a function of the inverse square root of ionic strength for the BAVF copolymer series (Cp=0.1 g/dL)	3-6
Figure 3.6	The reduced viscosity as a function of the inverse square root of ionic strength for the PSVF copolymer series (Cp=0.1 g/dL)	3-7
Figure 3.7	The reduced viscosity as a function of the inverse square root of ionic Strength for the AAVF copolymer series (Cp=0.1 g/dL)	3-8
Figure 3.8	Effect of polymer concentration on the apparent viscosity for the selected Copolymers	3-9
Figure 3.9	The intrinsic viscosity as a function of the inverse square root of ionic strength for the selected copolymers	3-10
Figure 3.10	Effect of the nature and concentration of electrolyte on the reduced viscosity for BAVF-56 (Cp=0.1 g/dL)	3-11
Figure 3.11	Effect of the nature and concentration of electrolyte on the reduced viscosity for PSVF-56 (Cp=0.1 g/dL)	3-11
Figure 3.12	Effect of the nature and concentration of electrolyte on the reduced viscosity for AAVF- 62 (Cp=0.1 g/dL)	3-12
Figure 3.13	Effect of urea concentration on the reduced viscosity for the selected copolymers (Cp=0.025 g/dL)	3-13

Figure 3.14 Effect of urea concentration on the reduced viscosity for the selected Copolymers (C _p =0.025 g/dL)	3-13
Figure 3.15 Effect of urea concentration on the reduced viscosity for the selected Copolymers (C _p =0.025 g/dL)	3-14
Figure 3.16 Effect of sodium chloride and urea concentration on the upper Critical solution temperature (U.C.S.T.) for AAVF-62. (C _p =0.1 g/dL)	3-14
Scheme 4.1 Synthetic pathway for the preparation of 4-(2-Acrylamido-2-Methylpropylidimethylammonio) Butanoate (AMPDAB)	4-3
Figure 4.1 ¹³ C NMR of 4-(2-Acrylamido-2-methylpropylidimethylammonio) butanoate (AMPDAB)	4-4
Scheme 4.2 ¹³ C NMR of 4-(2-Acrylamido-2-methylpropylidimethylammonio) butanoate (AMPDAB)	4-5
Figure 4.2 Mole percent AMPDAB incorporated into the copolymers as a function of comonomer composition in the feed	4-7
Figure 4.3 Apparent viscosity of DABAM copolymers at pH 7.5 as a function of copolymer concentration	4-10
Figure 4.4 Intrinsic viscosity of DABAM copolymers as a function of NaCl Concentration	4-12
Figure 4.5 Reduced viscosity as a function of increasing ionic strength of various salts (Polymer concentration of 0.1 g/dL)	4-13
Figure 4.6 Apparent viscosities of DABAM copolymers at pH 3 and pH 7.5 as a function of copolymer concentration	4-14
Figure 4.7 Apparent viscosities of DABAM copolymers as a function of the mol% AMPDAB found in the copolymers. (Determined at pH 3 and a polymer concentration of 0.1 g/dL)	4-14
Figure 4.8 Reduced Viscosity of DABAM copolymers as a function of the inverse square root of ionic strength. (Determined at pH 3 and a polymer concentration of 0.1 g/dL)	4-15
Figure 4.9 Apparent viscosities of DABAM and DAPSAM copolymers as a function of pH. (Polymer concentration of 0.1 g/dL)	4-16
Scheme 5.1 Synthetic pathway for preparation of 2-(2-acrylamido-2-methylpropylidimethylammonio)ethanoate (AMPDAE)	5-3
Scheme 5.2 Structural composition of copolymer of acrylamide with 2-(2-acrylamido-2-methylpropylidimethylammonio)ethanoate and with 4-(2-acrylamido-2-methylpropyl dimethylammonio) butanoate	5-4
Figure 5.1 ¹³ C n.m.r. spectrum of 2-(2-acrylamido-2-methylpropylidimethylammonio)-ethanone (AMPDAE)	5-5
Figure 5.2 Intrinsic viscosities of DAEAM copolymers as a function of NaCl Concentration	5-9
Figure 5.3 Reduced viscosities for DAEAM 25 and DAEAM 40 as a function of increasing ionic strength in various salts (C _p =0.3 g/dL ⁻¹)	5-10
Figure 5.4 Apparent viscosities of DAEAM copolymers at various pH values	

($C_p=0.3 \text{ g dl}^{-1}$)	5-11
Figure 5.5 Reduced viscosities of DAEAM 25 in deionized water and NaCl solutions as a function of pH ($C_p=0.3 \text{ g dl}^{-1}$)	5-12
Figure 5.6 Intrinsic viscosities of DEAM 25, DABAM 25, and DAEAM 60 as a function of the inverse square root of ionic strength for NaCl	5-14
Figure 5.7 Apparent viscosities of DAEAM 25 and DABAM 25 in deionized water as a function of pH ($C_p=0.1 \text{ g dl}^{-1}$)	5-15
Figure 6.1 PEO Solutions	6-3
Figure 6.2 PAM Solutions	6-3
Figure 6.3 ATABM Solutions	6-3
Figure 6.4 Q_{yield} vs. d_h^b	6-5
Figure 6.5 Coil Volume vs. Coil Viscosity	6-6
Figure 7.1 Apparent Viscosity vs. Shear Rate	7-2
Figure 7.2 Cable Rheometer	7-3
Figure 7.3 Cup and Bob Details	7-5
Figure 7.4 Cone Shaped Bob Bottom	7-6
Figure 7.5 Axis Adjustments	7-6
Figure 7.6 Bob Components	7-6
Figure 7.7 Twist Angle vs. Time of Operation	7-7
Figure 7.8 Twist Angle vs. Cup Speed	7-8

ABSTRACT

A coordinated research program has been initiated with the aim of developing environmentally responsive copolymers for Improved Oil Recovery (IOR). These novel polymer systems possess amphipathic microstructures which allow reversible pH-, salt, shear-, or temperature-responsiveness in aqueous media. Viscosity, fluid flow behavior, polymer interactions with reservoir rock and entrapped oil, and phase behavior can be changed by altering pH or salt concentration or by adjusting flow rates. The objectives of this work are to: synthesize responsive, amphiphilic systems; characterize molecular structure and solution behavior; measure rheological properties of the aqueous fluids including behavior in fixed geometry flow profiles and beds; and to tailor final polymer compositions for *in situ* rheology control under simulated reservoir conditions. This report focuses on a) synthesis, characterization, and solution studies of pH and salt responsive thickeners and b) development of procedures and an apparatus for measuring extentional flow. Polymers have been prepared from N-vinylformamide (NVF), sodium 3-acrylamido-3-methylbutanoate (NaAMBA), sodium 2-acrylamido-2-methylpropanesulfonate (NaAMPS), sodium acrylate (NaA), acrylamide (AM), 4-(2-acrylamido-2-methylpropylidimethylammonio)butanoate] (DABAM series), 3-(2-acrylamido-2-methylpropylidimethylammonio)propanesulfonate (DAPSAM series) and 2-(2-acrylamido-2-methylpropylidimethylammonio) ethanoate (DAEAM series). The hypothesis that polymer coils will only extend when the rate of coil expansion is greater than the rate of recovery was examined and the minimum fluid extension rate was shown to be inversely proportional to the hydrodynamic diameter of the coil. A low shear bob and cone rheometer has been designed in our laboratories for accurate measurement of rheological behavior of aqueous fluids in dilute solutions.

CHAPTER 1: Executive Summary: Background, Objectives, and Overview of Research during FY 2000

Introduction

A coordinated research program has been initiated with the aim of developing environmentally responsive copolymers for Improved Oil Recovery (IOR). These novel polymer systems possess amphipathic microstructures that allow reversible pH-, salt-, shear-, or temperature-responsiveness in aqueous media. Changes in the copolymer conformations in response to these controllable variables results in substantial changes in viscosity and phase behavior. These characteristics are of potential utility in controlling both fluid mobility and conformance, particularly for *in situ* processes. Responsive polymers have attributes that should overcome limitations inherent in even the best conventional IOR polymers. Salt and pH "triggers" strategically placed along the macromolecular backbone determine hydrodynamic volume and, thus, rheological behavior. Viscosity, fluid flow behavior, polymer interactions with reservoir rock and entrapped oil, and phase behavior can be changed by altering pH or salt concentration or by adjusting flow rates. Polymers are targeted to act alone or with surfactant to significantly alter the flow of fluids through porous media. Utilization of the responsiveness of the copolymers can result in the fluid viscosity and the permeability of the substrate being altered.

Research Objectives

The objectives of this work are to: synthesize responsive copolymer systems; characterize molecular structure and solution behavior; measure rheological properties of aqueous fluids in fixed geometry flow profiles; and to tailor final polymer compositions for *in situ* rheology control under simulated conditions. This report focuses on the synthesis and characterization of novel stimuli responsive copolymers, the investigation of dilute polymer solutions in extensional flow and the design of a rheometer capable of measuring very dilute aqueous polymer solutions at low torque.

Responsive Polymers: Synthesis, Characterization, and Behavior in Aqueous Media

A. Polyelectrolytes of NVF with NaAMBA, NaAMPS, and NaA. Chapters 2 and 3 detail the synthesis of copolymers of *N*-vinylformamide (NVF) with various negatively charged comonomers. An alternating incorporation tendency of the comonomers was determined by ^{13}C NMR. The resulting copolymers exhibited typical polyelectrolyte behavior by demonstrating a decrease in solution viscosity with added electrolytes. Molecular weights were determined and found to be dependent on the amount of NVF incorporated into the copolymers for the BAVF and PSVF series; reaching a maximum around 40 mol% NVF. This dependency was

not found for the AAVF series which exhibited higher molecular weights as the mol% NVF incorporated into the copolymers decreased. The phase behavior as a function of calcium ion concentration, pH, and temperature of each copolymer was studied. The PSVF series is stable in the presence of calcium chloride and with changes in pH of the aqueous media due to the weak basicity of the sulfonate group. For the BAVF series, copolymers containing 75 mol% or more of NaAMBA phase separate in the presence of calcium chloride at elevated temperatures. In addition, BAVF copolymers containing 38 mol% or more of NaAMBA phase separate at a critical pH value, dependent on the amount of NaAMBA incorporated into the copolymer. AAVF copolymers also phase separate in the presence of calcium chloride and at lower pH values dependent on the mol% of NaA in the copolymer. At pH 2, AAVF copolymers exhibit a USCT (upper critical solution temperature) which is influenced by added cosolutes.

B. pH and Electrolyte Responsive Copolymers of Acrylamide and Zwitterionic Betaine Monomers. In striving to synthesize polymers that show tolerance in the presence of added electrolytes, we have recently focused our attention on polyampholytes, polymers that possess both cationic and anionic pendant groups. This section describes the synthesis and characterization of polybetaines, polymers derived from zwitterionic monomers, that show the ability to sustain or increase their viscosity in the presence of added electrolytes that may be similar to that encountered in oil field applications for IOR.

In Chapter 4 the syntheses and characterization of copolymers of acrylamide with 4-(2-acrylamido-2-methylpropylidimethylammonio)butanoate] (DABAM series) and with 3-(2-acrylamido-2-methylpropylidimethylammonio)propanesulfonate (DAPSAM series) were considered. Experimentally determined reactivity ratios indicated random incorporation of the monomers into the final copolymers. The effects of pH, copolymer composition, and added electrolyte on the solution viscosity of the copolymers are described herein. The copolymers exhibit complex solubility and solution behavior due to hydrogen bonding, charge-charge interactions, molecular weight, and configurational effects. The copolymers at pH 3 display polyelectrolyte behavior due to the cationic nature of the polymer. At pH 8, the copolymers exhibit both intermolecular and intramolecular interactions depending on the amount of AMPDAB incorporated into the copolymer. The poly(vinyl carboxybetaines) are more soluble in deionized water than the analogous poly(vinyl sulfobetaines) as well as being more responsive to changes in the pH of the aqueous medium.

Chapter 5 describes the synthesis, characterization, and solution viscosity properties of a novel copolymer of acrylamide with 2-(2-acrylamido-2-methylpropylidimethylammonio) ethanoate (DAEAM series). The impetus behind this study is to further investigate structure-property relationships of

polyzwitterions composed of structurally similar zwitterionic monomers. The zwitterionic monomer of the DAEAM series differs from that of the DABAM series by the number of methylene units between the quaternary ammonium group and the carboxylate group (one vs. three). The intention of this study is to show that the spatial proximity of the quaternary ammonium and carboxylate groups has a significant effect on the basicity of the latter, greatly affecting solution behavior. Copolymers of acrylamide with 2-(2-acrylamido-2-methylpropylidimethyl-ammonio) ethanoate were prepared by free radical polymerization in an aqueous NaBr solution. Reactivity ratios and copolymer microstructures were determined and indicate random incorporation of both comonomers. Weight average molecular weights in the range of $6.3\text{-}10.4 \times 10^6 \text{ mol}^{-1}$ have been determined for the copolymer series. Second virial coefficients were found to decrease as the mol% of AMPDAE incorporated into the copolymers increased. All of the polymers in DAEAM series are soluble in deionized water. Intrinsic viscosity studies as a function of NaCl concentration suggest a decrease in intermolecular associations and an increase in intramolecular associations as the mol% of AMPDAE incorporated into the copolymers increases. Copolymers containing 60 mol% or more show an enhancement in viscosity as the concentration of added electrolytes is increased as a result of the shielding of intramolecular associations between the zwitterionic groups. The nature of added electrolytes also influences the solution behavior; the larger, more polarizable ions enhance viscosity more than smaller ions and trend with the Hoffmeister series. The presence of carboxylate groups renders the copolymers responsive to changes in pH of the aqueous environment. As pH is lowered, the carboxylate groups are progressively protonated, resulting in an enhancement in viscosity; however, the addition of electrolytes negates the increase in viscosity due to shielding effects. Solution properties of DAEAM-25 and DABAM-25 are similar at high pH values. As pH is lowered, DABAM-25 displays a much more dramatic increase in viscosity. This behavior is likely a result of the much lower pH required to protonate the carboxylate group of the AMPDAE mer unit.

C. Rheology of Dilute Aqueous Polymer Solutions. Chapter 6 describes an investigation of the previous assumption that a polymer coil to volume fraction, C^* , of 0.1 would give dilute polymer solutions capable of being analyzed using a screen rheometer. A hypothesis was formulated that presumes that polymer coils will only extend when the rate of coil expansion is greater than the rate of recovery. The minimum fluid extension rate was shown to be inversely proportional to the hydrodynamic diameter of the coil. This finding implies that in typical reservoir flooding where fluid extension rates are very low, polymer coil extension that decreases displacing fluid mobility and improves oil recovery will occur only if the coil hydrodynamic diameter is extremely large. Large coil hydrodynamic diameters are formed with very high molecular weight polymers having large intrinsic viscosities.

Chapter 7 details the construction of a bob and cone rheometer capable of measuring viscosities of dilute polymer solutions at low shear rates (5 sec^{-1} or less). This instrument was needed as an alternative to the Contraves Low Shear Model 30 rheometer that has been used previously but is currently no longer commercially available. The presently configured cable rheometer has a shear rate range from 1.0 to 2.7 sec^{-1} and can measure viscosities of most dilute aqueous polymer solutions in the first Newtonian shear rate region. Therefore, intrinsic viscosity values can be determined using the cable rheometer and studies can now be continued on the flow properties of polymer solutions.

CHAPTER 2. Polyelectrolytes of N-vinylformamide with Sodium-3-Acrylamido-3-Methylbutanoate, Sodium-2- Acrylamido- 2- Methyl propanesulfonate, and Sodium Acrylate: Synthesis and Characterization.

SYNOPSIS

Copolymers of N-vinylformamide(NVF) with sodium-3-acrylamido-3-methyl butanoate(NaAMBA), sodium-2-acrylamido-2-methylpropanesulfonate(NaAMPS), and sodium acrylate(NaA) were prepared by free radical polymerization in aqueous solution using 2,2'-azobis(N,N'-dimethyleneisobutyramidine) dihydrochloride as the water soluble azo initiator. Copolymer compositions were determined utilizing ^{13}C NMR by integration of the carbonyl resonances. Reactivity ratios were determined for NVF(M_1)/NaAMBA(M_2) (the BAVF series) and NVF(M_1)/NaAMPS(M_2) (the PSVF series). Both series, with r_1 and r_2 less than 1 and $r_1r_2 < 0.075$, are representative of copolymers that display alternating tendencies. Weight average molecular weights range from 0.9 to 7.5×10^6 gm/mol and were determined by low angle laser light scattering in 1 M NaCl solution.

INTRODUCTION

Water-soluble and water-dispersible copolymers represent one of the fastest growing classes of industrial products. The growth has been stimulated by the demand for environmentally compliant systems prepared in and processed from water. Applications include water treatment, remediation, coatings and personal care formulations, viscosity modification, and frictional drag reduction.¹⁻⁸

Although a large number of monomers are capable of polymerization into polymers with water solubility, only a few have sufficient water solubility and reactivity with appropriate comonomers to yield commercially viable systems. N-vinylformamide (NVF), an isomer of acrylamide (AM), has recently received renewed attention since purification procedures have been refined and high molecular weights are easily attainable.⁹⁻¹³ Both NVF and AM yield water soluble homopolymers by free radical polymerization; however, the structural differences of the monomers significantly alter copolymerization tendencies with various comonomers and microstructural attributes. Knowledge of reactivity ratios of NVF and AM with specific comonomers, therefore, is an important factor in tailoring microstructure for desired rheological characteristics.

Previous studies in our laboratories confirmed that NVF copolymerizes with electron deficient monomers such as acrylamide and maleic anhydride to form copolymers with strongly alternating tendencies.^{14,15} In this paper we report the synthesis and molecular characterization of copolymers of NVF with sodium-3-acrylamido-3-methyl butanoate (NaAMBA), sodium-2-acrylamido-2-methylpropane sulfonate (NaAMPS), and sodium acrylate (NaA). The reactivity ratios for the copolymers with NaAMBA and NaAMPS were determined by several methods and then used to statistically predict the microstructures of the resulting copolymers. Additionally, the molecular weight values were also determined by low angle laser light scattering. These studies complement previous research in our laboratories on copolymers of acrylamide with the same comonomer systems.¹⁶⁻²⁴

EXPERIMENTAL

Materials.

N-vinylformamide (N VF) from Air Products and Chemicals Inc. was vacuum distilled prior to use (72° C @ 5 torr). Acrylic acid from Aldrich Chemical Co. was vacuum distilled prior to use. 3-Acrylamido-3-methylbutanoic acid was synthesized via a Ritter reaction of equimolar amounts of 3,3-dimethylacrylic acid with acrylonitrile as reported by Hoke and Robins²⁵ and as modified by McCormick and Blackmon^{16,19}. 2-Acrylamido-2-methylpropanesulfonic acid from Aldrich Chemical Co. was recrystallized from methanol and vacuum dried at room temperature. 2,2'-Azobis(N,N'-dimethyleneisobutyramidine) dihydrochloride (VA-044) from Wako Chemicals USA, Inc. was used as received.

Poly(N-vinylformamide-co-Sodium 3-acrylamido-3-methylbutanoate) and Poly(N-vinylformamide-co-Sodium 2-acrylamido-2-methylpropane sulfonate).

The copolymers of N-vinylformamide (N VF) and Sodium 3-acrylamido-3-methylbutanoate (NaAMBA), the BAVF series, and copolymers of N-vinylformamide (N VF) and Sodium 3-acrylamido-3-methylbutanoate (NaAMPS), the PSVF series, were prepared in an aqueous solution at 45° C using 0.1 mol % VA-044 as the initiator. Each reaction was conducted in a 500 mL, three necked flask equipped with a mechanical stirrer and a nitrogen inlet tube. A designated amount of either 3-acrylamido-3-methyl butanoic acid or 2-acrylamido-2-methylpropane sulfonic acid was added to a specific volume of deionized water. To this was added an equimolar amount of sodium hydroxide and the pH of this mixture was adjusted to a pH= 8.5. Once the materials were completely dissolved, the appropriate amount of N VF was added and the mixture was then deaerated with oxygen-free nitrogen for 30 minutes and placed in a water bath at 45° C. After the reaction mixture had equilibrated, VA-044 dissolved in 5mL of deionized water was injected into the stirring solution. The total monomer concentration was held constant at 0.5 M in each reaction. A low conversion aliquot was taken for the determination of reactivity ratios. High conversion was terminated at less than 40% due to the high viscosity of the polymerization medium and as a precaution against copolymer drift. Polymerizations were terminated by precipitation into reagent grade acetone. The low conversion samples were further purified by reprecipitation into acetone followed by vacuum drying for 2 days. High conversion samples were purified by dialysis (using Spectra/Por 4 dialysis bags with molecular weight cutoffs of 12,000 to 14,000 g/mol) against deionized water adjusted to a pH=8 for 10 days. After dialysis, the polymer solutions were frozen and isolated by lyophilization. Conversions were determined gravimetrically from the purified samples.

Poly(N-vinylformamide-co-sodium acrylate).

The copolymers of N-vinylformamide (N VF) and sodium acrylate (NA) were prepared in an aqueous solution as reported previously except for AAVF-100 in

which the monomer concentration was 1.0 M.¹⁵ Polymer purification was performed in the same manner as discussed above.

Copolymer Characterization.

¹³C NMR spectra of the copolymers were obtained at 50.3 MHz on a Bruker AC200 spectrometer using 15-20 wt % aqueous (D₂O) polymer solutions with 3-(trimethylsilyl)-1-propane-sulphonic acid, sodium salt (DSS) as a reference. A recycle delay of 8 s, 90° pulse length, and gated decoupling to remove all NOE were used for quantitative spectral analysis with an accuracy of \pm 6%. Molecular weight studies were performed on a Chromatix KMX-6 low angle laser light scattering instrument at 25°C in 1M NaCl at pH=8.5 and accurate to within \pm 5-10%. Refractive index increments were obtained using a Chromatix KMX-16 laser differential refractometer.

RESULTS AND DISCUSSION

Compositional Studies

Copolymers of N-vinylformamide with sodium-3-acrylamido-3-methylbutanoate (BAVF series), sodium-2-acrylamido-2-methylpropanesulfonate (PSVF series), and sodium acrylate (AAVF series) were prepared at designated feed compositions described in the experimental section. The structures of the various monomers utilized in the syntheses are shown in Figure 1. Tables I-III compare initial feed ratios which were varied over the entire compositional range to resultant copolymer composition. The latter were determined by integration of appropriate carbonyl resonances obtained by ¹³C NMR spectroscopy. Tables I and II are for the BAVF and PSVF copolymer series, respectively, and represent low conversion samples. Table III is for the AAVF copolymer series and is representative of high conversion samples. The mol% NVF found in the AAVF copolymers from the high conversion samples agrees favorably with past results reported from our laboratories for low conversion samples¹⁵. This finding suggests that there is no significant drift in the compositions of the copolymers at these conversions.

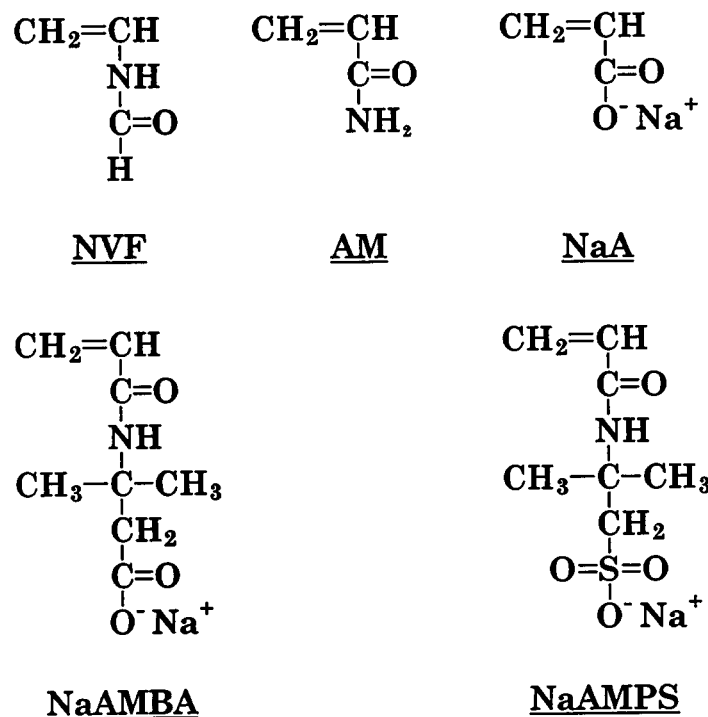


Figure 1. Structures for the monomers N-vinylformamide (N VF), acrylamide (AM), sodium acrylate (NaA), sodium 3-acrylamido-3-methylbutanoate (NaAMBA), and sodium 2-acrylamido-2-methylpropanesulfonate (NaAMPS).

Table I. Reaction Parameters for the Copolymerization of N-Vinylformamide (M_1) and Sodium 3-Acrylamido-3-methylbutanoate (M_2)

Sample	Feed ratio (mol%) (N VF : NaAMBA)	Rxn. Time (min.)	% Conv.	N VF found ^a (mol %)
BAVF 23	90.0 : 10.0	55	4.0	77.0±4.6
BAVF 38	75.0 : 25.0	65	12.0	62.0±3.7
BAVF 47	60.0 : 40.0	40	4.5	53.0±3.2
BAVF 56	40.0 : 60.0	30	15	44.0±2.6
BAVF 65	25.0 : 75.0	30	5.0	35.0±2.1
BAVF 75	10.0 : 90.0	18	17	25.0±1.5
BAVF 100	0.0 : 100.0	—	—	0.0 ^b

^a Determined from ^{13}C NMR.

^b Theoretical Value

Table II. Reaction Parameters for the Copolymerization of N-Vinylformamide (M₁) and Sodium 2-Acrylamido-2-methylpropanesulfonate (M₂)

Sample	Feed ratio (mol%) (NVF : NaAMPS)	Rxn. Time (min.)	% Conv.	NVF found ^a (mol %)
PSVF 21	90.0 : 10.0	45	15	79.0±4.7
PSVF 40	75.0 : 25.0	40	12	60.0±3.6
PSVF 45	60.0 : 40.0	50	12	55.0±3.3
PSVF 56	40.0 : 60.0	20	12	44.0±2.6
PSVF 64	25.0 : 75.0	25	11	36.0±2.2
PSVF 70	10.0 : 90.0	20	15	30.0±1.8
PSVF 100	0.0 : 100.0	—	—	0.0 ^b

^a Determined from ¹³C NMR.

^b Theoretical Value

Table III. Reaction Parameters for the Copolymerization of N-Vinylformamide (M₁) and Sodium Acrylate(M₂)

Sample	Feed ratio (mol%) (NVF : NaAMBA)	Rxn. Time (min.)	% Conv.	NVF found ^a (mol %)
AAVF 22	88.0 : 12.0	60	25	78.0±4.5
AAVF 49	60.0 : 40.0	35	27	51.0±3.0
AAVF 62	40.0 : 60.0	30	24	37.5±2.2
AAVF 82	12.0 : 88.0	30	38	17.5±1.0
AAVF 100	0.0 : 100.0	—	—	0.0 ^b

^a Determined from ¹³C NMR.

^b Theoretical Value

In Figures 2-4, copolymer composition plots of the mol% NVF in the copolymer versus the mol% NVF in the feed for the BAVF, PSVF, and AAVF series, respectively, are shown. In addition, these figures also contain previous results from our laboratories for copolymers of AM with NaAMBA¹⁶, NaAMPS^{20,22}, and NaA²³. The short dashed lines which pass through the origin represent ideal incorporation while the curves through the data points were obtained by a spline smoothing fit. Copolymers of NVF exhibit a significant deviation from the dashed line. The azeotropic point is approximately 50 mol% for the BAVF and PSVF series and 40 mol% for the AAVF series. Below this point, more NVF is incorporated into the copolymers than is present in the feed while above this point, less NVF is incorporated. This behavior is typical of copolymerizations which exhibit an alternating tendency. The copolymers with acrylamide do not exhibit this preference of cross addition. In fact, acrylamide is preferentially added at all compositions, this behavior being more prevalent for the carboxylate containing comonomers and may be suggestive of some type of hydrogen bonding interaction with acrylamide. The dissimilarity in the reactivity between NVF and AM can tentatively be ascribed to the electronic differences in the vinyl bond and will be addressed later.

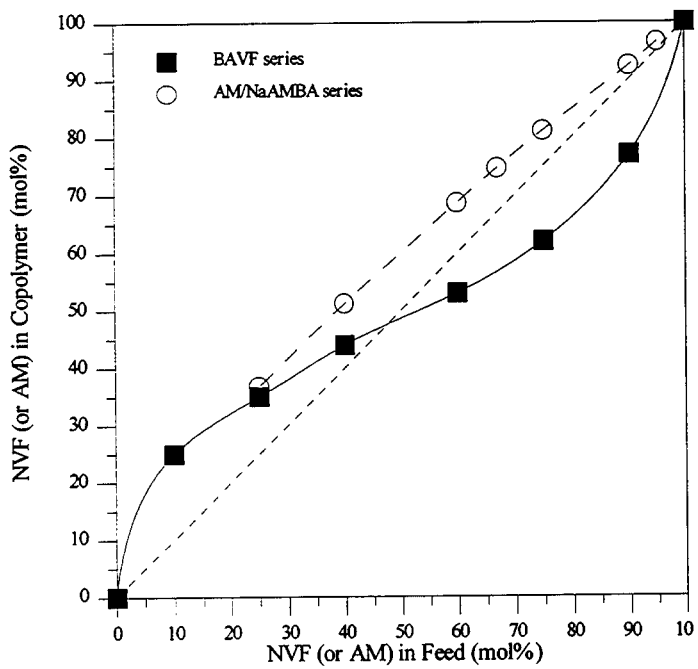


Figure 2. Mole percent NVF (■) or AM (○) incorporated into copolymers with NaAMBA as a function of comonomer feed ratio. The short dashed line represents ideal random incorporation.

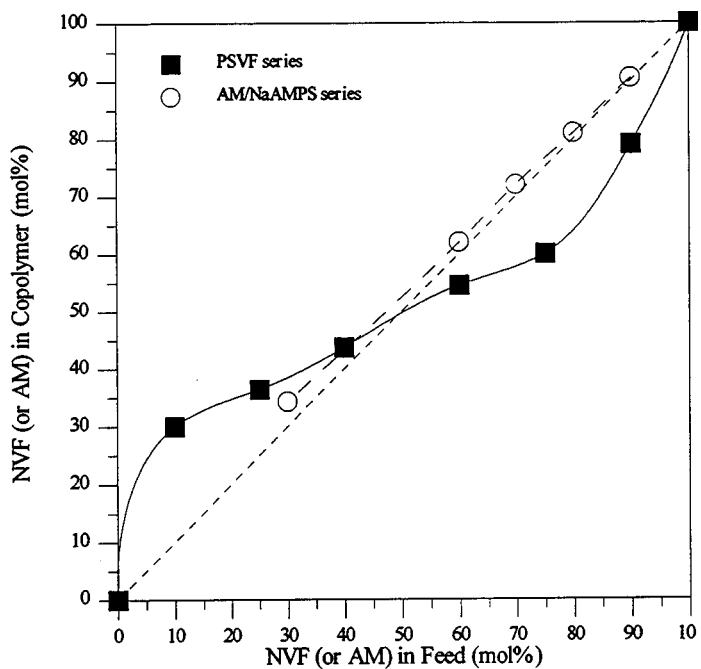


Figure 3. Mole percent NVF (■) or AM (○) incorporated into copolymers with NaAMPS as a function of comonomer feed ratio. The short dashed line represents ideal random incorporation.

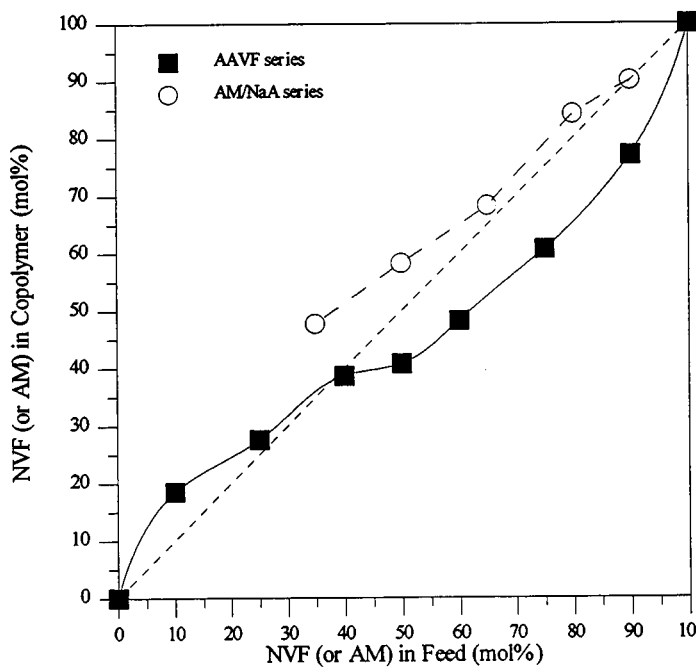


Figure 4. Mole percent NVF (■) or AM (○) incorporated into copolymers with NaA as a function of comonomer feed ratio. The short dashed line represents ideal random incorporation.

Reactivity Ratio Studies

To further investigate the alternating behavior of the copolymers, reactivity ratios were determined. Fineman-Ross²⁶, Kelen-Tudos (K-T)²⁷, and nonlinear least-squares (NLS)²⁸ methods were employed to calculate the r_1 , r_2 values and the results obtained are listed in Table IV. In each study r_1 and r_2 were determined designating NVF as M_1 and the anionic comonomer as M_2 . Comparing values obtained by the NLS method, both the BAVF, $r_1=0.26$ and $r_2=0.28$, and PSVF series, $r_1=0.25$ and $r_2=0.22$, have nearly identical values for r_1 and r_2 . Furthermore, copolymers of AM with NaAMBA and NaAMPS (Table IV) also yield similar r_1 , r_2 values. These results are not unexpected and likely due to the structural similarity of the anionic comonomers. The BAVF and PSVF series, however, have much lower $r_1 \cdot r_2$ values than those calculated for the AM copolymers (0.075 vs. 0.5-0.6). Again, this implies a greater tendency for the NVF copolymers to polymerize in an alternating fashion. The AAVF copolymers also tend to alternate as previously reported, this response being more prevalent when greater than 50 mol% NVF is present in the feed.¹⁵ Compared to the AM copolymers, the AAVF series yields a r_1/r_2 ratio (K-T values) approximately eight times less than obtained for the AM/NaA series. This observation may be attributable, in part, to the higher stability of the AM versus NVF radical on a propagating chain end. The ability of AM to polymerize to high molecular weight is well known and is a result of the high ratio of propagation to termination rate constants (k_p/k_t).

Table IV. Reactivity Ratios for N-Vinylformamide(M_1) and Acrylamide(M_1) with various Anionic Comonomers(M_2)

Comonomer Pair	Fineman-Ross	Kelen-Tudos	NLS
N-Vinylformamide and Sodium 3-Acrylamido-3-methylbutanoate	$r_1 = 0.27 \pm 0.02$ $r_2 = 0.33 \pm 0.02$	$r_1 = 0.25 \pm 0.02$ $r_2 = 0.29 \pm 0.02$	$r_1 = 0.26 \pm 0.02$ $r_2 = 0.28 \pm 0.02$
N-Vinylformamide and Sodium 2-Acrylamido-2-methylpropanesulfonate	$r_1 = 0.32 \pm 0.02$ $r_2 = 0.39 \pm 0.02$	$r_1 = 0.25 \pm 0.02$ $r_2 = 0.24 \pm 0.02$	$r_1 = 0.25 \pm 0.02$ $r_2 = 0.22 \pm 0.02$
N-Vinylformamide and Sodium Acrylate	$r_1 = 0.29 \pm 0.11$ $r_2 = 0.65 \pm 0.03$	$r_1 = 0.22 \pm 0.09$ $r_2 = 0.52 \pm 0.05$	$r_1 = 0.20 \pm 0.04$ $r_2 = 0.50 \pm 0.05$
Acrylamide and Sodium 3-Acrylamido-3-methylbutanoate	$r_1 = 1.23 \pm 0.02$ $r_2 = 0.50 \pm 0.04$	$r_1 = 1.20 \pm 0.02$ $r_2 = 0.47 \pm 0.05$	-----
Acrylamide and Sodium 2-Acrylamido-2-methylpropanesulfonate	$r_1 = 0.98 \pm 0.09$ $r_2 = 0.49 \pm 0.02$	$r_1 = 1.00 \pm 0.08$ $r_2 = 0.52 \pm 0.07$	-----
Acrylamide and Sodium Acrylate	$r_1 = 1.05 \pm 0.08$ $r_2 = 0.19 \pm 0.04$	$r_1 = 1.11 \pm 0.10$ $r_2 = 0.32 \pm 0.09$	-----

Statistical Microstructure Studies

The statistical distribution of monomer sequences for the BAVF and PSVF series were determined by the methods of Igarashi.²⁹ The reactivity ratios determined by the K-T method were used to calculate the mol% blockiness (M_1 - M_1 and M_2 - M_2), mol% alternation (M_1 - M_2), and the mean sequence lengths of M_1 and M_2 . The results are shown in Tables V and VI. Values obtained for the AAVF series have been previously reported.

As suggested earlier, both the BAVF and PSVF copolymer series tend to form alternating copolymers. This observation is further supported by the values presented in Tables V and VI. Both the BAVF and PSVF series have significantly high values for M_1 - M_2 , the mol% alternation. These values are graphically compared to the values obtained for the AM copolymers in Figure 5. All copolymers of NVF yield higher values than AM when the mol% incorporation of NVF and AM are approximately the same. The copolymers of NVF attain a maximum value of approximately 80 mol% alternation while those of acrylamide approach 60 mol%. In addition, the majority of the copolymers for the BAVF, PSVF, and AAVF series exhibit values of less than two for the mean sequence lengths. These low mean values imply the absence of any long runs of either comonomer further substantiating the alternating tendency.

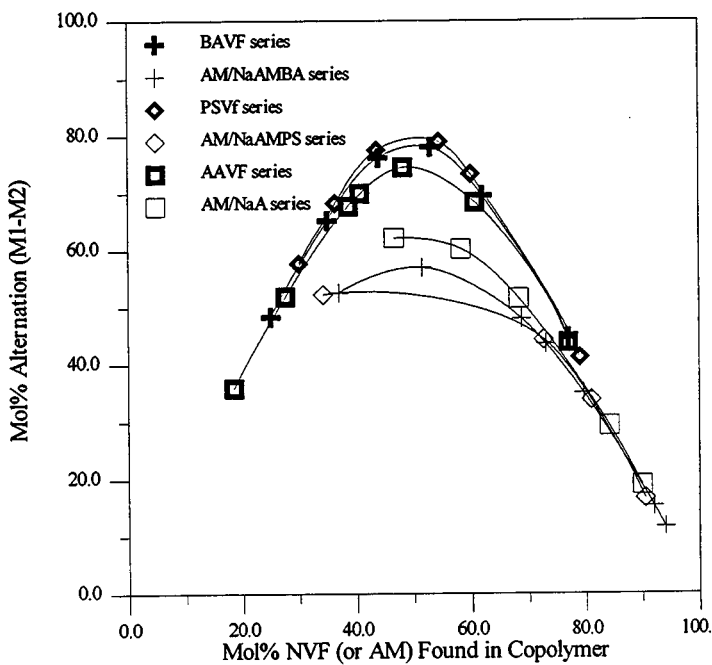


Figure 5. Mol% Alternation (M_1 - M_2) versus mol% NVF or AM incorporated into copolymers.

Table V. Structural Data for the Copolymers of N-Vinylformamide (M₁) with Sodium-3-Acrylamido-3-Methylbutanoate (M₂)

Sample Number	M1 in Copolymer (mol %)	Blockiness Mole % M ₁ -M ₁ M ₂ -M ₂	Alternation Mole % M ₁ -M ₂	Mean Seq. Length M ₁ M ₂
BAVF 23	77.0	54.66 0.66	44.67	3.27 1.03
BAVF 38	62.0	27.23 3.23	69.55	1.76 1.10
BAVF 47	53.0	13.94 7.94	78.11	1.38 1.19
BAVF 56	44.0	5.89 17.89	76.21	1.17 1.43
BAVF 65	35.0	2.39 32.39	65.23	1.08 1.86
BAVF 75	25.0	0.83 50.83	48.33	1.03 3.59

Table VI. Structural Data for the Copolymers of N-Vinylformamide (M₁) with Sodium 2-Acrylamido-2-methylpropanesulfonate (M₂)

Sample Number	M1 in Copolymer (mol %)	Blockiness Mole % M ₁ -M ₁ M ₂ -M ₂	Alternation Mole % M ₁ -M ₂	Mean Seq. Length M ₁ M ₂
PSVF 21	79.0	58.42 0.42	41.16	3.22 1.03
PSVF 40	60.0	23.32 3.32	73.35	1.74 1.08
PSVF 45	54.5	15.00 6.00	79.00	1.37 1.16
PSVF 56	43.7	4.94 17.54	77.52	1.16 1.35
PSVF 64	36.4	2.28 29.48	68.25	1.08 1.70
PSVF 70	30.0	1.16 41.16	57.67	1.03 3.11

Comparable behavior has been observed for copolymers of NVF and AM. The propensity for cross addition suggests the presence of some type of donor-acceptor characteristics between NVF and acrylamido-based monomers. The latter are expected to be an electron-accepting type monomer due to the strong electron withdrawing nature of the amide group. On the other hand, NVF is expected to be a an electron donating type monomer because of the lone pair of electrons on the nitrogen atom adjacent to the vinyl group. These electron poor/ electron rich

characteristics may favor a cross addition polymerization mechanism comparable, but to a lesser extent, than that frequently observed for maleic anhydride copolymerizations. Similar behavior has been observed by Schulz et al. for copolymers of N-vinylpyrrolidone (NVP) with various monomers possessing an acrylamide functionality.³⁰ The vinyl bonds of NVF and NVP should possess similar electronic characteristics since both are covalently bonded to the nitrogen atom of an amide functionality. In addition to these electronic effects, other structural features of both NaAMBA and NaAMPS may induce alternating tendencies. Both NaAMBA and NaAMPS are inherently bulky, therefore steric repulsions may favor cross-additions with NVF. Another factor to be considered is that both NaAMBA and NaAMPS are anionically charged and coulombic repulsions required by homoaddition are less favored than addition of NVF. This effect is likely a major factor in the AAVF series as the vinyl bond of NaA is electronically rich, therefore, precluding any type of donor-acceptor interactions. Evidence for coulombic repulsions influencing polymer composition has been reported by Salazar and McCormick for copolymers of NaAMBA with acrylamide.¹⁹ In that study, addition of NaCl to the polymerization medium led to a more ideal incorporation of NaAMBA into the copolymer, a result of the shielding effect between NaAMBA comonomers by the addition of NaCl.

Light Scattering Studies

Molecular weights and second virial coefficients (A_2) were determined for all of the copolymers in this study at 25°C in 1.0M NaCl at pH=8.5. The values obtained are displayed in Tables VI-IX. For the BAVF series, the molecular weights ranged from 1.2 to 6.8×10^6 g/mol and the A_2 values ranged from 12.5 to 2.8×10^{-4} ml·mol/g². These molecular weights are considerably lower than those of the AM/NaAMBA copolymers which ranged from 12.9 to 15.6×10^6 g/mol. For the PSVF series, the molecular weights ranged from 0.9 to 7.5×10^6 g/mol and the A_2 values ranged from 44.3 to 1.0×10^{-4} ml·mol/g². The trend for these two series is that the molecular weight reaches a maximum value when there are approximately 44 mol% of NVF units incorporated into the copolymers. This may be a result of a faster rate of alternating propagation when nearly equimolar amounts of comonomers are incorporated into the copolymer. Interestingly, A_2 reaches a minimum value at the same copolymer composition which may be a result of the higher molecular weights. For the AAVF series, the molecular weights ranged from 0.9 to 12.0×10^6 g/mol and the A_2 values ranged from 14.8 to 2.8×10^{-4} ml·mol/g². The trend for this series is that the molecular weights increase as the mol% of NVF incorporated into the copolymers decreases. The A_2 values exhibit the opposite trend, decreasing in value as less NVF is incorporated into the copolymers.

Table VII. Molecular Weight and Second Virial Coefficient Data for the Copolymers of N-Vinylformamide (M_1) with Sodium 3-Acrylamido-3-methylbutanoate(M_2)

Sample	NVF Found ^a (mol %)	$M_w \times 10^{-6}$ (g / mol)	$A_2 \times 10^4$ (ml·mol/g ²)	$DP \times 10^{-4}$
BAVF 23	77.0	1.2	12.5	1.3
BAVF 38	62.0	2.4	4.0	2.0
BAVF 47	53.0	4.6	4.6	3.6
BAVF 56	44.0	6.8	2.8	4.9
BAVF 65	35.0	5.4	4.7	3.6
BAVF 75	25.0	5.7	5.3	3.5
BAVF 100	0.0 ^b	1.3	8.6	0.7

^a Determined from ^{13}C NMR.

^b Theoretical Value

Table VIII. Molecular Weight and Second Virial Coefficient Data for the Copolymers of N-Vinylformamide (M_1) with Sodium 2-Acrylamido-2-methylpropanesulfonate (M_2)

Sample	NVF found ^a (mol %)	$M_w \times 10^{-6}$ (g / mol)	$A_2 \times 10^4$ (ml·mol/g ²)	$DP \times 10^{-4}$
PSVF 21	79.0	0.9	44.3	0.9
PSVF 40	60.0	2.6	12.0	1.9
PSVF 45	54.5	2.3	11.1	1.6
PSVF 56	43.7	7.5	1.0	4.7
PSVF 64	36.4	6.9	1.6	4.0
PSVF 70	30.0	4.5	2.8	2.5
PSVF 100	0.0 ^b	1.7	8.0	0.7

^a Determined from ^{13}C NMR.

^b Theoretical Value

Table IX. Molecular Weight and Second Virial Coefficient Data for the Copolymers of N-Vinylformamide (M_1) with Sodium Acrylate (M_2)

Sample	NVF found ^a (mol %)	$M_w \times 10^{-6}$ (g / mol)	$A_2 \times 10^4$ (ml \cdot mol/g 2)	DP $\times 10^{-4}$
AAVF 22	78.0	0.9	14.8	1.2
AAVF 49	51.0	2.9	7.8	3.5
AAVF 62	37.5	3.9	5.1	4.6
AAVF 82	17.5	6.6	3.2	7.3
AAVF 100	0.0 ^b	12.0	2.8	12.7

^a Determined from ^{13}C NMR.

^b Theoretical Value

CONCLUSIONS

Copolymers of N-vinylformamide with sodium-3-acrylamido-3-methyl butanoate, sodium-2-acrylamido-2-methylpropanesulfonate, and sodium acrylate were prepared by free radical polymerization in aqueous solution. ^{13}C NMR was used to determine the copolymer compositions by integration of the carbonyl peaks. The reactivity ratios were determined by two methods and indicate random copolymerization with a strong alternating tendency. This alternating tendency was further confirmed by calculating the copolymer microstructures by the method of Igarashi. Molecular weights were determined and found to be dependent on the amount of NVF incorporated into the copolymers for the BAVF and PSVF series; reaching a maximum around 40 mol% NVF. This dependency was not found for the AAVF series which exhibited higher molecular weights as the mol% NVF incorporated into the copolymers decreased.

References

- 1) Jones, G. D. In *Polyelectrolytes*; Frisch, K. C.; Klemper, D.; Patsis, A.V. Eds.; Technomic Publishing Co., Inc.: Westport, CT., 1976; p144.
- 2) Molyneux, P. *Water-Soluble Synthetic Polymers: Properties and Behavior*, Vol. I and II; CRC Press: Boca Raton, FL., 1984.
- 3) Shalaby, S.; Butler, G.; McCormick, C. L.; Eds.; *Water-Soluble Polymers*, ACS Symposium Series no. 467; American Chemical Society: Washington, D.C., 1991.
- 4) Schulz, D.; Glass, J. E. Eds.; *Polymers as Rheology Modifiers*; ACS Symposium Series no. 462, American Chemical Society: Washington, D.C., 1991.
- 5) McCormick, C. L.; Bock, J.; Schulz, D. In *Encyclopedia of Polymer Science and Engineering*, Vol. 17; Wiley Press: New York, 1989; p730.
- 6) Dubin, P.; Bock, J.; Davies, R. M.; Schulz, D.; Thies, C. Eds.; *Macromolecular Complexes in Chemistry and Biology*; Springer-Verlag: New York, 1994.
- 7) Bekturov, E. A.; Bakauova, Z. Bh. *Synthetic Water-Soluble Polymers in Solution*; Huethig and Wepf Press: New York, 1986.
- 8) Sorbie, K. S. *Polymer-Improved Oil Recovery*; CRC Press: Boca Raton, FL., 1991.
- 9) U.S. Pat. 4,772,359 Linhart, F.; Degen, H.; Auhorn, W.; Kroener, M.; Hartmann, H.; Heide, W. 1988.
- 10) U. S. Pat. 4,774,285 Pfohl, S., Kroener, M., Hartmann, H., and Denzinger, W., 1988.
- 11) U. S. Pat. 4,795,770 Lai, T.; Vijayendran, B. 1989.
- 12) U. S. Pat. 4,814,505 Kroener, M.; Schmidt, W.; Proll, T.; Hartmann, H. 1989.
- 13) Badesso, R.J., Lai, T. W., Pinschmidt, R. K., Sagl, D. J., and Vijayendran, B. R., *Polymer Preprints* 1991, 32(2), 110.
- 14) Chang, Y. ; McCormick, C. L. *Macromolecules* 1993, 26, 4814.
- 15) Kathmann, E. E.; McCormick, C. L. *Macromolecules* 1993, 26, 5249.
- 16) McCormick, C. L.; Blackmon, K. P. *J. Polym. Sci., Polym. Chem. Edn.* 1986, 24, 2635.
- 17) McCormick, C. L.; Blackmon, K. P.; Elliot, D. L. *J. Polym. Sci., Polym. Chem. Edn.* 1986, 24, 2619.
- 18) McCormick, C. L.; Elliot, D. L. *Macromolecules* 1986, 19, 542.
- 19) McCormick, C. L.; Salazar, L. C. *J. Macro. Sci., Pure Appl. Chem.* 1992, A29(3), 193.
- 20) McCormick, C. L.; Chen, G. S.; Hutchinson, B. H. *J. Appl. Polym. Sci.* 1982, 27, 3103.
- 21) Neidlinger, H. H.; Chen, G. G.; McCormick, C. L. *J. Appl. Polym. Sci.* 1984, 29, 713.

22) McCormick, C. L.; Chen, G. S. *J. Polym. Sci., Polym. Chem. Edn.* **1982**, *20*, 817.

23) Chen, G. S. *PhD. Dissertation*, University of Southern Mississippi, May 1986

24) Newman, J. K.; McCormick, C. L. *Macromolecules* **1994**, *27*, 5114.

25) Hoke, D.; Robins, R. *J. Polym. Sci.* **1971**, *10*, 3311.

26) Fineman, M.; Ross, S. *J. Polym. Sci.* **1950**, *5*, 259.

27) Kelen, T.; Tudos, F. *J. Macromol. Sci., Chem.* **1975**, *A9*, 1.

28) Tidwell, P. W.; Mortimer, G. A. *J. Polym. Sci.: Part A* **1965**, *3*, 369.

29) Igarashi, S. *J. Polym. Sci., Polym. Lett. Ed.* **1963**, *1*, 359.

30) Schulz, D. N.; Kitano, K.; Danik, J. A.; Kaladas, J. J. *Polymers in Aqueous Media: Performance Through Associations*; Glass, J. E., Ed.; Advances in Chemistry 223; American Chemical Society: Washington D.C., 1989; p165.

CHAPTER 3. Polyelectrolytes of N-vinylformamide with Sodium-3-Acrylamido-3-Methylbutanoate, Sodium- 2- Acrylamido- 2- Methyl propanesulfonate, and Sodium Acrylate: Solution Behavior.

SYNOPSIS

Dilute solution properties of copolymers of N-vinylformamide (NVF) with sodium-3-acrylamido-3-methylbutanoate (NaAMBA), sodium-2-acrylamido-2-methylpropanesulfonate (NaAMPS), and sodium acrylate (NaA) of known molecular weight and compositions have been studied in regard to added cosolutes, pH and temperature. Phase separation studies have also been performed. All copolymers display typical polyelectrolyte behavior as observed by a reduction in viscosity in the presence of added electrolytes. Copolymers from all three series display losses of viscosity in the presence of urea at pH=8.5. With the exception of a few copolymers of NVF with NaA (AAVF-100,-82,-49), all copolymers investigated exhibit no phase separation in the presence of calcium chloride at 25°C. Copolymers of NVF with NaAMPS (PSVF series) are soluble throughout the pH range investigated, while most copolymers from the BAVF and AAVF series phase separate as the pH of the aqueous medium is lowered. At low pH, phase separation at the lower critical solution temperature is observed for the BAVF series. Conversely, the phase separation of the AAVF copolymers is representative of an upper critical solution temperature and is affected by the presence of added cosolutes such as sodium chloride and urea.

INTRODUCTION

Water-soluble polymers with sulfonate or carboxylate functionality have commercial utility in a number of applications.¹⁻³ The sulfonate group is a weak base and remains charged throughout the useful pH range from » 2 to 12. Counterion binding along the polyelectrolyte chain is less site specific for sulfonate groups than that observed with carboxylates.⁴⁻⁶ The degree of ionization, number of ionic sites, and distance from the polymer backbone influence rheological properties, phase behavior, and responsiveness to pH and electrolyte changes.

In this work, we investigate the solution properties of copolymers of N-vinylformamide (NVF) with sodium-3-acrylamido-3-methylbutanoate (NaAMBA), sodium-2-acrylamido-2-methylpropanesulfonate (NaAMPS), and sodium acrylate (NaA). In depth synthesis and structural characterization is reported in the accompanying paper of this series.¹⁷

EXPERIMENTAL

Materials

Copolymers of NVF with NaAMBA, NaAMPS, and NaA were prepared at 45°C in aqueous solution at a pH=8.5 using 2,2'-Azobis(N,N'-

dimethyleneisobutyramidine)dihydrochloride.¹⁷ All other materials were used as received.

Copolymer Characterization

The copolymer compositions were determined from ¹³C NMR data. Molecular weights were determined by using low angle laser light scattering. These procedures and values are reported in the accompanying paper in this series.¹⁷

Viscosity Measurements

Aqueous stock solutions of electrolytes and urea were prepared in deionized water. Stock polymer solutions were prepared at a concentration of 0.3 g/dL and pH=8-8.5. Care was taken to avoid excessive shear during the dissolution of the polymers to limit degradation. Dilutions were performed isoionically and solutions allowed to age 2-3 weeks. Viscosity measurements were performed with a Contraves LS-30 rheometer at 25°C and a shear rate of 6 sec⁻¹. Duplicate runs were conducted and reproducibility found to be within \pm 3-7% dependent on the magnitude of the viscosity values. Unless otherwise stated, all viscosity measurements were performed at pH of 8.3-8.5. Precautions were taken to assure that the data used in the calculation of the intrinsic viscosities were from the region of concentration below the critical overlap concentration. Intrinsic viscosities were evaluated using the Huggins equation.

Turbidimetry

The cloud points were obtained using a Brinkman PC 800 Colorimeter with a 620nm light filter. The sample of polymer solution (15mL) was stirred by a magnetic stirrer and was heated slowly by an air-heating system. A thermometer immersed in the solution was used to determine the temperature at which the phase transition occurred. Reported values were taken when the transmittance was approximately 50%. The values reported are accurate to within \pm 0.8°C.

RESULTS AND DISCUSSION

Polyelectrolytes (Figure 1) comprised of NVF with the comonomers NaA, NaAMBA, and NaAMPS have been prepared with microstructural control. These copolymer series, designated AAVF, BAVF, and PSVF respectively, have been extensively characterized as to microstructure, overall composition, molecular weight, and extent of polymer solvent interaction. Representative compositions and molecular weights are shown in Table 1. The numbers following the acronym represent the mol% of the anionic comonomer found in the final copolymer.

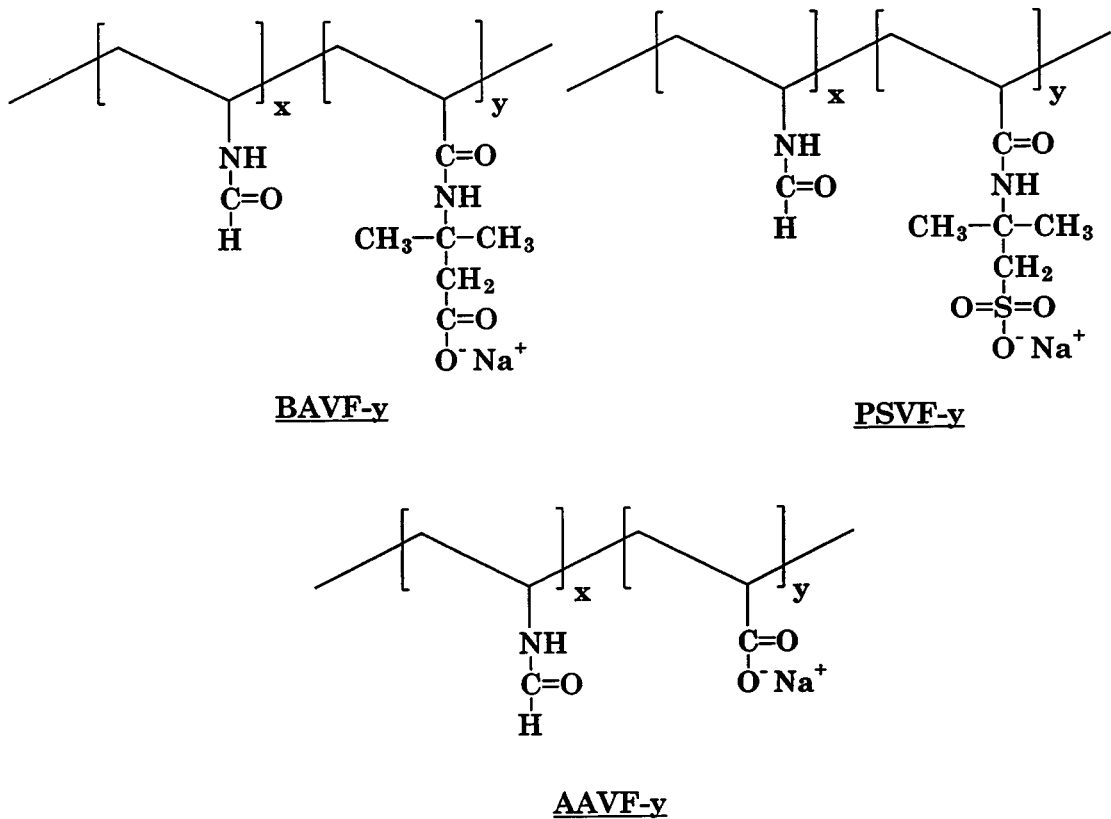


Figure 1. Copolymers of N-vinylformamide with Sodium-3-Acrylamido-3-Methylbutanoate (BAVF series), Sodium-2-Acrylamido-2-Methylpropane sulfonate (PSVF series), and Sodium Acrylate (AAVF series)

Effects of Polymer Concentration

The effects of polymer concentration on the apparent viscosity for the BAVF, PSVF, and AAVF copolymer series are shown in Figures 2-4. The measurements were conducted at pH=8.5 and hence almost all of the anionic comonomers should be neutralized. Because of the polyelectrolytic nature of the copolymers, relatively high apparent viscosities are observed at low polymer concentration due to coulombic repulsions between the anionically charged comonomers.

An interesting trend is also noted for all three copolymer series. The homopolyelectrolytes (BAVF-100, PSVF-100, and AAVF-100) and the copolymers containing the lowest incorporation of charged comonomers (BAVF-23, PSVF-21, and AAVF-22) consistently exhibit the lowest apparent viscosities. Previously, we have found that for similar polyelectrolytes incorporating AM instead of NVF, that the copolymers always yielded higher viscosity values than the homopolyelectrolytes. Furthermore, for the AM

copolymers, the highest viscosity values were obtained when there was »10-35 mol% incorporation of either NaAMBA^{7,8} or NaAMPS⁹, while for AM-NaA copolymers¹⁰, 50 mol% NaA incorporation yielded the highest viscosity. For the NVF copolymers, those containing a slight molar excess of the anionic comonomer (ca. 60 mol%) attain the highest apparent viscosity. This behavior results from numerous factors which affect the hydrodynamic volume, including molecular weight, mol% of anionic comonomer, and the extent of hydration of the polymer coil. Additionally, intramolecular hydrogen bonding of adjacent mer units can stiffen the polymer backbone resulting in a larger hydrodynamic volume. This has been previously observed for copolymers of AM and NaA.¹³⁻¹⁵ Another effect which influences solvation of polyelectrolytes is that of counterion condensation which effectively neutralizes a portion of the anionic charge, thereby reducing charge repulsion effects. Intramolecular hydrogen bonding, counterion condensation, and charge-charge repulsions are stronger with the AAVF series in which the anionic group is closer to the macromolecular backbone.

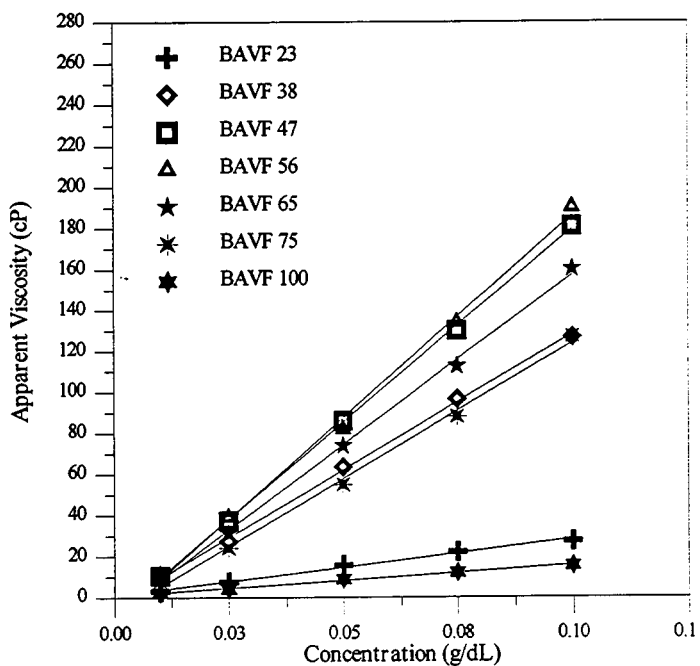


Figure 2. Effect of polymer concentration on the apparent viscosity for the BAVF copolymer series.

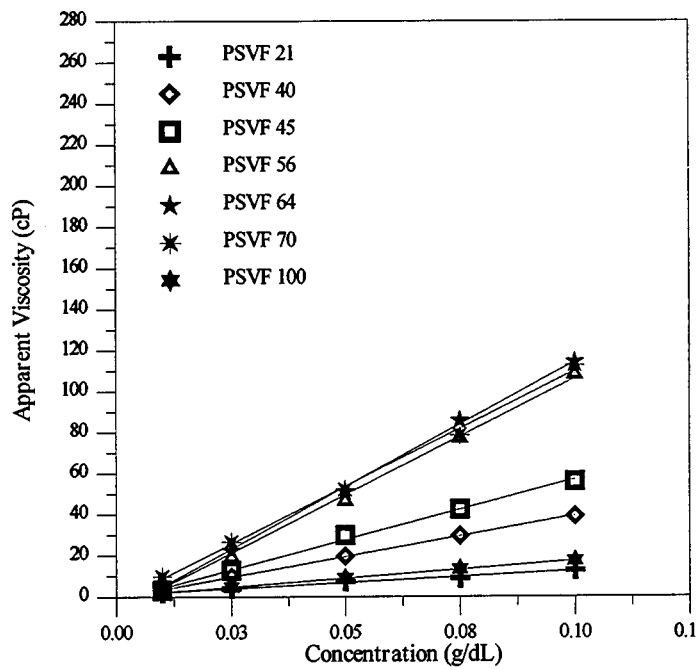


Figure 3. Effect of polymer concentration on the apparent viscosity for the PSVF copolymer series.

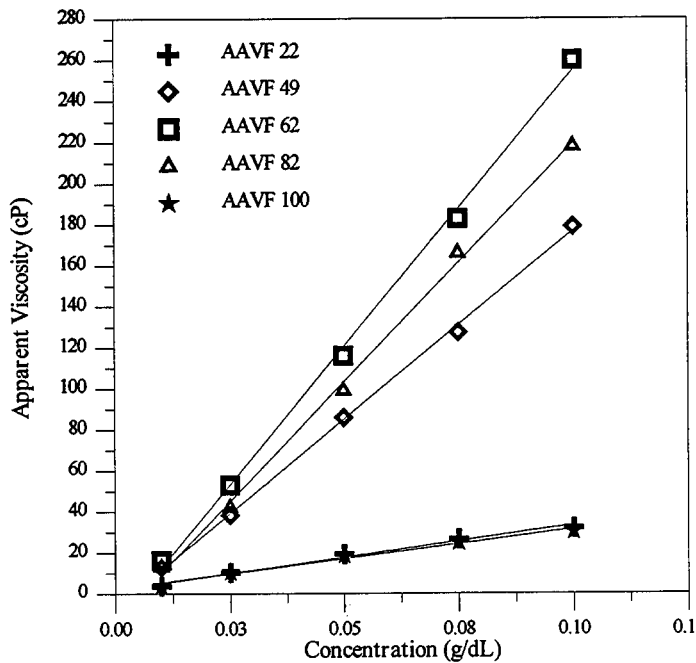


Figure 4. Effect of polymer concentration on the apparent viscosity for the AAVF copolymer series.

Effects of Added Electrolytes

The effects of sodium chloride on the reduced viscosity were also examined and displayed in Figures 5-7. Polyelectrolyte behavior is observed

as evidenced by the linear dependence of the reduced viscosity as a function of the inverse square root of ionic strength. As the concentration of electrolyte is increased (from right to left in the figures), the Debye-Huckel reciprocal screening length decreases. This, in turn, leads to a screening of the electrostatic repulsions along the polyelectrolyte which in turn allows the polymer chain to acquire a more random coil-like configuration. Furthermore, by examining the magnitude of the slopes in the figures, the extent of conformational change induced by the addition of electrolytes can be assessed. Higher slope values indicate that the polymer coil is more susceptible to undergo conformational changes as the concentration of electrolyte is increased. From the figures, the copolymers incorporating the carboxylate group exhibit higher slopes than the sulfonate copolymers and may be indicative of enhanced counterion binding. Other factors which affect the hydration and conformation of the coil, such as the degree of hydrophobicity and steric repulsions, are also likely operative. The effects of polymer composition on the reduced viscosity follows similar trends as mentioned earlier. Namely, the copolymers with approximately 40-80 mol% of charged comonomer maintain higher viscosities even in the presence of electrolytes. This behavior still prevails in 1.0M NaCl, conditions in which polymer conformation is only negligibly influenced by charge-charge repulsions.

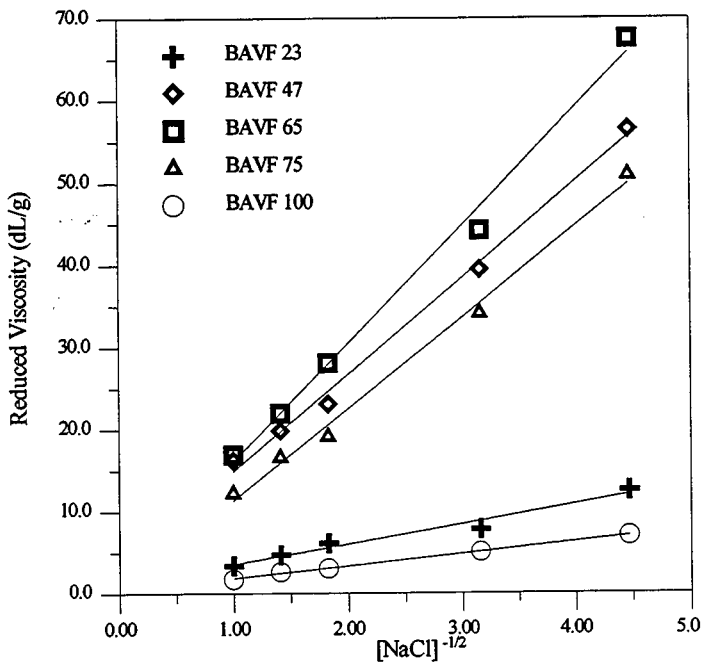


Figure 5. The reduced viscosity as a function of the inverse square root of ionic strength for the BAVF copolymer series (Cp=0.1 g/dL).

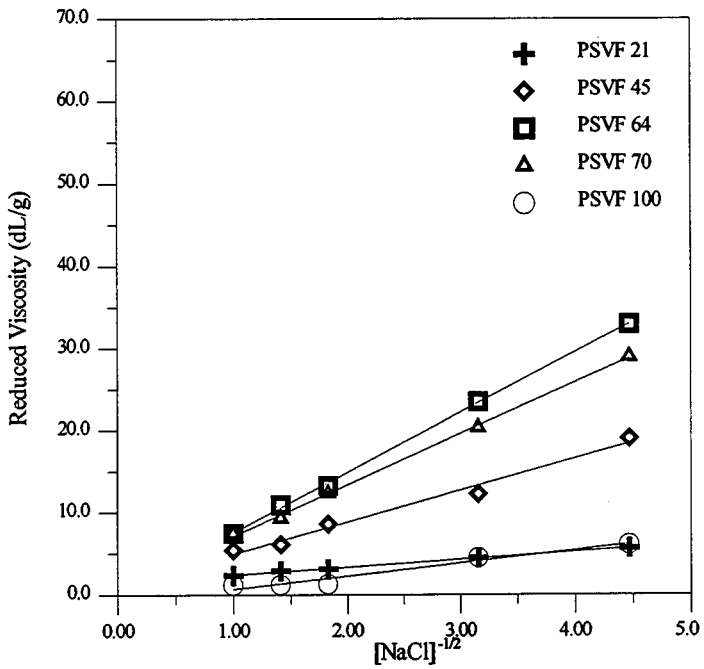


Figure 6. The reduced viscosity as a function of the inverse square root of ionic strength for the PSVF copolymer series ($C_p=0.1$ g/dL).

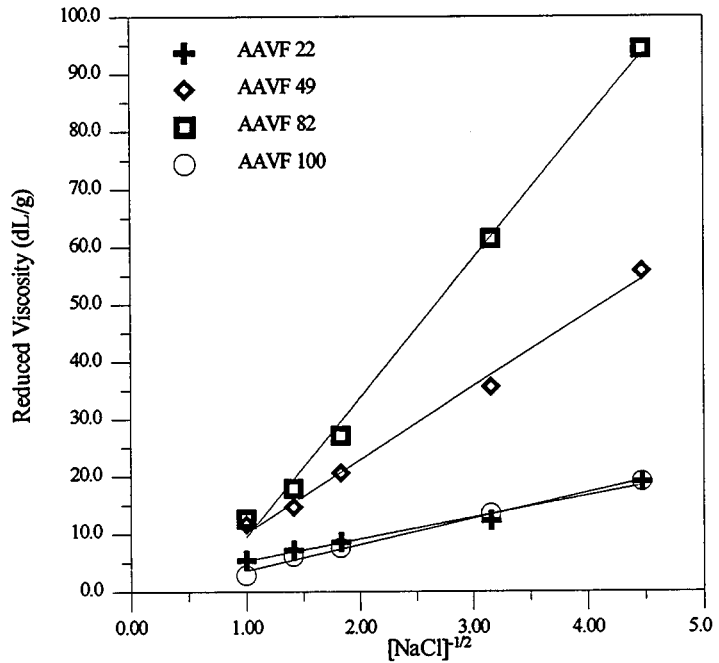


Figure 7. The reduced viscosity as a function of the inverse square root of ionic strength for the AAVF copolymer series ($C_p=0.1$ g/dL).

Effects of the Nature of the Anionic Comonomer

In an effort to gain an understanding of the influence of the nature of the anionic comonomer on the solution behavior, viscosity studies were conducted on BAVF-38 and -56, PSVF-40 and -56, and AAVF-62. Since these pairs possess similar degrees of polymerization and essentially equivalent molar compositions of charged species, structure/property comparisons may be made. Molecular weight values and degrees of polymerization are shown in Table I.

Table I. Molecular Weight and Second Virial Coefficient Data for Copolymers of NVF with NaAMBA, NaAMPS, and NaA.

Sample	NVF found ^a (mol %)	$M_w \times 10^{-6}$ (g / mol)	$A_2 \times 10^4$ (ml \cdot mol/g 2)	$DP \times 10^4$
BAVF 38	62.0	2.4	4.0	2.0
PSVF 40	60.0	2.6	12.0	1.9
BAVF 56	44.0	6.8	2.8	4.9
PSVF 56	44.0	7.5	1.0	4.7
AAVF 62	38.0	3.9	5.1	4.6

^a Determined from ^{13}C NMR

The apparent viscosities of the copolymers in deionized water at pH=8.5 are shown in Figure 8. AAVF-62 has the highest apparent viscosity followed by BAVF-56 and PSVF-56. The ionic groups of AAVF are both closer to the polymer backbone and to adjacent anionic groups compared to BAVF and PSVF series. The forces resulting from charge-charge repulsions therefore cause a greater extension of the polymer backbone and subsequently larger hydrodynamic volumes. For the BAVF and PSVF copolymers, the charged centers are farther removed from the backbone and more conformational side chain motion allows charge-charge repulsions to be diminished. The BAVF copolymers consistently display higher viscosities than the PSVF copolymers. The difference between the two copolymers is the nature of the anionic species, BAVF possessing a carboxylate group and PSVF possessing a sulfonate group. Past studies in our laboratories have shown similar behavior for copolymers of acrylamide with NaAMBA and NaAMPS⁷⁻¹². In those studies, the copolymers containing the NaAMBA comonomer exhibited higher viscosities than those with NaAMPS. This behavior was attributed to both intramonomer and intermonomer hydrogen bonding between the carboxylate moiety and the acrylamido moieties. The

carboxylate group is a stronger base than the sulfonate group and should therefore be a stronger hydrogen bond acceptor. Other factors such as enhanced solvation of the carboxylate group as compared to the sulfonate group and differing degrees of polarizability of the two groups may also be operative.

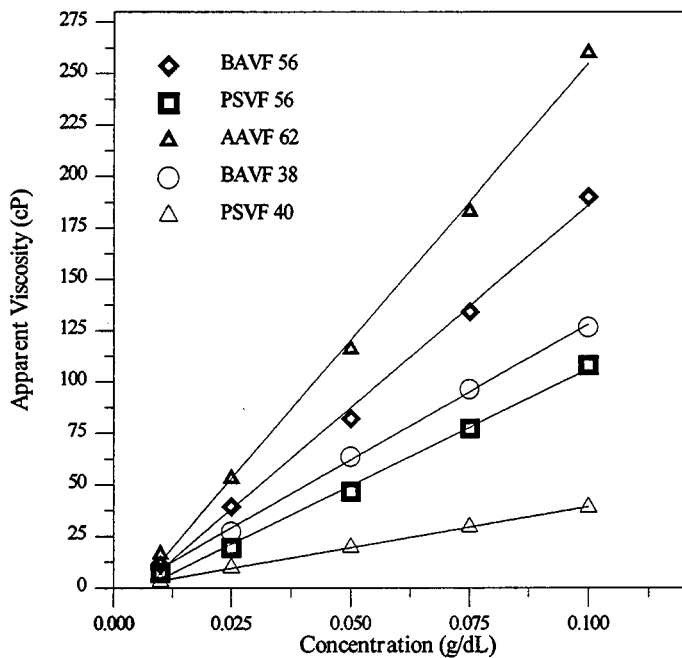


Figure 8. Effect of polymer concentration on the apparent viscosity for the selected copolymers.

Figure 9 shows the effect of sodium chloride on the intrinsic viscosities of BAVF-38 and -56, PSVF-40 and -56, and AAVF-62. As before, there is a linear dependency of the intrinsic viscosity on the inverse square root of ionic strength. The BAVF copolymers exhibit higher slopes and therefore experience more conformational changes as the concentration of electrolytes is increased. Furthermore, the BAVF copolymers display an enhanced viscosity compared to the PSVF copolymers while the AAVF copolymer exhibit behavior intermediate to the BAVF and PSVF series. Similar trends have previously been observed for AM copolymers with NaAMPS and NaAMBA in the presence of electrolytes. Enhanced chain stiffness caused by hydrogen bonding interactions may, in part, reflect the observed differences in salt response.

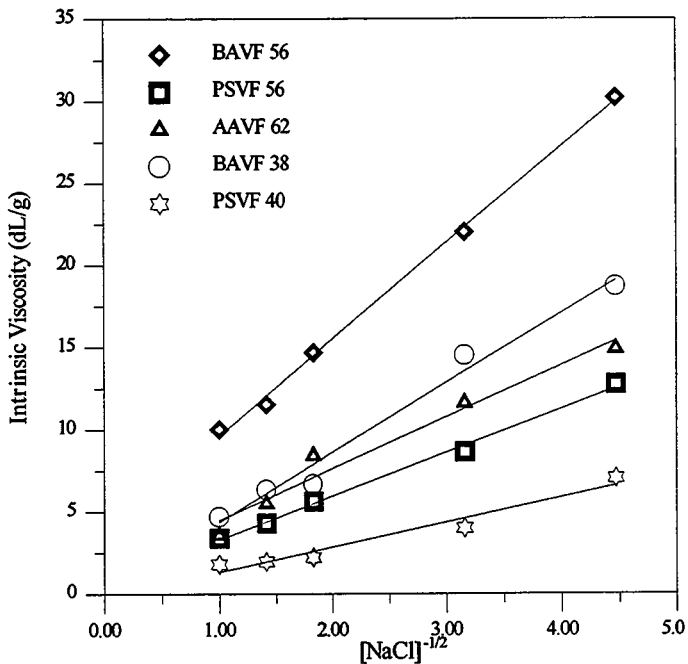


Figure 9. The intrinsic viscosity as a function of the inverse square root of ionic strength for the selected copolymers.

Figures 10-12 illustrate the effect of the nature of the added electrolyte on the reduced viscosity of the copolymers containing approximately 60 mol% anionic groups. For the electrolytes examined in this study, the reduced viscosity is relatively unaffected by the nature of the small molecule anion or cation as evidenced by essentially the same viscosity profile and values as the concentration of electrolyte is increased. This behavior suggests that there is no detectable interaction between the copolymer and the monovalent electrolyte.

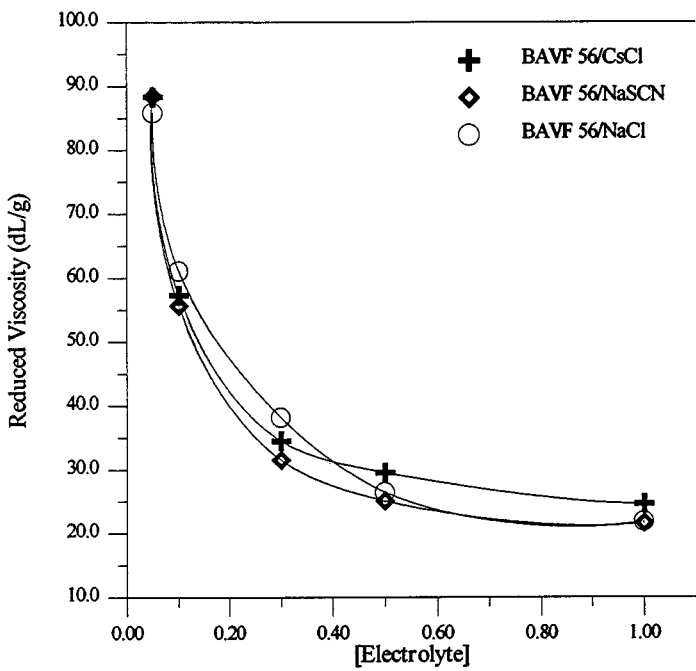


Figure 10. Effect of the nature and concentration of electrolyte on the reduced viscosity for BAVF-56 (Cp=0.1 g/dL).

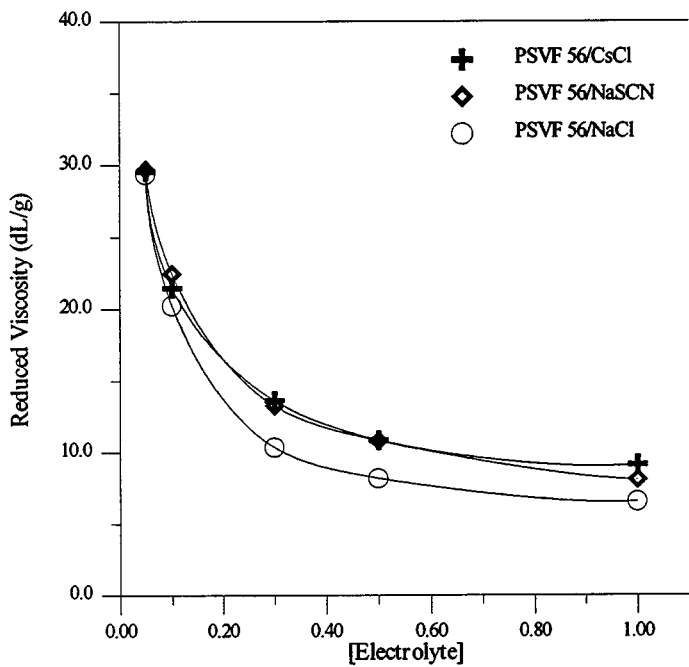


Figure 11. Effect of the nature and concentration of electrolyte on the reduced viscosity for PSVF-56 (Cp=0.1 g/dL).

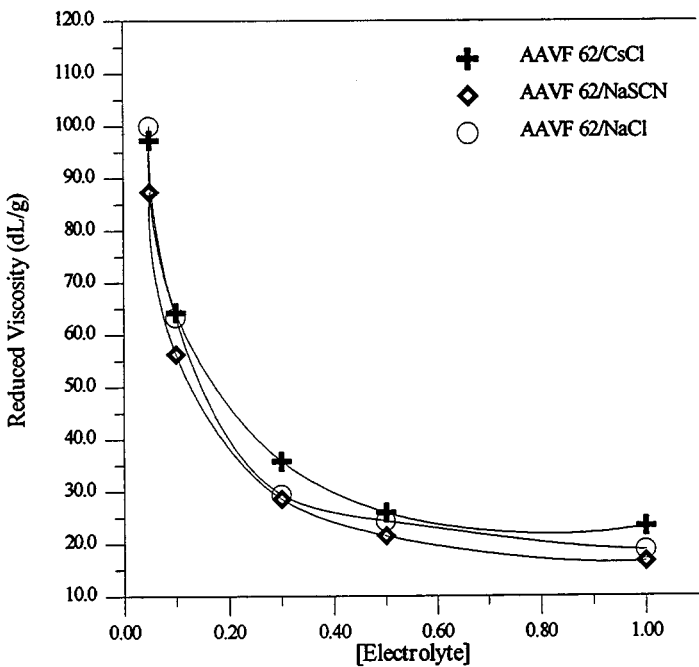


Figure 12. Effect of the nature and concentration of electrolyte on the reduced viscosity for AAVF-62 (Cp=0.1 g/dL).

Effects of Urea

The effects of urea on the solution behavior of the copolymers were examined in the absence of added electrolytes and the results are shown in Figures 12-15. Interestingly, urea has the same effect as small molecule electrolytes, that is a reduction in the reduced viscosity as concentration is increased. The dramatic loss of hydrodynamic volume implies a decrease in the solvent/polymer interaction as opposed to a shielding effect as is the case for added electrolytes. Whether this effect is due to specific interactions of urea with the polymer and/or a result of the perturbation of the water structure cannot be decisively concluded by viscosity studies alone. It should also be noted that this phenomenon is observed for all three copolymer series, thus implying that the results are independent of the structure of the anionic comonomer and the mol% incorporated into the copolymer.

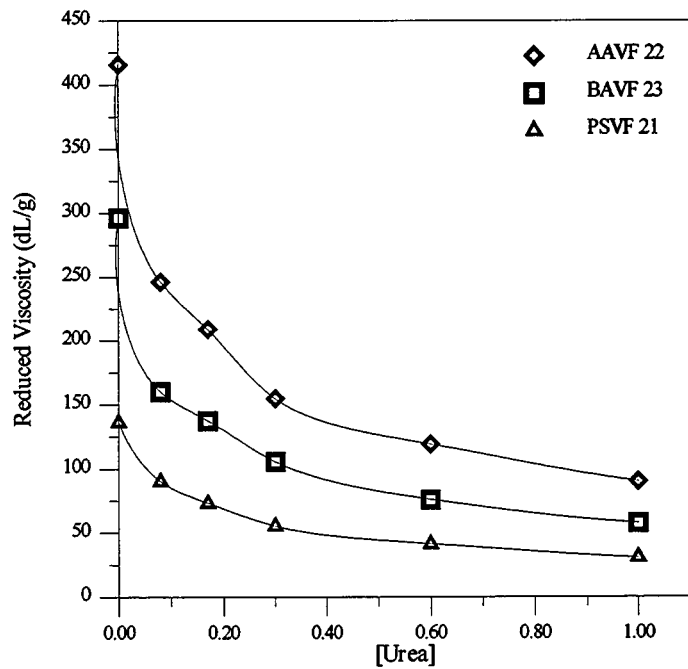


Figure 13. Effect of urea concentration on the reduced viscosity for the selected copolymers. ($C_p=0.025$ g/dL).

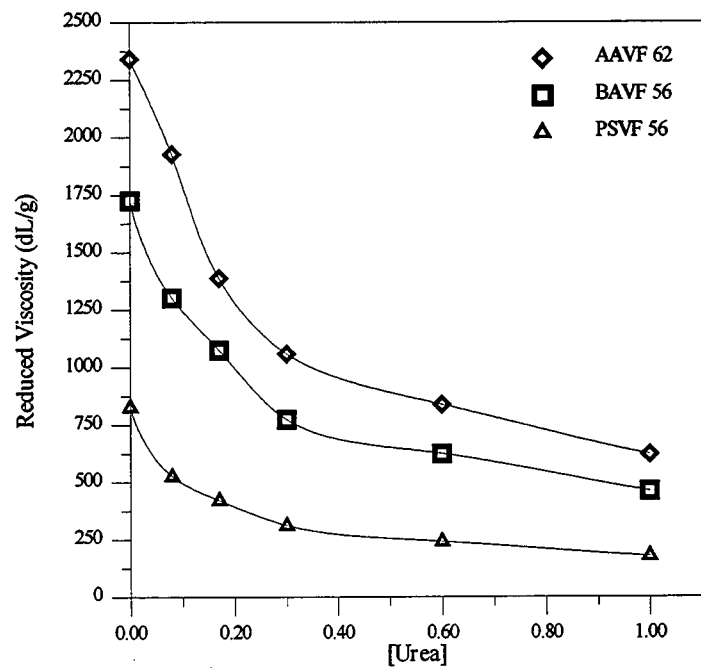


Figure 14. Effect of urea concentration on the reduced viscosity for the selected copolymers. ($C_p=0.025$ g/dL).

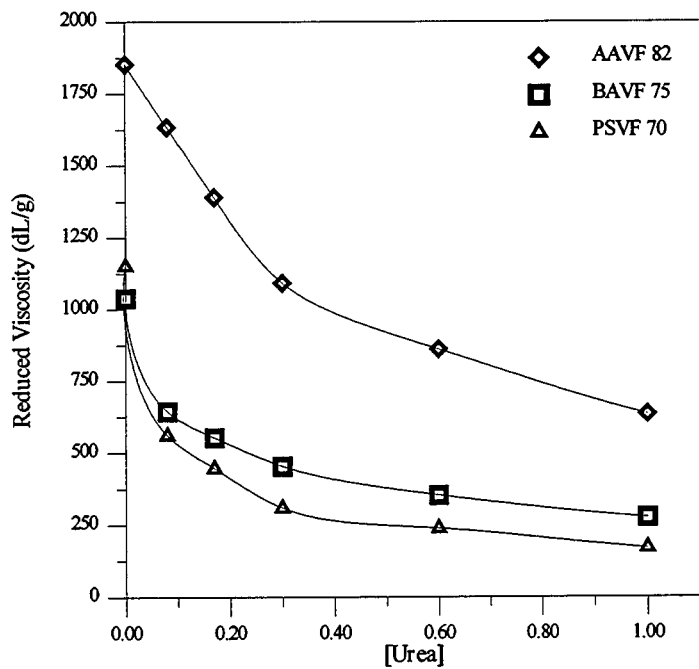


Figure 15. Effect of urea concentration on the reduced viscosity for the selected copolymers. ($C_p=0.025$ g/dL).

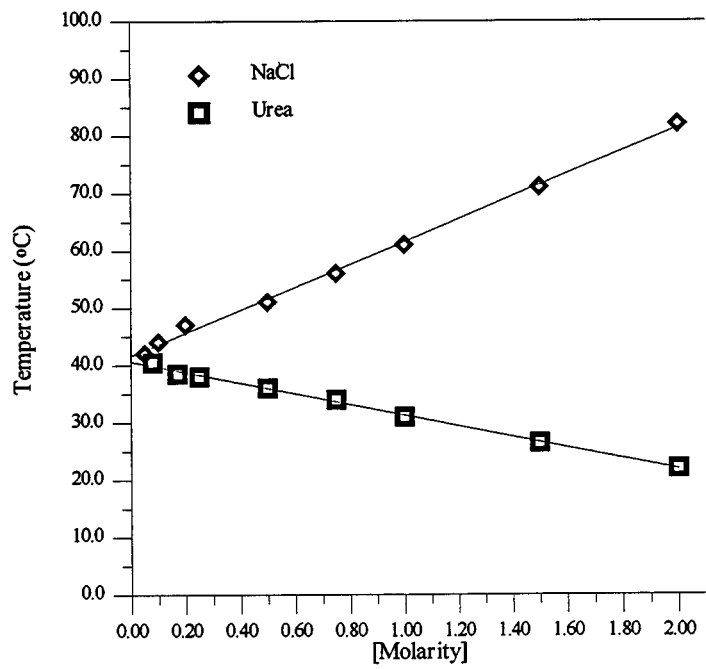


Figure 16. Effect of sodium chloride and urea concentration on the upper critical solution temperature (U.C.S.T.) for AAVF-62. ($C_p=0.1$ g/dL).

Phase Behavior

Many polymers possessing anionic moieties are known to undergo phase separation in the presence of divalent electrolytes such as calcium chloride and magnesium chloride.^{4-6,11} This phenomenon is attributed to a strong site binding of the anionic moieties with divalent cations. The effects of calcium chloride as well as changes in the pH of the aqueous medium have been assessed for the BAVF, PSVF, and AAVF copolymer series.

The phase behavior of the AAVF, BAVF, and PSVF copolymers in the presence of calcium chloride was studied at 25°C and at polymer concentrations of 0.2 g/dL at pH=8.5. The behavior of the AAVF copolymer series is similar to that of copolymers of acrylamide and sodium acrylate. In the presence of calcium chloride all of the copolymers, with the exception of AAVF-21, phase separate. The BAVF and PSVF copolymers, however, are soluble in the presence of calcium chloride (0-2M) at 25°C. Similar phase stability for copolymers of acrylamide with NaAMBA in the presence of calcium chloride has previously been reported by our group.⁷ It should also be noted that both BAVF-100 and BAVF-75 phase separate at higher temperatures. For example, BAVF-75 in the presence of 0.1M CaCl_2 exhibits a lower critical solution temperature (L.C.S.T.) of 86 °C., while BAVF-100 exhibits a L.C.S.T. of 76°C. In the presence of 0.3M CaCl_2 , the L.C.S.T. for BAVF-75 falls to 82°C while the L.C.S.T. for BAVF-100 falls to 71°C. For copolymers containing 65 mol% or less of NaAMBA, no phase separation was observed in 0.3M CaCl_2 up to 100°C. The PSVF copolymers were stable in the presence of CaCl_2 at all temperatures. The differences in the solubility behavior between the BAVF and PSVF copolymer series may be attributed to the stronger affinity for the calcium ion of the carboxylate group compared to the sulfonate group.

The phase behavior of the copolymers was also examined as a function of pH in deionized water at a polymer concentration of 0.05g/dL. To avoid hydrolysis, the lowest pH value examined was approximately 1. The PSVF copolymers were soluble over the entire pH range. This behavior is directly attributable to the weak basicity of the sulfonate groups which are essentially disassociated at this pH value. With the exception of BAVF-23, all of the BAVF copolymers phase separate at a critical pH value dependent on the mol% NaAMBA incorporated into the copolymers. For example, BAVF-100 phase separates as the pH approaches 5.4 while BAVF-38 does not precipitate until the pH approaches 3.4. The phase separation may be explained by the fact that as the pH is lowered, more NaAMBA comonomer units will be progressively protonated and thus rendered nonionic. As this occurs, the polymer becomes more hydrophobic; at a critical pH value the polymer phase separates. This transition will be affected by changes in the aqueous media, such as ionic strength and temperature, as well as changes in the polymer composition and molecular weight. For example, BAVF-38 will

resolubilze at 11°C or lower, which is representative of a L.C.S.T. under these conditions (pH=3.0).

The phase behavior of the AAVF series is also dependent on polymer composition and temperature. AAVF-100 was not examined as the solution behavior of polyacrylic acid is well documented.¹ At 25°C, AAVF-82 precipitates as the pH approaches 2.3 while AAVF-62 precipitates as the pH approaches 2.7. AAVF-40 and AAVF-22 do not precipitate under these conditions. The effect of temperature on the phase stability of the AAVF copolymers was studied at pH=2. With the exception of AAVF-22, all copolymers exhibit an upper critical solution temperature (U.C.S.T.) in contrast to the BAVF copolymers. The upper critical solution temperatures for AAVF-82,-62,-40 are 38°C, 42°C, and, 19°C, respectively. When the samples are heated above their respective temperatures, the copolymer resolubilizes and one phase results. In contrast to the BAVF series which phase separates due to hydrophobic interactions, the hydrogen bonding interactions between the carboxylic acid and the formamide group in the AAVF series is likely responsible for phase separation. This behavior has been cited previously for copolymers of acrylic acid and acrylamide.¹⁶ The effects of sodium chloride and urea on the U.C.S.T. of AAVF-62 were also examined and the results are shown in Figure 16. The presence of sodium chloride, which slightly enhances water structure, increases the U.C.S.T. of AAVF-62. In contrast, urea, which disrupts water structure, decreases the U.C.S.T. of AAVF-62. This behavior is a result of solvent perturbation in the presence of the added cosolute which in turn affects the polymer-solvent interaction.

CONCLUSIONS

The solution behavior of copolymers of NVF with NaA, NaAMBA, and NaAMPS has been investigated as a function of pH, added electrolytes, and temperature. Polyelectrolyte behavior is observed for all three copolymer series. In deionized water, copolymers containing approximately 60 mol% of the anionic comonomer exhibit the highest viscosities. Furthermore, the closer the charged group is spatially located to the polymer backbone, the higher the viscosity. The nature of the anionic species of the comonomer also affects the solution behavior as evidenced by the enhanced viscosity of the BAVF series versus the PSVF series at pH 8.5. The addition of electrolytes to all three copolymer series causes a marked reduction in viscosity due to shielding effects. Urea also induces a reduction in the hydrodynamic volume of the copolymers. The PSVF series is stable in the presence of calcium chloride and with changes in pH of the aqueous media due to the weak basicity of the sulfonate group. For the BAVF series, copolymers containing 75 mol% or more of NaAMBA phase separate in the presence of calcium chloride at elevated temperatures. In addition, BAVF copolymers containing 38 mol% or more of NaAMBA phase separate at a critical pH value,

dependent on the amount of NaAMBA incorporated into the copolymer. AAVF copolymers also phase separate in the presence of calcium chloride and at lower pH values dependent on the mol% of NaA in the copolymer. At pH 2, AAVF copolymers exhibit a U.C.S.T which is influenced by added cosolutes.

References

- 1) Molyneux, P. *Water-Soluble Synthetic Polymers: Properties and Behavior, Vol. II*; CRC Press: Boca Raton, FL., 1984.
- 2) McCormick, C. L.; Bock, J.; Schulz, D. in *Encyclopedia of Polymer Science and Engineering*, Vol. 17; Wiley PressL New York, 1989; p730.
- 3) Bekturov, E. A.; Bakauova, Z. Bh., *Synthetic Water-Soluble Polymers in Solution*; Huethig and Wepf Press: New York, 1986.
- 4) Ikegami, A.; Imai, N. *J. Polym. Sci.* **1962**, *56*, 133.
- 5) Schwartz, T.; Francois, J. *Makromol. Chem.* **1981**, *182*, 2775.
- 6) Truong, D. N.; Galin, J. C.; Francois, J.; Pham, Q. T. *Polym. Comm.* **1984**, *25*, 208.
- 7) McCormick, C. L.; Blackmon, K. P.; Elliot, D. L. *J. Polym. Sci., Polym. Chem. Edn.* **1986**, *24*, 2619.
- 8) McCormick, C. L.; Salazar, L. C. *J. Macro. Sci., Pure Appl. Chem.* **1992**, *A29(3)*, 193.
- 9) Neidlinger, H. H.; Chen, G. G.; McCormick, C. L. *J. Appl. Polym. Sci.* **1984**, *29*, 713.
- 10) Chen, G. S. *PhD. Dissertation*, University of Southern Mississippi, May 1986.
- 11) Newman, J. K.; McCormick, C. L. *Macromolecules* **1994**, *27*, 5114 .
- 12) McCormick, C. L.; Elliot, D. L. *Macromolecules* **1986**, *19*, 542.
- 13) Kulicke, K. M.; Horl, H. H. *Colloid and Polym. Sci.* **1985**, *263*, 530
- 14) Klein, J.; Heitzmann, R. *Makromol. Chem.* **1978**, *179*, 1895.
- 15) Smets, G. *Makromol. Chem.*, **1959**, *29*, 190.
- 16) Klenna, O. V.; Lebedeva, L. G. *J. Polym. Sci. (U.S.S.R.)* **1983**, *25*, 2380.
- 17) Kathmann, E. E.; White, L. A.; McCormick, C. L. *previous paper in the series.*

CHAPTER 4. pH and Electrolyte Responsive Copolymers of Acrylamide and the Zwitterionic Monomer 4-(2-Acrylamido-2-Methyl propyldimethylammonio) Butanoate: Synthesis and Solution Behavior

SYNOPSIS.

A novel carboxybetaine monomer, 4-(2-acrylamido-2-methylpropyl-dimethyl ammonio) butanoate (AMPDAB), has been synthesized and copolymerized with acrylamide in an aqueous NaBr solution. The feed ratio of AM (M_1):AMPDAB(M_2) was varied from 90:10 to 0:100 mol %. Low conversion samples were collected and copolymer compositions were determined with ^{13}C NMR by integration of the carbonyl resonances. Reactivity ratios were determined and the nonlinear least-squares method yielded values of $r_1=1.01$ and $r_2=0.99$, indicating random incorporation of monomers into the final copolymer. Molecular weights were determined and range from 3.9 to 12.0×10^6 g/mol. The solution behavior of the above copolymers was studied as a function of pH and added electrolytes. With the exception of the copolymers containing 60 and 75 mol% AMPDAB, homogeneous solutions were obtained in deionized water. At high pH, the polyzwitterions show an enhancement in viscosity as the concentration of added electrolyte is increased. In deionized water, as the pH of the aqueous media is lowered, the copolymers exhibit a dramatic increase in viscosity as the carboxylate groups are protonated and charge-charge repulsions of the quaternary ammonium groups induce polyelectrolyte behavior. The solution behavior is compared to structurally similar sulfobetaines which do not exhibit any responsiveness to changes in pH.

INTRODUCTION

The synthesis of electrolyte-tolerant, water-soluble polymers that contain ionic pendant groups has been the goal of academic and industrial laboratories for the past several years. Such polymers have applications in water treatment, remediation, drag reduction, petroleum recovery, viscosification, formulation of coatings, cosmetics, and pharmaceuticals. In striving to synthesize polymers that show tolerance in the presence of added electrolytes, we have recently focused our attention on polyampholytes, polymers which possess both cationic and anionic pendant groups.¹⁻⁶ The ionic groups may be located on separate monomer units or may be incorporated into one zwitterionic monomer. Polyampholytes can exhibit enhancements in viscosity and solubility in the presence of added electrolytes due to shielding of columbic attractions.⁷⁻¹⁴ This behavior renders these systems useful in areas which require performance in the presence of additives such as electrolytes and surfactants.

Previous work in our laboratories dealt with the synthesis and characterization of copolymers of acrylamide and the sulfopropylbetaine monomer, 3-(2-acrylamido-2-methylpropanedimethylammonio)-1-propanesulfonate (AMPDAPS).⁴ The solution behavior was dependent on the amount of AMPDAPS incorporated into the copolymers. When 25 mol% or less of AMPDAPS was incorporated, the copolymers were soluble in deionized water and displayed a tendency to intermolecularly associate. Peiffer and Lundberg reported the tendency

for intermolecular associations of other low-charge density polyampholytes.¹⁵ Higher incorporation of AMPDAPS (≥ 60 mol%) led to water insoluble copolymers that required the addition of a critical amount of electrolyte to achieve solubility in aqueous solution. This behavior is typical of poly(vinylsulfobetaines) and has been observed in numerous studies.¹⁶⁻¹⁸

Another class of zwitterionic polymers are poly(vinylcarboxybetaines) in which the anionic group is a carboxylate functionality. The carboxylate moiety can be protonated at low pH values, allowing behavior as polycations or polyampholytes depending on the pH of the aqueous medium. Ladenheim and Morawetz¹⁹ synthesized the first poly(vinylcarboxybetaines) by reacting poly(4-vinylpyridine) with ethylbromoacetate followed by hydrolysis of the ester functionality. Topchiev et al.²⁰ reported the polymerization of a carboxybetaine monomer and solution behavior of the resulting homopolymer. Polymerization rates and viscosity studies were dependent on the pH of the aqueous medium. More recently, Wielema et al.²¹ reported the synthesis of several monomeric carboxybetaines with varying alkyl groups between charged centers. By adjusting the pH, polyelectrolyte or polyampholyte behavior was observed depending on the degree of ionization of the carboxylate functionality.

In this paper we report the synthesis and characterization of a series of copolymers of acrylamide with a novel carboxybetaine monomer. The purpose of the present work is to study the compositional effects of carboxybetaine comonomer incorporation on the properties of the resulting copolymers. In particular, the viscosity responsiveness of the copolymers has been studied as a function of pH and added electrolytes. The results are compared to the behavior of structurally similar poly(vinylsulfobetaines) and interpreted in terms of the differing anionic pendent groups in the respective copolymers.

EXPERIMENTAL SECTION

Materials

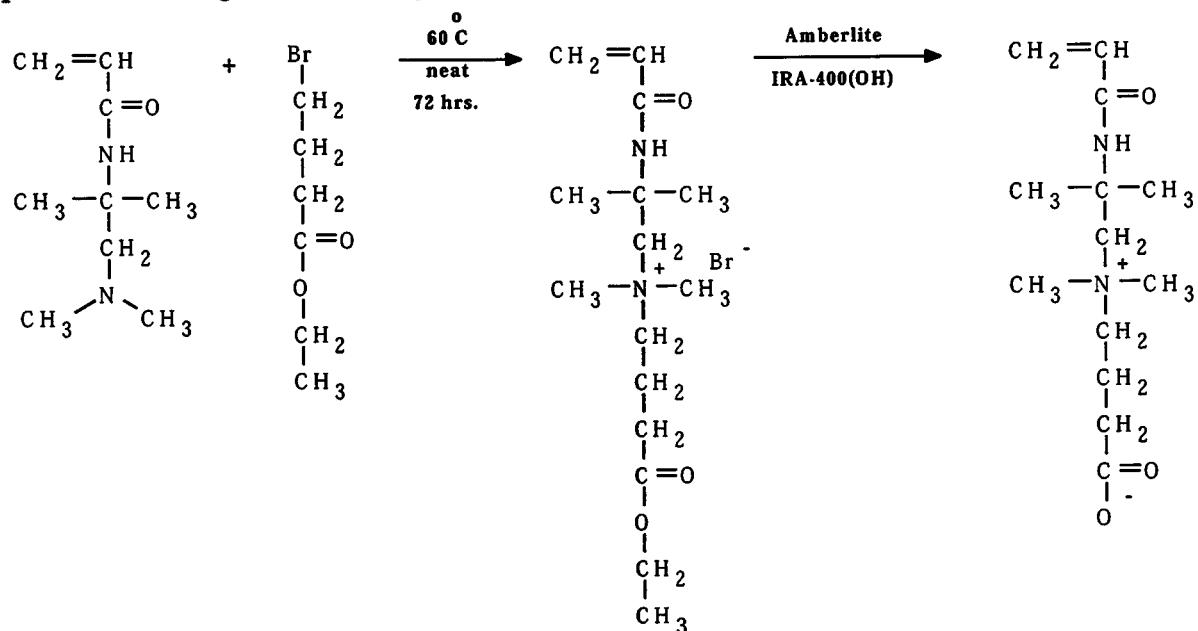
Acrylamide (AM) from Aldrich was recrystallized twice from acetone and vacuum dried at room temperature. Potassium persulfate from J. T. Baker was recrystallized twice from deionized water.

Monomer Synthesis

(4-carboxypropyl)2-acrylamido-2-methylpropanedimethylammonium bromide (Scheme 1)

The synthesis of (4-carboxypropyl)-2-acrylamido-2-methylpropanedimethyl ammonium bromide (AMPDAB) involved a similar procedure employed by Laughlin and others to synthesis various carboxybetaine surfactants²²⁻²⁴ a multistep procedure. 2-Acrylamido-2-methylpropanedimethyl-amine, AMPDA,^{25,26} (0.5 mol) was dissolved in ethyl 4-bromobutyrate (0.55 mol) and the reaction allowed to proceed for 72 hours at 60°C. The solid that formed was then dissolved in methanol

and precipitated in diethyl ether. The precipitate was filtered, thoroughly dried, and recrystallized from 2-propanol. Following recrystallization, the product was dissolved in water and passed over Amberlite IRA-400(OH) ion-exchange resin. The water was removed under reduced pressure at 50°C to yield the zwitterionic product as an oil. The product was dissolved in water, chilled on an ice bath, and one equivalent of HBr. The water was once again removed under reduced pressure at 50°C to yield the cationic monomer. The product was subsequently recrystallized in ethanol, dissolved in methanol, and precipitated into diethyl ether to yield pure AMPDAB (yield 70-80%). M.p. 185-187°C (dec). Analysis for C₁₁H₂₁N₂O₃Br: Calculated- C, 46.4%; H, 7.4%; N, 8.3%. Found- C, 47.5%; H, 7.3%; N, 8.3%. F.T.I.R. (KBr pellet) acid O-H, 3600-2600 cm⁻¹; aliphatic C-H, 2970 cm⁻¹; acid C=O, 1732 cm⁻¹; amide C=O, 1653 cm⁻¹ and 1556 cm⁻¹; acid C-O, 1259 cm⁻¹. ¹³C NMR (D₂O with 3-(trimethylsilyl)-1-propane-sulfonic acid, sodium salt (DSS) as the reference): 20.03, 29.47, 32.36, 54.33, 56.04, 68.06, 69.31, 130.37, 132.53, 170.45, and 177.96 ppm. Peak assignments are given in Figure 1.



Scheme 1. Synthetic pathway for the preparation of 4-(2-Acrylamido-2-Methylpropyldimethylammonio) Butanoate (AMPDAB).

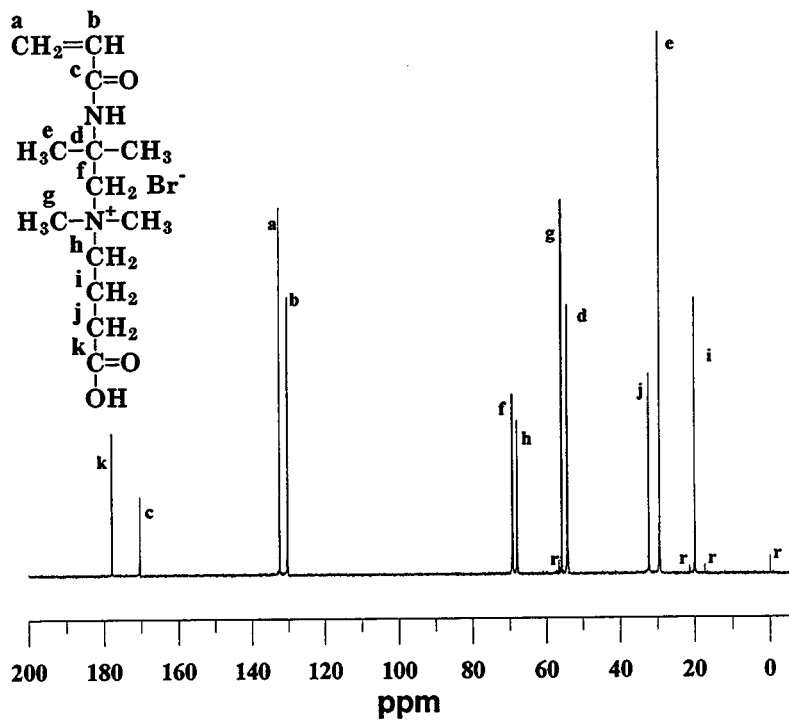


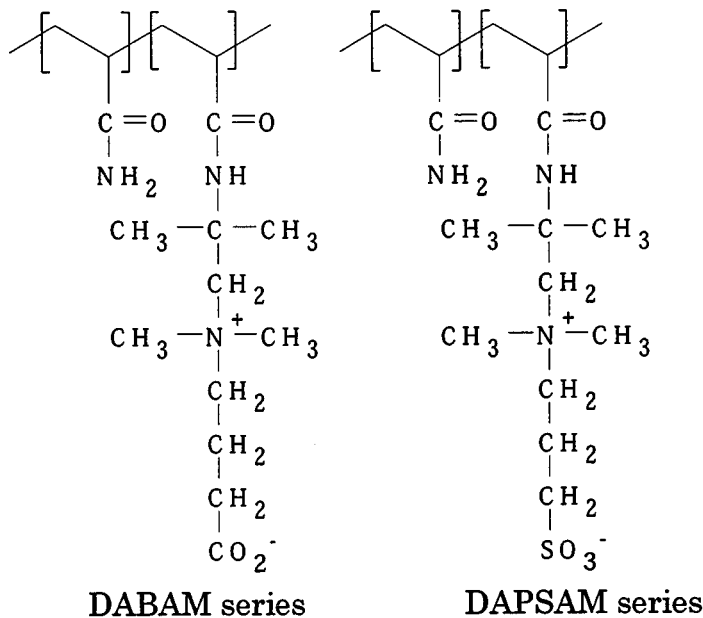
Figure 1. ^{13}C NMR of 4-(2-Acrylamido-2-methylpropyl)dimethylammonium butanoate (AMPDAB).

Synthesis of Copolymers of 4-(2-acrylamido-2-methylpropane dimethylammonio)butanoate with Acrylamide (Scheme 2)

The homopolymer of AMPDAB and the copolymers of AMPDAB with AM (the DABAM series) were synthesized by free radical polymerization in a 0.5M aqueous NaBr solution under nitrogen at 30°C using 0.1 mol % potassium persulfate as the initiator. The feed ratio of AM:AMPDAB was varied from 90:10 to 25:75 mol % with the total monomer concentration held constant at 0.45M. 0.5M NaBr in the reaction medium was used as a precaution to insure that polymers with high AMPDAB content remained homogeneous during polymerization.

In a typical synthesis, specified quantities of each monomer were dissolved in small volumes of deionized water. The separate solutions were then combined and one equivalent of sodium hydroxide per equivalent of AMPDAB was added and the pH adjusted to 8. The necessary quantity of NaBr was added to achieve a 0.5M NaBr solution. The reaction mixture was then sparged with nitrogen and initiated with 0.1 mol % potassium persulfate. A low conversion sample was acquired for reactivity ratio studies. The reaction was terminated around 50% conversion due to the high viscosity of the reaction medium and as a precaution against copolymer drift. The polymers were precipitated in acetone, redissolved in deionized water,

then dialyzed using Spectra/Por 4 dialysis bags with molecular weight cutoffs of 12,000 to 14,000 g/mol.



Scheme 2. Structural composition of copolymers of acrylamide with 4-(2-Acrylamido-2-Methylpropylidimethylammonio) Butanoate (the DABAM series) and with 3-(2-Acrylamido-2-Methylpropylidimethylammonio) Propanesulfonate (the DAPSAM series)

Synthesis of the Copolymer of 3-(2-acrylamido-2-methylpropanedimethylammonio)-1-propanesulfonate with Acrylamide (Scheme 2)

The polymerization procedure for DAPSAM-25 was conducted 0.5M NaCl in a similar manner as previously reported.⁴

Copolymer Characterization

¹³C NMR spectra of the copolymers were obtained at 50.3 MHz on a Bruker AC200 spectrometer using 15-20 wt % aqueous (D₂O) polymer solutions with DSS as a reference. A recycle delay of 8 s, 90° pulse length, and gated decoupling to remove all NOE were used for quantitative spectral analysis. Molecular weight studies were performed on a Chromatix KMX-6 low angle laser light scattering instrument. Refractive index increments were obtained using a Chromatix KMX-16 laser differential refractometer.

Viscosity Measurements

Polymer solutions were made by dissolving designated amounts of polymer in the stock electrolyte solutions. The solutions were then isoionically diluted to appropriate concentrations and allowed to age for seven to ten days before being analyzed with a Contraves LS-30 rheometer. Duplicate runs were conducted and reproducibility found to be within \pm 3-7% dependent on the magnitude of the viscosity values. Intrinsic viscosities were evaluated using the Huggins equation.

RESULTS AND DISCUSSION

Monomer Synthesis

The novel carboxybetaine monomer, AMPDAB, was synthesized utilizing a method commonly used to prepare small molecule surfactants with carboxybetaine head groups. The advantages of the method versus typical base hydrolysis procedures (using alkali hydroxides) are the relatively mild conditions and the absence of inorganic electrolyte by-products which, due to the limited solubility of zwitterions in organic solvents, may be difficult to remove. In brief, the synthesis involves quaternization of the monomeric tertiary amine by the reaction with ethyl 4-bromobutyrate. The bromide ion affiliated with cationic product is replaced by the hydroxide ion after percolation through an anionic exchange resin of the hydroxide form (OH^-). The associated hydroxide ion promotes hydrolysis of the ester functionality with ethanol as the by-product to yield the zwitterionic product. Due to the hygroscopic nature of the product, however, the monomer had to be isolated as a bromide salt by addition of one equivalent of HBr. A ^{13}C NMR spectrum of the monomer is shown in Figure 1.

Compositional and Reactivity Ratio analysis

Based on previous studies, the number and distribution of charged groups incorporated into polyampholytes dictates the solution behavior of the resulting polymers^{4,12}. Inter- and incorporated into polyampholytes dictate the solution behavior of the resulting polymers. Inter- and intramolecular associations as well as solubility have been shown to be directly related to the charge density of the systems^{4,15}. To investigate this issue for the novel poly(vinylcarboxybetaines) of this study, a series of copolymers was synthesized and reactivity ratios determined. The compositions of low conversion copolymer samples were determined by integration of the carbonyl peaks observed by ^{13}C NMR spectroscopy (Table I). Reactivity ratios for the AM(M1) / AMPDAB(M2) comonomer pair were determined by the methods of Fineman-Ross,²⁷ Kelen-Tudos,²⁸ and nonlinear least squares (NLS).²⁹ The Fineman-Ross method yielded values of $r_1=0.88$ and $r_2=0.92$, the Kelen-Tudos method yielded values of $r_1=0.88$ and $r_2=0.93$, and the NLS method yielded values of $r_1=1.01$ and $r_2=0.99$. The experimentally determined copolymer composition as a function of feed composition is shown in Figure 2, the dashed line represents ideal random incorporation. The random incorporation is in agreement with that previously observed by our group for a similar zwitterionic monomer.⁴

Table I. Reaction Parameters for the Copolymerization of Acrylamide (M_1) with 4-(2-Acrylamido-2-Methylpropylidemethylammonio) Butanoate(M_2)

Sample	Feed ratio (mol%) (AM : AMPDAB)	Rxn. Time (hrs.)	% Conv.	AMPDAB found ^a (mol %)
DABAM 10	90.0 : 10.0	2.0	7.3	11.2
DABAM 25	75.0 : 25.0	0.3	8	22.4
DABAM 40	60.0 : 40.0	0.3	14	40.7
DABAM 60	40.0 : 60.0	0.3	12	61.1
DABAM 75	25.0 : 75.0	0.4	13	73.3
DABAM 100	0.0 : 100.0	-----	-----	100.0 ^b

^a Determined from ^{13}C NMR

^b Theoretical Value

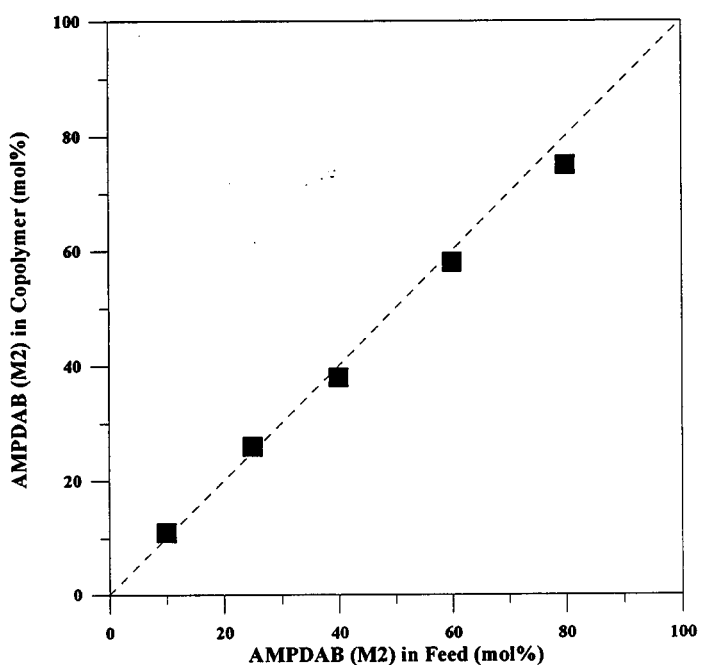


Figure 2. Mole percent AMPDAB incorporated into the copolymers as a function of comonomer composition in the feed.

The methods of Igarashi³⁰ were employed to determine the microstructural composition and are presented in Table II. Similar values for all three categories (blockiness, alternation, and, mean sequence length) are observed for DABAM-25 and -75 as well as DABAM-40 and -60. For example, DABAM-40 has a mean sequence length of 2.4 for M₁ and 1.59 for M₂ while DABAM-60 has a mean sequence length of 1.62 for M₁ and 2.33 for M₂. Again, these values are consistent with a random microstructure.

Table II. Structural Data for the Copolymers of Acrylamide (M1) with 4-(2-Acrylamido-2-Methylpropylidemethylammonio) Butanoate (M2)

Sample Number	M1 in Copolymer (mol %)	Blockiness		Alternation Mole % M1-M2	Mean Seq. Length	
		Mole % M1-M1	M2-M2		M1	M2
DABAM 10	88.8	78.68	1.08	20.24	9.39	1.10
DABAM 25	77.6	59.67	4.47	35.07	3.80	1.30
DABAM 40	59.3	34.07	15.47	50.46	2.40	1.59
DABAM 60	38.9	14.07	36.27	49.65	1.62	2.33
DABAM 75	26.7	6.42	53.02	40.55	1.31	3.66

Low angle laser light scattering. Table III shows the weight-average molecular weights determined by classical low-angle laser light scattering at 25°C in 1M NaCl. The molecular weights for the DABAM series vary from 3.9 to 12.0 x 10⁶g mol⁻¹. The values decrease as more AMPDAB is incorporated into the copolymer feed. Also shown in Table 2 is DAPSAM-25. This copolymer possesses a sulfonate group instead of a carboxylate group as the anionic moiety. Both DABAM-25 and DAPSAM-25 have similar molecular weights allowing meaningful comparisons and assessments of the effects of the anionic moiety on the solution behavior of polyzwitterions.

Table III. Classical Light Scattering Data for the Copolymers of Acrylamide (M_1) with 4-(2-Acrylamido-2-Methylpropylidemethylammonio) Butanoate(M_2)

Sample	AMPDAB Found ^a (mol %)	$M_W \times 10^{-6}$ (g / mol)	$A_2 \times 10^4$ (ml \cdot mol/g 2)	$DP \times 10^{-4}$
DABAM 10	11.2	12.0	6.0	13.4
DABAM 25	22.4	10.2	0.8	8.7
DABAM 40	40.7	9.8	0.6	6.7
DABAM 100	100 ^b	3.9	0.8	1.5
DAPSAM 25	25.8 ^c	12.4	0.6	9.8

^a Determined from ^{13}C NMR

^b Theoretical Value

^c mol % AMPDAPS found

The second virial coefficients (A_2) for the DABAM series have been determined and are also presented in Table 2. With the exception of DABAM-10, all of the copolymers have A_2 values below 1×10^4 ml \cdot mol/g 2 in 1M NaCl. This behavior is representative of polyampholytic systems which normally have low A_2 values under these conditions.

Solution Behavior

Copolymer Composition and Solubility

The carboxybetaine monomer, AMPDAB, was copolymerized with AM in varying molar ratios to yield polyampholytic systems. These polymers behave as a polyelectrolytes or a polyampholytes depending on the pH of the solution due to the presence of the carboxylate functionality incorporated into the AMPDAB mer unit. The presence of the carboxylate functionality, however, induces complex solution behavior as discussed below. The viscosity behavior of the above copolymers was studied with a Contraves LS-30 rheometer as a function of pH and added electrolytes at 25°C and a shear rate of 6 sec $^{-1}$.

The solubility of the DABAM series is a function of the amount of AMPDAB incorporated into the copolymer. The numbers appended to DABAM in the following discussions indicate the mole percent of AMPDAB present in the copolymer feed and therefore representative of the mol% incorporated into the copolymer. DABAM- 10, -25, and -40 are readily solubilized in deionized water and salt solutions at all pH values studied. DABAM-60 and DABAM-75, however, are

not completely soluble over the pH range (1-13). The copolymer stock solutions (0.3 g/dL) are optically clear solutions but visibly heterogeneous as noted by the presence of a number of small, microgel-like particles suspended in solution. The solutions are viscous, however, indicating complete dissolution of most of the sample. Furthermore, aggregates remain even when diluted to 0.01g/dL. The addition of NaCl, NaSCN, and, CsCl, or known protein denaturants (urea and guanidine hydrochloride) over a wide range of concentrations (0-3M) fail to disperse the microgel particles. This implies some other mechanism for intermolecular aggregation other than electrostatic interactions. Polyzwitterions previously studied in our labs, based on sulfobetaine comonomers (DAPSAM series), did not display this behavior and were molecularly dissolved in the presence of added electrolytes⁴. Interestingly, DABAM-100 is soluble in deionized water at all pH values investigated (pH 1-13). This suggests the incomplete solubility of DABAM-60 and -75 is due to the presence of the acrylamide comonomer. Whether this is a molecular weight effect or a conformational effect is not currently resolved and is under investigation.

The apparent viscosities of the copolymers in deionized water at pH=7.5 are shown in Figure 3. Due to obvious microheterogeneity, the viscosities for DABAM-60 and -75 were determined at least five times and found to be consistent to within \pm 7% of the reported values. DABAM-60 and DABAM-75 display higher viscosities than DABAM-25 and DABAM 40. This is probably a result of the more aggregative nature of the copolymers containing a higher incorporation of AMPDAB as previously discussed. Molecular weights could not be determined for DABAM-60 and -75.

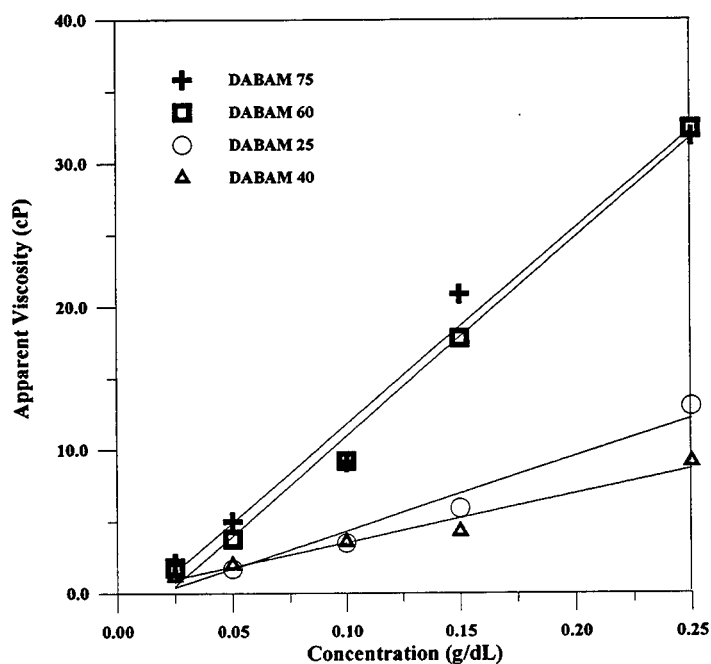


Figure 3. Apparent viscosity of DABAM copolymers at pH 7.5 as a function of copolymer concentration.

Effects of Added Electrolytes

Intrinsic viscosities were determined for DABAM-10, -25, -40, and -100, as well as DAPSAM-25, in varying ionic strengths of NaCl at pH 8 (Figure 4). At this pH, essentially all of the AMPDAB mer units are zwitterionic. The copolymers of DABAM-10, DABAM-25, and DABAM-40 display complex solution behavior. At low concentrations of NaCl, there is an initial decrease in the intrinsic viscosity likely due to the elimination of intermolecular interactions with the increasing ionic strength. This behavior has been observed previously for other low charge density polyampholytic systems.^{4,15,19,31} Upon addition of a critical concentration of NaCl, the polymers display polyampholytic behavior as evidenced by an increase in intrinsic viscosity as intramolecular attractions are reduced. DABAM-100 exhibits an increase in intrinsic viscosity as the ionic strength increases, indicating the shielding of intramolecular coulombic attractions. As mentioned earlier, DABAM-100 is soluble in deionized water in contrast to the sulfobetaine homopolymer previously studied in our group, DAPSAM-100, which requires the addition of a critical concentration of NaCl for dissolution. The only structural difference in these two polymers is the nature of the anionic group; DABAM-100 possesses a carboxylate functionality while DAPSAM-100 possesses a sulfonate functionality. The differences in solubility are likely due to the more hydrophilic nature of the carboxylate functional group as compared to the sulfonate group. This behavior has been observed for small molecule zwitterionic surfactants.^{23,24,32} The more hydrated the carboxylate moiety is, the weaker the attraction with neighboring ammonium groups, and therefore an enhancement in solvation for the polymer coil. Another interesting feature is that DABAM-25 exhibits a much higher intrinsic viscosity than DAPSAM-25, even though the two copolymers have similar molecular weights and A_2 values.

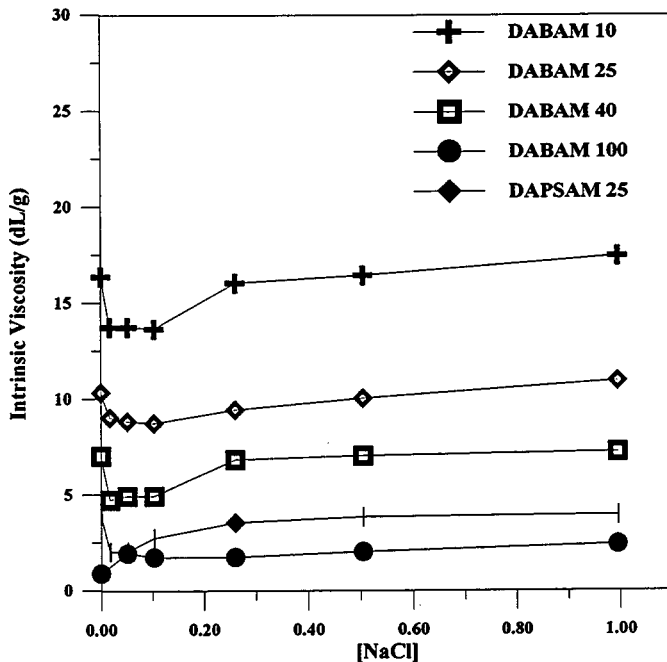


Figure 4. Intrinsic viscosity of DABAM copolymers as a function of NaCl concentration.

The reduced viscosities were also examined as a function of increasing electrolyte concentration of various salts. Figure 5 displays the results of this study for DABAM-25 and DAPSAM-25. Both copolymers show an enhancement in viscosity as the concentration of electrolyte is increased in accord with polyampholytic behavior. In addition, the aqueous solutions which have soft counterions (Cs^+ and SCN^-) yield higher viscosity values than those which possess relatively hard counterions (Na^+ and Cl^-). This behavior is in accord with the Hoffmeister effect³³ and has been observed for other polyzwitterionic systems.¹⁶⁻¹⁸ Salamone et al. have proposed that this effect is a result of specific counterion condensation.¹⁷ Other effects, such as the influence the added ions have on water structure, should also be considered.

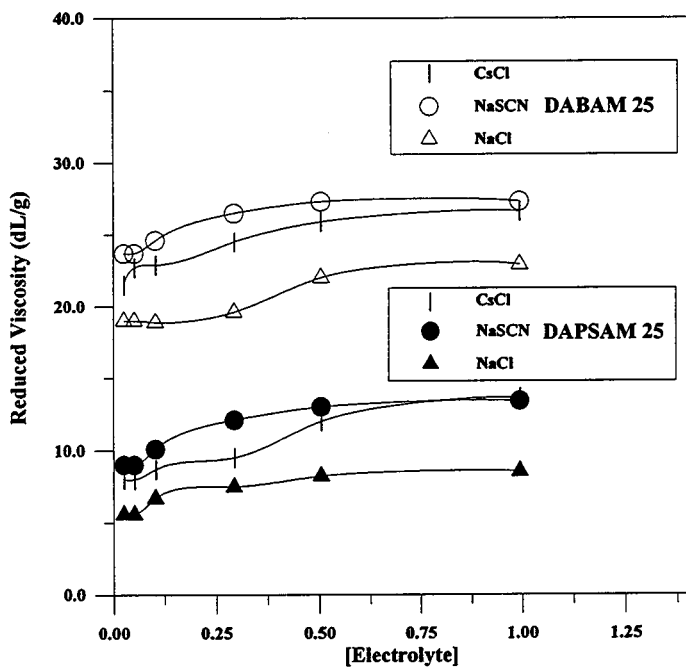


Figure 5. Reduced viscosity as a function of increasing ionic strength of various salts. (Polymer concentration of 0.1 g/dL)

Effects of pH

Figure 6 shows the effects of increasing polymer concentration on the apparent viscosity of DABAM-25 and -40 at pH 3 and pH 7.5. At low pH, the carboxylate group incorporated in the AMPDAB mer unit is protonated and the polymer acquires an overall positive charge due to the remaining ammonium group. The polycationic nature of the copolymer induces a larger hydrodynamic volume since charge-charge repulsions result in an extended conformation. As the pH is raised the carboxylic acid is ionized and the coulombic repulsions essentially become coulombic attractions. These attractions lead to a restricted conformation and much smaller hydrodynamic volumes as evidenced by the lower viscosity values. The effect of copolymer composition on the apparent viscosity at pH 3 is presented in Figure 7. The maximum viscosity occurs when approximately 20-30 mol% AMPDAB is incorporated into the copolymer and is likely the result of molecular weight differences as well as charge density effects.

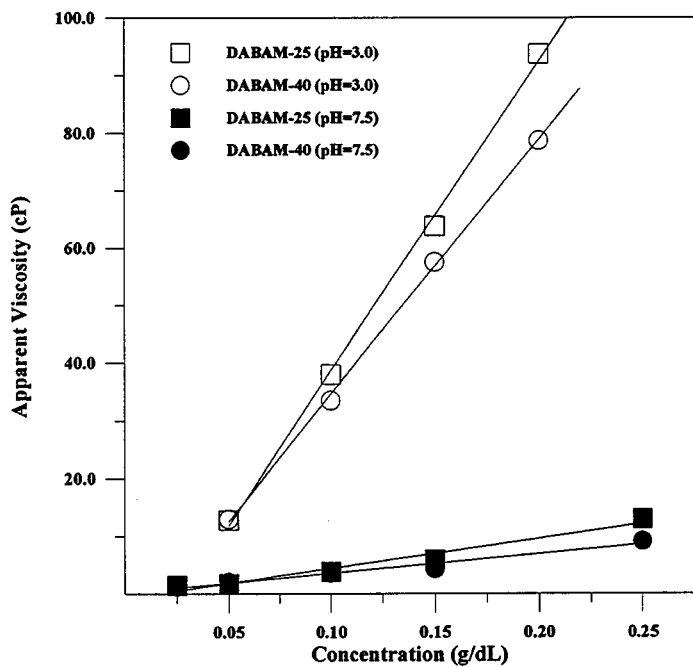


Figure 6. Apparent viscosities of DABAM copolymers at pH 3 and pH 7.5 as a function of copolymer concentration.

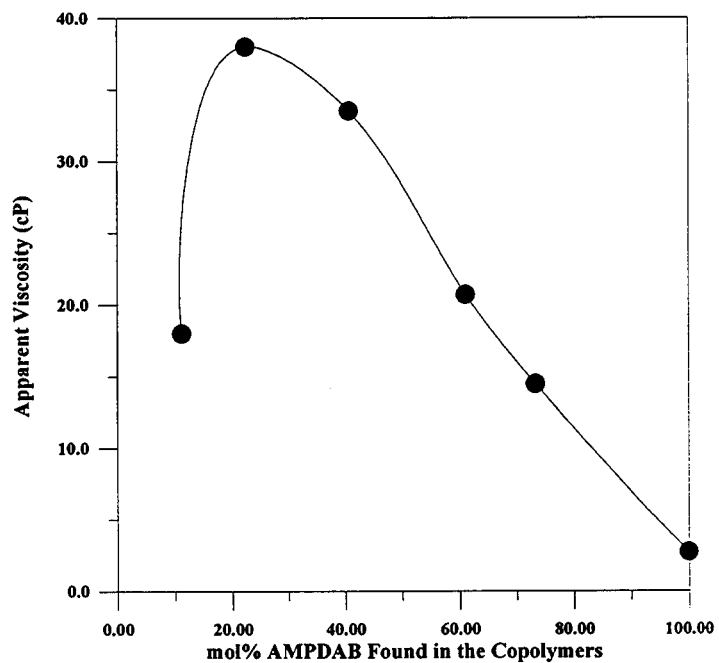


Figure 7. Apparent viscosities of DABAM copolymers as a function of the mol% AMPDAB found in the copolymers. (Determined at pH 3 and a polymer concentration of 0.1 g/dL)

The effects of added electrolytes on the solution behavior of the DABAM copolymers at pH 3 are shown in Figure 8. As anticipated, there is a decrease in viscosity as the concentration of NaCl increases as charge-charge repulsions are shielded and the polymer coil contracts. Linear dependency of the reduced viscosity on the inverse square root of ionic strength is typical behavior for polyelectrolytes.³⁴ Furthermore, the magnitude of the slope gives an indication of the degree of conformational change induced by the addition of electrolytes. From Figure 8, DABAM-25 exhibits the smallest slope while DABAM-75 has the highest slope. This behavior is, in part, due to enhanced hydrophobicity of the AMPDAB mer unit at low pH due to the conversion of the carboxylate group to the carboxylic acid group. Thus, through the addition of NaCl, not only are charge-charge repulsions shielded but also hydrophobic interactions are enhanced as water structuring events lead to a 'salting-out' effect. As more AMPDAB is incorporated into the copolymers, this effect is magnified.

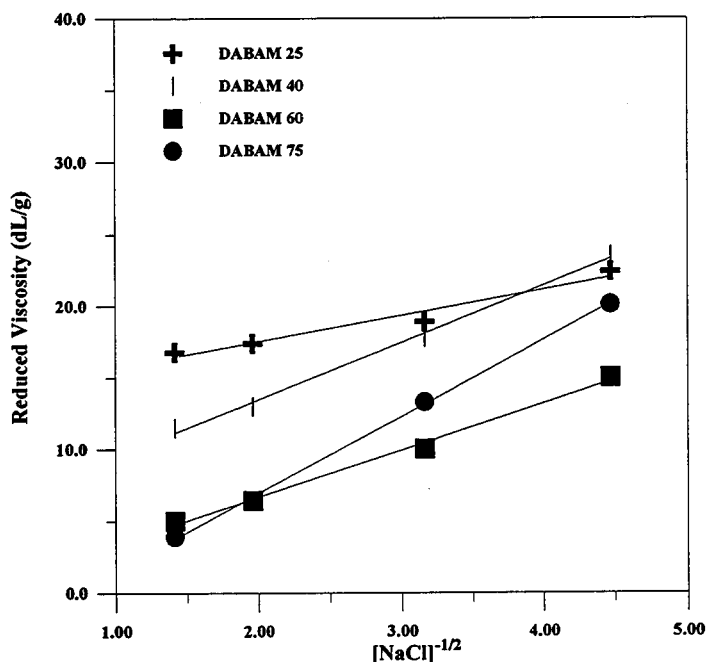


Figure 8. Reduced Viscosity of DABAM copolymers as a function of the inverse square root of ionic strength. (Determined at pH 3 and a polymer concentration of 0.1 g/dL)

The apparent viscosity as a function of decreasing pH was also examined for copolymers with different anionic substituents (Figure 9). DABAM-25, which incorporates the carboxylate functionality, exhibits a magnitude of order increase in the apparent viscosity as the pH is lowered from 8 to 3. DAPSAM-25 which

contains the sulfonate functionality is relatively insensitive to changes in the pH of the aqueous solution. The dramatic pH responsiveness of the carboxybetaine mer units is in direct contrast with that of the sulfobetaine mer units. The sulfonate group is a much weaker base than the carboxylate group and cannot be protonated at pH values which will not degrade the polymer backbone. Thus, the AMPDAPS mer units of DAPSAM-25 remain in the zwitterionic state throughout the useful pH range. In contrast, DABAM-25, which contains carboxylate groups, may be converted from the zwitterionic to the cationic state by lowering of pH. At pH values less than 3, a reduction in the apparent viscosity is observed for DABAM-25. This behavior probably results from a shielding of the cationic charges as the concentration of hydronium and chloride ions increases as the pH is lowered. The increase in hydrophobicity as more of the carboxylate groups are protonated is also partially responsible for loss of hydrodynamic volume in aqueous media.

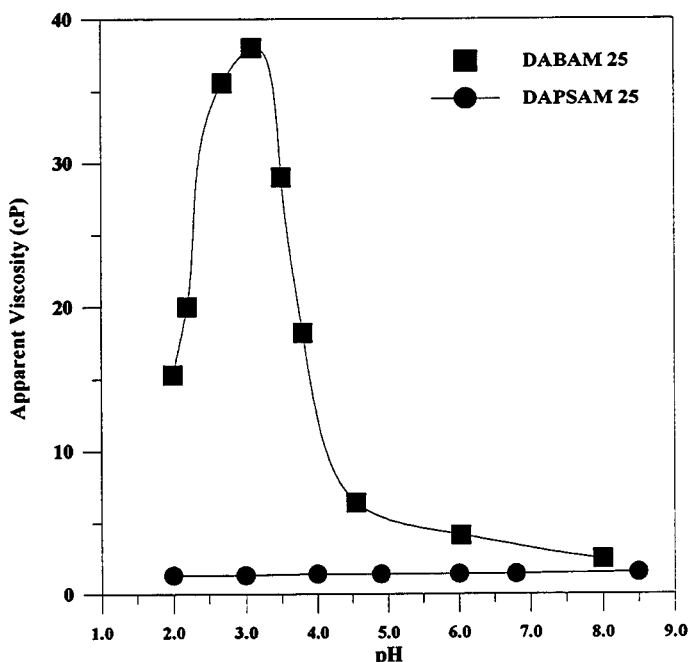


Figure 9. Apparent viscosities of DABAM and DAPSAM copolymers as a function of pH. (Polymer concentration of 0.1 g/dL)

CONCLUSIONS

A novel series of polyampholytes based on copolymers of acrylamide (AM) and 4-(2-Acrylamido-2-methylpropylidemethyl ammonio) butanoate (AMPDAB) has been synthesized by free radical polymerization in 0.5M NaBr. Reactivity ratios and copolymer microstructures were determined indicating random incorporation of the comonomers. Weight average molecular weights range from 3.9 to 12.0×10^6 gm/mol as determined by low angle laser light scattering. The copolymers exhibit complex

solubility and solution behavior due to hydrogen bonding, charge-charge interactions, molecular weight, and configurational effects. The copolymers at pH 3 display polyelectrolyte behavior due to the cationic nature of the polymer. At pH 8, the copolymers exhibit both intermolecular and intramolecular interactions depending on the amount of AMPDAB incorporated into the copolymer. The poly(vinyl carboxybetaines) are more soluble in deionized water than the analogous poly(vinyl sulfobetaines) as well as being more responsive to changes in the pH of the aqueous medium.

References

1. McCormick, C. L.; Johnson, C. B. *Macromolecules* **1988**, *21*, 687.
2. McCormick, C. L.; Johnson, C. B. *Macromolecules* **1988**, *21*, 694.
3. McCormick, C. L.; Salazar, L. C. *Polymer*, **1992**, *33*, 4384.
4. McCormick, C. L.; Salazar, L. C. *Polymer* **1992**, *33*, 4617.
5. McCormick, C. L.; Salazar, L. C. *Macromolecules* **1992**, *25*, 1896.
6. McCormick, C. L.; Salazar, L. C. *J. Appl. Poly. Sci.* **1993**, *48*, 1115.
7. Salamone, J. C.; Volksen, W.; Israel, S. C.; Olson, A. P.; Raia, D. C.; *Polymer* **1977**, *18*, 1058.
8. Monroy Soto, V. M.; Galin, J. C. *Polymer* **1984**, *25*, 121.
9. Monroy Soto, V. M.; Galin, J. C. *Polymer* **1984**, *25*, 254.
10. Higgs, P. G. and Joanny, J. F., *J. Chem. Phys.* **1991**, *94*, 1543.
11. Schulz, D. N.; Peiffer, P. K.; Agarwal, J.; Larabee, J.; Kaladas, J. J.; Soni, L.; Handwerker, B.; Garner, R. T. *Polymer* **1986**, *27*, 1734.
12. Salamone, J. C.; Quach, L.; Watterson, A. C.; Krauser, S.; and Mahmud M. U. *J. Macromol. Sci., Part A* **1985**, *22*, 653.
13. Corpart, J.; Candau, F. *Macromolecules* **1993**, *26*, 1333.
14. Skouri, M.; Munch, J. P.; Candau, S. J.; Neyret, S.; Candau, F. *Macromolecules* **1994**, *27*, 69.
15. Peiffer, D. G.; Lundberg, R. D. *Polymer* **1985**, *26*, 1058.
16. Liaw, D. J.; Lee, W. F.; Whung, Y. C.; Lin, M. C. *J. Appl. Polym. Sci.* **1987**, *37*, 999.
17. Salamone, J. C.; Volksen, W.; Israel, S. C.; Olson, A. P. *Polymer*, **1978**, *19*, 1157.
18. Schulz, D. N.; Kitano, K.; Dannik, J. A.; Kaladas, J. J. *Polym. Mater. Sci. Eng.* **1987**, *147*, 149.
19. Ladenheim, H.; Morawetz, H. *J. Polym. Sci.*, **1957**, *26*(113), 251.
20. Topichiev, D. A.; Mkrtchyan, R. A.; Simonyan, R. A.; Kabanov, V. A. *Polym. Sci., U.S.S.R. (Eng. Transl.)* **1977**, *A19*, 580.
21. Wielma, T., *PhD Dissertation*, University of Groningen, 1989.
22. Laughlin, R.G. *U.S. Patent 4,287,174*, **1981**.
23. Chevalier, Y.; Storet, Y.; Pourchet, S.; LePerche, P. *Langmuir*, **1991**, *7*, 848.
24. Weers, J. G.; Rathman, J. F.; Axe, F. U.; Crichlow, C. A.; Foland, L.D.; Scheuing, D. R.; Wiersema, R.J.; Zielske, A. G. *Langmuir*, **1991**, *7*, 854.

25. McCormick, C.L.;Salazar, L.C *J. Polym. Sci., Part A* **1993**, *31*, 1099.
26. McCormick, C.L.;Blackmon, K.P. *Polymer*, **1986**, *27*, 1971.
27. Fineman, M.; Ross, S. *J. Polym. Sci.*, **1950**, *5*, 259.
28. Kelen, T.; Tudos, F. *J. Macromol. Sci., Chem.*, **1975**, *A9*, 1.
29. Tidwell, P. W.; Mortimer, G. A. *J.Polym. Sci.:Part A*, **1965**, *3*, 369.
30. Igarashi, S. *J. Polym. Sci., Polym. Lett. Ed.*, **1963**, *1*, 359.
31. Salamone, J. C.; Ahmed, I.; Rodriguez, E. L.; Quach, L.; Watterson, A. C. *J. Macromol. Sci. Chem., Part A* **1988**, *25*, 811.
32. Laughlin, R.G. In *Advances in Liquid Crystals*; Brown G.H.,Ed.; Academic Press: New York, **1978**; Vol. 3, p41 and p99.
33. Collins, K.D.; Washabaugh, M. W. *Quat. Rev. of Biophys.*, **1985**, *18*(4), 323.
34. Molyneux, P. *Water-Soluble Synthetic Polymers: Properties and Behavior*, Vol. *II*; CRC Press: Boca Raton, FL., 1984.

CHAPTER 5. Effects of methylene *versus* propylene spacers in the pH and electrolyte responsiveness of zwitterionic copolymers incorporating carboxybetaine monomers

SYNOPSIS

Water-soluble polyzwitterions have been synthesized by free radical copolymerization of acrylamide with the novel carboxybetaine monomer, 2-(2-acrylamido-2-methylpropyl-dimethylammonio) ethanoate (AMPDAE). Feed ratios of 10 to 100 mol% AMPDAE were employed to give the polyzwitterion series, DAEAM. Copolymer compositions of low conversion samples were determined from ^{13}C n.m.r. by integration of the carbonyl resonances. Reactivity ratios were determined yielding an r_1r_2 value of 0.6. Molecular weights range from 6.3 to 10.4×10^6 g mol $^{-1}$ as determined by low angle laser light scattering. Dilute solution properties of the copolymers have been studied as a function of added electrolytes and pH. Intrinsic viscosity behavior in NaCl solutions is dependent on the mol% of AMPDAE incorporated into the copolymers. Reduced viscosities were also examined as a function of the nature of added electrolytes, displaying higher viscosity values in accord with the Hoffmeister lyotropic series. The copolymers exhibit an enhancement in viscosity as pH is lowered due to protonation of the carboxylate groups which renders the polymer coil cationic due to the presence of quaternary ammonium groups. The solution behavior of the copolymer containing 25 mol% AMPDAE, which possess methylene unit between the quaternary ammonium group and the carboxylate group, is compared to that of a copolymer containing 25 mol% 4-(2-acrylamido-2-methylpropyl-dimethylammonio) butanoate, which possesses three methylene units between the charged centers.

INTRODUCTION

Polyampholytes based on zwitterionic or dipolar ions have recently become the subject of synthetic and theoretical investigations due to their unique behavior. Typically, the cationic species is based on an ammonium group while the anionic species has been comprised of several different anionic moieties¹⁻²². The majority of the studies involve the aqueous solution behavior of poly(sulfobetaines)¹⁻¹⁶. These systems were first prepared by Hart and Timmerman by polymerizing the product of the reaction of 2- and 4-vinylpyridine with 1,4-butanesultone¹. The polymer derived from 4-vinyl-pyridine was insoluble in deionized water and required the addition of a critical concentration of salt to achieve solubility in aqueous solution. The insolubility of other poly(sulfobetaines) in deionized water and subsequent solubilization in the presence of added electrolytes has been the typical behavior; however, a few systems have been reported which are soluble in deionized water^{1,8,9}. Unlike poly(sulfobetaines), systems in which the anionic species is a carboxylate group (poly(carboxybetaines)) have received far less attention¹⁷⁻²². Topchiev *et al.*

reported kinetic studies of the free radical polymerization of 2-(N,N-dimethyl-N-(2-methacryloyloxyethylene))propiobetaine as well as solution behavior¹⁹. Wielma *et al.* have investigated poly(carboxybetaines) based on vinylimidazole with varying numbers of methylene units between the charged centers²⁰. Solubility behavior of these systems was complex and dependent on the ionic strength, pH, and nature of the added electrolyte.

Recently we initiated studies of polyampholytes prepared from zwitterionic monomers which are structurally identical except for the nature of the anionic group^{13,14}. Copolymers of acrylamide with 3-(2-acrylamido-2-emthylpropanedimethylammonio)-1-propane-sulfonate (DAPSAM series) were prepared and the solution behavior found to be dependent on the mol% of sulfobetaine incorporated into the copolymers¹³. By comparison, copolymers of acrylamide with 4-2-(acrylamido-2-emthylpropanedimethylammonio)butanoate (DABM series) in which the anionic species is a carboxylate group were similarly prepared and studied²². It was found that changes in the nature of the anionic group can lead to substantially different solution behavior. The carboxylate group was found to increase solubility and viscosity at low pH.

In this paper we report the synthesis and characterization of copolymers of acrylamide with the novel carboxybetaine monomer 2-(2-acrylamido-2-methylpropylidimethylammonio) ethanoate (DAEAM series). The impetus behind this study is to further investigate structure-property relationships of polyzwitterions composed of structurally similar zwitterionic monomers. The zwitterionic monomer of the DAEAM series differs from that of the DABAM series by the number of methylene units between the quaternary ammonium group and the carboxylate group (one vs. three). The solution behavior of the DAEAM series has been investigated as a function of added electrolytes and pH and compared to that of copolymers of the DABAM series. In this paper it is shown that the spatial proximity of the quaternary ammonium and carboxylate groups has a significant effect on the basicity of the latter, greatly affecting solution behavior.

EXPERIMENTAL

Materials

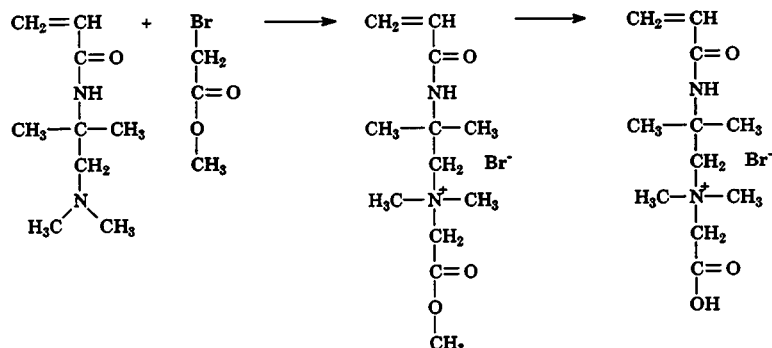
Acrylamide (AM) from Aldrich was recrystallized twice from acetone and vacuum dried at room temperature. Potassium persulfate from J. T. Baker was recrystallized twice from deionized water.

Monomer synthesis.

(4-carboxyethyl)2-acrylamido-2-methylpropylidimethylammonium bromide (Scheme 1)

The synthesis of (4-carboxyethyl)-2-acrylamido-2-methylpropylidimethylammonium bromide (AMPDAE) involved a procedure

employed by Laughlin and others to synthesize various carboxybetaine surfactants⁴⁶. 2-Acrylamido-2-methylpropyltrimethylamine, AMPDA^{5,6} (0.5 mol) was dissolved in 200ml of acetonitrile followed by the addition of an excess of methyl bromoacetate (0.75 mol). The reaction was allowed to proceed for 72 h at 45°C under a nitrogen atmosphere. The solid product that formed was then washed twice with 700 ml of acetone. The precipitate was filtered and thoroughly dried (yield: 75%). Once dried, the product was dissolved in water and passed over Amberlite IRA-400(OH) ion-exchange resin. The water was removed under reduced pressure at 50°C to yield the zwitterionic product in an oily state. The oil was dissolved in water, chilled on an ice bath, and one equivalent of HBr was added. The water was once again removed under reduced pressure at 50°C to yield the cationic monomer as a white, cakey powder. The monomer was washed with acetone, dried, and subsequently recrystallized from ethanol to yield pure AMPDAE (yield: 80%). M.p. 120-122°C (dec). Analysis for C₁₁H₂₁N₂O₃Br⁺H₂O: Calculated--C, 40.37%; H, 7.03%, N, 8.56%. Found--C, 40.81%; H, 6.78%; N, 8.78. FTIR (KBr pellet) acid O-H, 3600-2600cm⁻¹; aliphatic C-H, 2970cm⁻¹; acid C=O, 1724cm⁻¹; amide C=O, 1664cm⁻¹ and 1537cm⁻¹; acid C-O, 1260cm⁻¹. ¹³C n.m.r. (D₂O with 3-(trimethylsilyl)-1-propane-sulfonic acid, sodium salt (DSS as the reference): 29.52, 55.83, 56.38, 64.92, 69.94, 130.36, 132.61, 168.70, and 170.54 ppm.

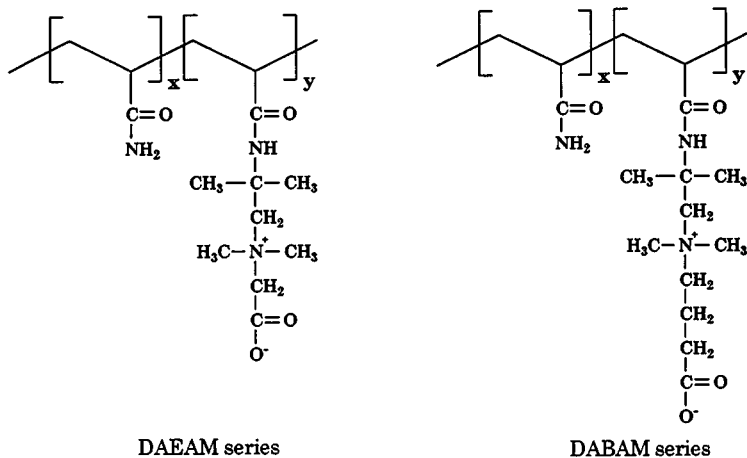


Scheme 1 Synthetic pathway for preparation of 2-(2-acrylamido-2-methylpropyltrimethylammonio)ethanoate (AMPDAE).

Synthesis of copolymers of 4-(2-acrylamido-2-methylpropyltrimethylammonio)ethanoate with acrylamide (Scheme 2)

The homopolymer of AMPDAE and the copolymers of AMPDAE with AM (the DAEAM series) were synthesized by free radical polymerization in a 0.5 M aqueous NaBr solution under nitrogen at 30°C using 0.1 mol% potassium persulfate as the initiator. The feed ratio of AM/AMPDAE was varied from 90/10 to 0/100 mol% with the total monomer concentration held constant at 0.45 M. 0.5 M NaBr in the reaction medium was used as a precaution in ensure homogeneity during polymerization.

In a typical synthesis, specified quantities of each monomer were dissolved in small volumes of deionized water. The separate solutions were then combined and one equivalent of sodium hydroxide per equivalent of AMPDAE was added and the pH adjusted to 8. The necessary quantity of NaBr was added to achieve a 0.5M NaBr solution. The reaction mixture was then sparged with nitrogen and initiated with 0.1 mol% potassium persulfate. A low conversion sample was acquired to allow reactivity ratio studies. The reaction was terminated around 50% conversion due to the high viscosity of the reaction medium and as a precaution against copolymer drift. DABAM-25 was synthesized in a similar manner previously described⁷. The polymers were precipitated in acetone, redissolved in deionized water, then dialyzed using Spectra Por No. 4 dialysis membranes with MWCO = 12 000 to 14 000 g mol⁻¹. After dialysis, the polymers were isolated by lyophilization.



Scheme 2 Structural composition of copolymer of acrylamide with 2-(2-acrylamido-2-methylpropyltrimethylammonio)ethanoate and with 4-(2-acrylamido-2-methylpropyltrimethylammonio)butanoate.

Synthesis of the copolymer of 3-(2-acrylamido-2-methylpropyltrimethylammonio)-butanone with acrylamide (Scheme 2)

The polymerization procedure for DAPSAM-25 was conducted in 0.5M NaCl in a similar manner as previously reported⁷.

Copolymer characterization

¹³C n.m.r spectra of the copolymers were obtained at 50.3 MHz on a Bruker AC200 spectrometer using 15-20wt% aqueous (D₂O) polymer solutions with DSS as a reference. A recycle delay of 8 s, 90°C pulse length, and gated decoupling to remove all NOE were used for quantitative spectral analysis. Molecular weight studies were performed on a Chromatix KMX-6 low angle laser light scattering instrument. Refractive index increments were obtained using a Chromatix KMX-16 laser differential refractometer.

Viscosity Measurements

Polymer solutions were made by dissolving designated amounts of polymer in the stock electrolyte solutions. The solutions were then diluted to appropriate concentrations and allowed to age for seven to ten days before being analyzed with a Contraves LS-30 rheometer. Duplicate runs were conducted and reproducibility found to be within $\pm 3\text{-}7\%$ dependent on the magnitude of the viscosity values. Intrinsic viscosities were evaluated using the Huggins equation.

RESULTS AND DISCUSSION

Monomer synthesis

2-(2-acrylamido-2-methylpropylidemethylammonio)ethanone was synthesized utilizing a method commonly used to prepare small molecule surfactants with carboxybetaine head groups. The advantages of the method *vs.* typical base hydrolysis procedures (using alkali hydroxides) are the relatively mild conditions and the absence of inorganic electrolyte by-products which, due to the limited solubility of zwitterions in organic solvents, may be difficult to remove. Briefly, the synthesis involves quaternization of the monomeric tertiary amine by the reaction with ethyl 4-bromobutyrate. The bromide ion affiliated with cationic product is replaced by the hydroxide ion after percolation through an anionic exchange resin of the hydroxide form (OH^-). The associated hydroxide ion promotes hydrolysis of the ester functionality with ethanol as the by-product to yield the zwitterionic product. Due to the hygroscopic nature of the product, however, the monomer was isolated as a bromide salt by addition of the equivalent of $\text{HBr}^{3,7}$. A ^{13}C n.m.r. spectrum of the monomer is shown in *Figure 1*.

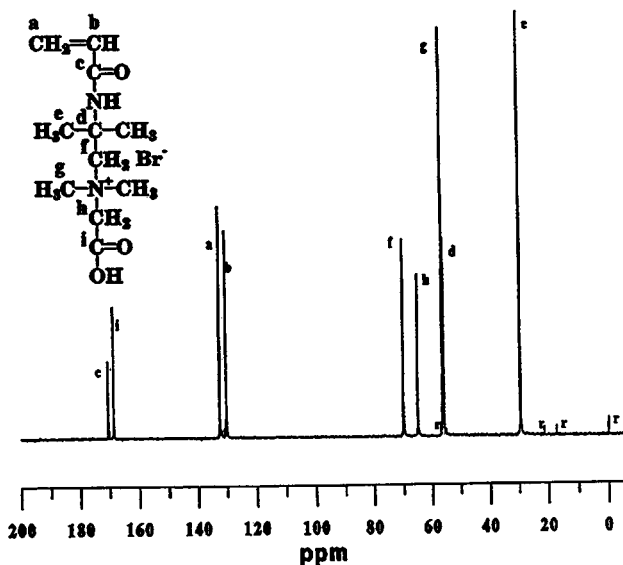


Figure 1. ^{13}C n.m.r. spectrum of 2-(2-acrylamido-2-methylpropylidemethylammonio)ethanone (AMPDAE).

Compositional and reactivity ratio analysis.

Table 1. Reaction parameters for the copolymerization of acrylamide (M_1) with 4-(2-acrylamido-2-methylpropylidemethylammonio) ethanoate (M_2)

Sample	Feed ratio (AM/AMPDAE) (mol %)	Reaction time (h)	Conversion (%)	AMPDAE found ^a (%)
DAEAM-10	90.0/10.0	3.1	4.0	11.0
DAEAM-25	75.0/25.0	1.5	9.5	26.0
DAEAM-40	60.0/40.0	1.4	18	38.0
DAEAM-60	40.0/60.0	1.4	15	58.0
DAEAM-80	20.0/80.0	2.0	17	75.0
DAEAM-100	0.0/100.0	-	-	100.0 ^b

^a Determined from ^{13}C n.m.r.

^b Theoretical value

The concentrations of charged groups incorporated into polyampholytic systems affect the solution behavior of the resulting polymers. Inter- and intramolecular associations as well as solubility have been shown to be directly related to the charge density of the systems^{1,7-9}. To investigate this issue for the novel poly(vinylcarboxybetaine) a series of copolymers were synthesized and reactivity ratios determined. The reaction parameters and compositions of low conversion copolymer samples, determined by integration of the carbonyl peaks, are presented in *Table 1*. From the experimental compositions, reactivity ratios for the AM(M_1)/AMPDAE(M_2) comonomers were determined by the methods of Fineman-Ross¹⁰, Kelen-Tudos¹¹, and non-linear squares (NLS)¹². The methods yielded values (± 0.05) of $r_1 = 0.86$ and $r_2 = 0.70$, $r_1 = 0.85$ and $r_2 = 0.69$, and $r_1 = 0.86$ and $r_2 = 0.70$, respectively. The random comonomer incorporation is in accord with the behavior of other acrylamido type monomers previously studied in our laboratories^{1-2,7}. The methods of Igarashi¹² were employed to determine the microstructure composition (*Table 2*) using the reactivity ratios from the Kelen-Tudos method.

Table 2. Structural data for the copolymers of acrylamide (M_1) with 4-(2-acrylamido-2-methylpropyl)dimethylammonio) ethanoate (M_2)

Sample	M ₁ in copolymer (mol %)	Blockiness (mol%) M ₁ -M ₁	M ₂ -M ₂	Alternation (mol%) M ₁ -M ₂	Mean Sequence Length M ₁	M ₂
DAEAM-10	89.0	78.78	0.8	20.00	8.67	1.08
DAEAM-25	74.0	52.93	4.93	42.14	3.56	1.23
DAEAM-40	62.0	35.56	11.56	52.88	2.28	1.46
DAEAM-60	42.0	14.53	30.53	54.94	1.57	2.03
DAEAM-80	25.0	4.52	54.52	40.96	1.21	3.76

Low angle laser light scattering

Table 3 shows the weight-average molecular weights determined by low-angle laser light scattering at 25°C in 1M NaCl. The molecular weight for the DAEAM series varies from 6.3 to 10.4×10^6 g mol⁻¹. The values demonstrate the high reactivity of acrylamido monomers. The second virial coefficients (A_2) for the DAEAM series have values between 2.7 to 0.8×10^{-4} ml·mol g⁻². This trend suggests that as more of the zwitterionic comonomer is incorporated into the copolymer, the lesser the extent of polymer/solvent interaction. This behavior is representative of polyampholytic systems in aqueous solutions which typically have low A_2 values.

Table 3. Classical light scattering data for the copolymers of acrylamide (M_1) with 4-(2-acrylamido-2-methylpropylidemethylammonio) ethanoate (M_2)

Sample	AMPDAE			
	found ^a (%)	$M_w \square 10^{-6}$ (g mol ⁻¹)	$A_2 \square 10^4$ (ml mol g ⁻²)	$DP \square 10^{-4}$
DAEAM-10	11.0	7.4	2.7	8.5
DAEAM-25	26.0	10.4	2.4	9.4
DAEAM-40	38.0	7.5	1.3	5.6
DAEAM-60	58.0	6.3	1.4	3.8
DAEAM-80	75.0	10.2	0.8	5.2
DAEAM-100	100.0 ^b	7.3	0.7	3.2
DABAM-25 ^c	22.4	10.2	0.8	8.7

^a Determined from ^{13}C n.m.r.

^b Theoretical value

^c Mol % AMPDAB found

Solution Behavior

Solubility of DAEAM series

AMPDAE was copolymerized with AM in varying molar ratios to yield water-soluble ionic copolymer systems. Since these polymers can behave as polyelectrolytes or polyampholytes depending on the pH of the solution, the viscosity behavior of the above copolymers was studied as a function of pH and added electrolytes at 25°C and a shear rate of 6 s⁻¹ utilizing a Contraves LS-30 rheometer.

The numbers to the right of DAEAM in the following discussion indicate the mol% of AMPDAE present in the polymerization. Copolymers of DAEAM series are soluble in deionized water at all pH values. Even DAEAM-100, a homopolymer of AMPDAE, is soluble. Most polyzwitterions require the addition of electrolytes to screen attractive charge-charge interactions to achieve solubility. The solubility of DAEAM-100 and other examples referenced in the Introduction indicate that structural features of the monomer units as well as the polymer backbone are important in determining solubility in aqueous media.

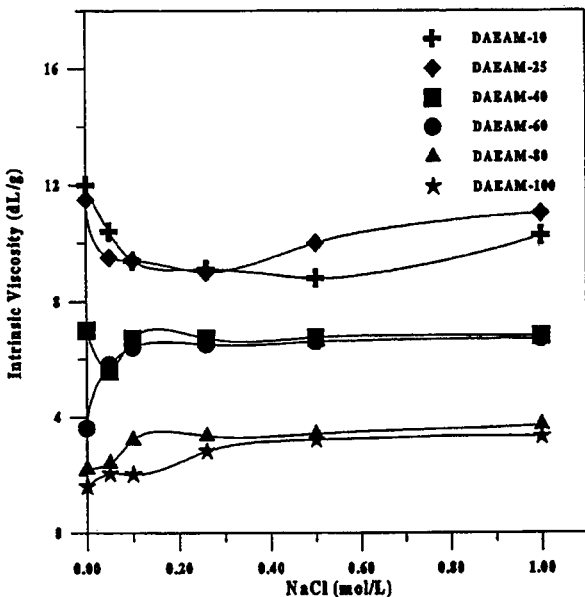


Figure 2. Intrinsic viscosities of DAEAM copolymers as a function of NaCl concentration

Effects of added electrolytes

The effect of sodium chloride on the intrinsic viscosities of the DAEAM copolymers at pH 8 is shown in Figure 2. Complex solution behavior is observed and is related to the amount of AMPDAE incorporated into the copolymers. For DAEAM-10, -25 and -40 a decrease in the intrinsic viscosity upon the addition of sodium chloride is observed. As more sodium chloride is added, the intrinsic viscosity increases. The concentration of sodium chloride required to induce this increase is dependent on the number of zwitterionic comonomers incorporated into the copolymer. The decrease in intrinsic viscosity at low concentration may be explained by the elimination of intermolecular coulombic interactions. Further addition of the electrolyte enhances the solvent quality as charge-charge interactions are screened and the hydrodynamic volume of the polymer increases. This behavior has been observed previously for low charge density polyampholytic systems^{13,22,32,33}. At incorporations of AMPDAE of 60 mol% or greater (DAEAM-60, -80, -100), this behavior is no longer observed. Instead, the intrinsic viscosity increases with addition of sodium chloride. This suggests that the coulombic interactions between the oppositely charged species are intramolecular in deionized water. Therefore, addition of sodium chloride acts to disrupt or shield these interactions and solvation of the polymer is enhanced.

The nature of the counterions of the added electrolyte has also been investigated. *Figure 3* shows the reduced viscosity of DAEAM-25 and DAEAM-40 as a function of increasing ionic strength utilizing NaCl, NaSCN, and CsCl. The order of the electrolytes in terms of increasing reduced viscosity is NaSCN>CsCl>NaCl in accord with Hoffmeister lyotropic series³⁵. This behavior has been attributed to a stronger interaction of the larger, more polarizable counterions with the charged moieties of the zwitterionic comonomer⁷. In addition, effects of the electrolyte species on the water structure and, therefore, polymer/solvent interactions must be considered.

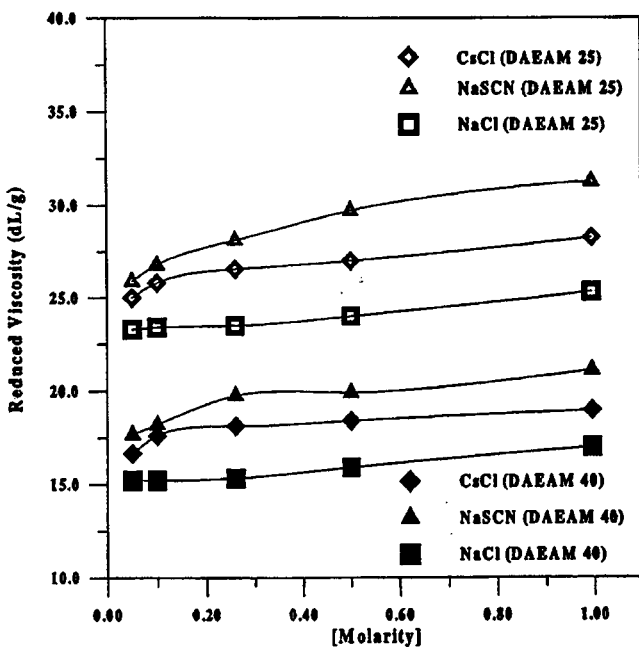


Figure 3. Reduced viscosities for DAEAM 25 and DAEAM 40 as a function of increasing ionic strength in various salts ($C_p=0.3 \text{ g dL}^{-1}$)

Effects of pH

The zwitterionic comonomer in the DAEAM series possesses a carboxylate moiety and thus should be sensitive to changes in the pH of the aqueous medium. Therefore studies were conducted on the copolymers as function of pH in deionized water and in the presence of added electrolytes.

Shown in *Figure 4* are the effects of pH on the apparent viscosity of DAEAM-25, -40 and -80. All of the copolymers display maxima. This behavior demonstrates the transition of the copolymers from polyzwitterions to polycations. As the pH is lowered, the carboxylic acid moieties are progressively protonated into the

carboxylic acid moiety. The polymer coil acquires an overall positive charge due to the quaternary ammonium species and charge repulsions force the coil to expand. Larger hydrodynamic volumes and therefore enhanced viscosities are observed. Further lowering the pH increases the concentration of hydronium and chloride ions which act to shield the charge repulsions between the ammonium moieties and, therefore, a reduction in the viscosity is observed. Hydrophobic effects may also be operative.

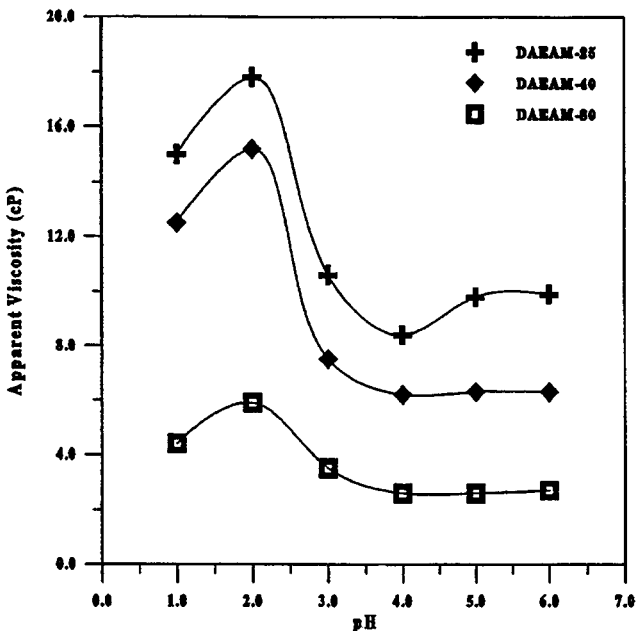


Figure 4. Apparent viscosities of DAEAM copolymers at various pH values ($C_p=0.3$ g dl^{-1})

DAEAM-25 and -40 show a greater enhancement in viscosity as the pH is lowered compared to DAAAM-80. The weight average molecular weights of DAEAM-25 and DAEAM-80 are similar (around 10 million) while the degree of polymerization of DAEAM-40 and DAEAM-80 are similar ($\approx 50\,000$). One would intuitively expect that the copolymer possessing the greatest number of charged groups would experience the greatest charge-charge repulsions and therefore attain the largest hydrodynamic volume leading to higher viscosity values. This behavior is not observed. The inherent bulkiness of AMPDAE comonomer may cause hindered rotation, thus restricting the degrees of freedom along the polymer backbone. Hydration of the polymer coil must also be considered since the acrylamide mer units are well solvated in aqueous media.

The pH value required to protonate the carboxylate moiety is obviously influenced by the neighboring ammonium moiety. Potentiometric studies by Laughlin and others^{26,27,34,36} and ^{13}C n.m.r. measurements by Chevalier and Le Perche³⁷ on small molecule carboxybetaines have clearly demonstrated this

behavior. Carboxybetaines with one methylene unit between the carboxylate and the quaternary ammonium groups have pK_a values near 2.0. This is considerably lower than the normal value of carboxylic acids, which typically have pK_a values around 4.5.

The effects of pH on the reduced viscosity for DAEAM-25 were also examined in the presence of added electrolytes and are shown in *Figure 5*. At pH values above 3, the copolymer has a slightly higher viscosity in the presence of 0.26 M NaCl than in deionized water or in 0.0167 M NaCl. The copolymer above pH 3 is zwitterionic in nature and thus charge-charge interactions are shielded in the presence of added electrolytes, leading to an enhancement in viscosity. At pH values below 3, the polymer becomes polycationic in nature for reasons discussed above. In 0.26M NaCl, these charges are sufficiently shielded and no enhancement in viscosity is observed as the pH is lowered. In 0.017 M NaCl, lower pH values are required before an increase in viscosity is observed. This may be explained by a shielding of the initial cationic charges, which are formed as a result of lowering the pH. Further lowering of the pH neutralizes more carboxylate anions yielding quaternary ammonium groups which are closer in proximity than the Debye shielding length. Thus, charge-charge repulsions arise leading to an expansion of the polymer coil. Similar viscosities are observed at pH = 1 in deionized water and in 0.017 M NaCl. Furthermore, no maximum is observed in 0.017 M NaCl. This supports the observation that the increase in ionic strength at low pH values is responsible for the decrease in viscosity in deionized water.

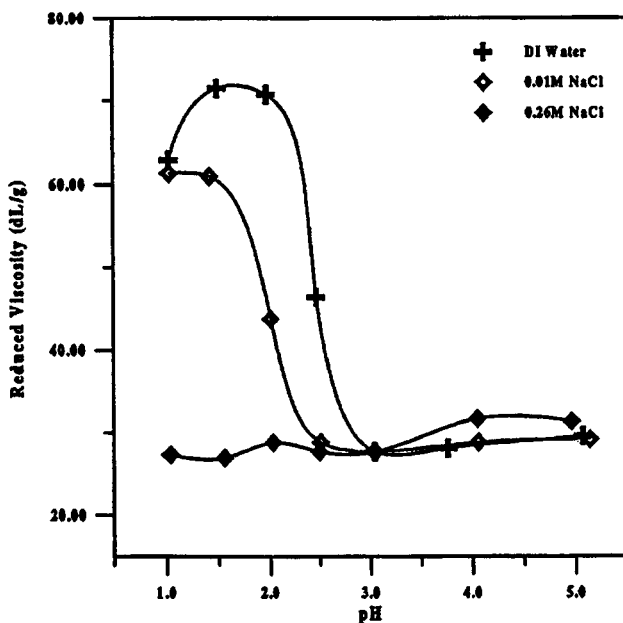


Figure 5. Reduced viscosities of DAEAM 25 in deionized water and NaCl solutions as a function of pH ($C_p=0.3$ g dl^{-1})

Effect of the number of methylene units between charges on the zwitterionic comonomer

In an effort to gain further understanding of polyzwitterions possessing carboxybetaine mer units, solution behavior has been studied for two polymeric systems that have different spacer lengths between the quaternary ammonium group and the carboxylate group. DAEAM-25 contains one methylene group between charges while DABAM-25 has three methylene groups (Scheme 2). Both copolymers have similar molecular weights with DAEAM-25 having a molecular weight of $10.4 \times 10^6 \text{ g mol}^{-1}$ and DABAM-25 a molecular weight of $10.2 \times 10^6 \text{ g mol}^{-1}$ (Table 3). Thus, a structural comparison may tentatively be drawn between the two systems.

In *Figure 6*, the intrinsic viscosity of DAEAM-25, DABAM-25, and DAEAM-60 as a function of the inverse square root of ionic strength of sodium chloride is shown. The intrinsic viscosities of polyelectrolytes normally display a linear relationship with a positive slope when plotted in this manner. In this case, no linearity in the graph is observed except possibly at the higher ionic strengths where the slope is negative. The deviation at the lower ionic strengths may be a result of the intermolecular associations discussed earlier. The curve for DAEAM-60, which does not exhibit intermolecular associations, deflects downward at the lowest ionic strength measured, while those for DAEAM-25 and DABAM-25 deflect upwards. The negative slope at the higher ionic strengths is opposite of that observed for polyelectrolytes and indicates an increase in hydrodynamic volume as the ionic strength is increased. The 'anti-polyelectrolyte' effect is normally observed of polyampholytes. At the higher electrolyte concentrations, both DAEAM-25 and DABAM-25 display essentially the same intrinsic viscosity. Therefore, at pH 8.5, no major differences in the hydrodynamic volume of the two copolymers in sodium chloride solutions are apparent. Although one might expect that increasing the number of methylene groups would enhance the hydrophobicity, small molecule studies of surfactants containing carboxybetaine head groups suggest that a spacer length of three methylene units results in a more hydrophilic head groups than a one methylene spacer unit^{26,27}. Chevalier and Le Perche have attributed this behavior to an increase in the dipole movement of the head groups, as the charged centers are moved farther apart³⁷. As the number of methylene groups increases to five or greater, however, hydrophobic effects dominate and the head group becomes less hydrophilic. Therefore a balance between the magnitude of the dipole movement, which enhances hydrophilicity, and the number of methylene groups in the spacer unit, which enhances hydrophobicity, influences the solution behavior of zwitterionic compounds.

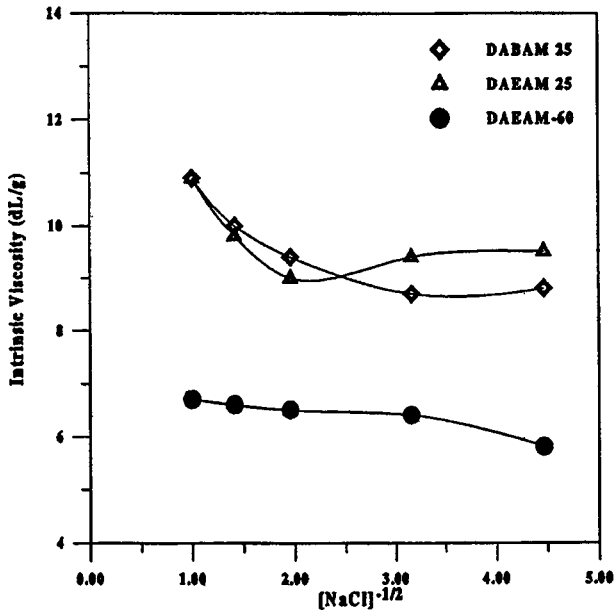


Figure 6. Intrinsic viscosities of DEAM 25, DABAM 25, and DAEAM 60 as a function of the inverse square root of ionic strength for NaCl

Solution behavior as a function of pH has also been determined for DAEAM-25 and DABAM-25 at a polymer concentration of 0.1 g dl^{-1} (Figure 7). At pH 8, both copolymers have essentially the same viscosity; however, as the pH of the solution is lowered, differences between the two copolymers become evident. DABAM-25 acquires a measurable positive charge at pH 6, as evidenced by an increase in viscosity, and displays a viscosity maximum around pH 3. The viscosity of DAEAM-25 remains relatively constant until the pH falls below 3, the viscosity maximum occurring around a pH of 1.5-2. The differences in the viscosity maxima can be attributed to the differences in basicity of the two distinct carboxylate groups. As discussed earlier, small molecule studies report a $\text{p}K_a$ value near 2 for a carboxybetaine with one methylene unit between charge centers. For a carboxybetaine with three methylene units between charge centers, this value increases to 4^{26,27,37}. This effect arises through induction from the positive field generated by the quaternary ammonium group which acts to lower the basicity of carboxylate group, the closer the two spatially become. In addition, the differences in the viscosity values between the observed maxima are almost an order of magnitude greater for DABAM-25. This behavior may be attributed to the low pH values required to protonate the carboxylate functionality of the DAEAM copolymers. As the pH is lowered, the higher concentrations of hydronium and chloride ions increase the ionic strength and effectively screen the cationic charge centers. This effect is also observed for DABAM-25 which exhibits a decrease in viscosity below pH 3. Other factors, such as hydrophobic and nearest neighbor effects, are also likely operative.

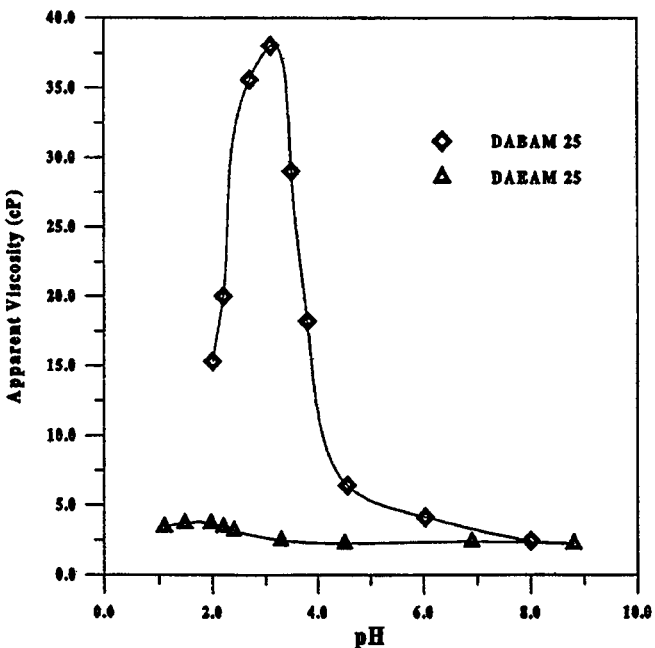


Figure 7. Apparent viscosities of DAEAM 25 and DABAM 25 in deionized water as a function of pH ($C_p=0.1 \text{ g dl}^{-1}$)

CONCLUSIONS

Copolymers of acrylamide with 2-(2-acrylamido-2-methylpropylidimethylammonio) ethanoate have been prepared by free radical polymerization in an aqueous NaBr solution. Reactivity ratios and copolymer microstructures were determined and indicate random incorporation of both comonomers. Weight average molecular weights in the range of $6.3\text{--}10.4 \times 10^6 \text{ mol}^{-1}$ have been determined for the copolymer series. Second virial coefficients were found to decrease as the mol% of AMPDAE incorporated into the copolymers increased. All of the polymers in DAEAM series are soluble in deionized water. Intrinsic viscosity studies as a function of NaCl concentration suggest a decrease in intermolecular associations and an increase in intramolecular associations as the mol% of AMPDAE incorporated into the copolymers increases. Copolymers containing 60 mol% or more show an enhancement in viscosity as the concentration of added electrolytes is increased as a result of the shielding of intramolecular associations between the zwitterionic groups. The nature of added electrolytes also influences the solution behavior; the larger, more polarizable ions enhance viscosity more than smaller ions and trend with the Hoffmeister series. The presence of carboxylate groups renders the copolymers responsive to changes in pH of the aqueous environment. As pH is lowered, the carboxylate groups are progressively protonated, resulting in an

enhancement in viscosity; however, the addition of electrolytes negates the increase in viscosity due to shielding effects. Solution properties of DAEAM-25 and DABAM-25 are similar at high pH values. As pH is lowered, DABAM-25 displays a much more dramatic increase in viscosity. This behavior is likely a result of the much lower pH required to protonate the carboxylate group of the AMPDAE mer unit.

REFERENCES

- 1 Hart, R. and Timmerman, D. *J. Polym. Sci.* 1958, **28**, 638
- 2 Schulz, D. N., Peiffer, D. G., Agarwal, P. K., Larabee, J., Kaladas, J. J., Soni, L., Handwerker, B. and Garner, R. T. *Polymer* 1986, **27**, 1734
- 3 Huglin, M. B. and Radwan, M. A. *Polym. Int.* 1991, **26**, 97
- 4 Schulz, D. N., Kitano, K., Danik, J. A. and Kaladas, J. J. *J. Polym. Mater. Sci. Eng.* 1987, **147**, 149
- 5 Liaw, D., Lee, W., Whung, Y. and Lin, M. *J. Appl. Polym. Sci.* 1987, **34**, 999
- 6 Salamone, J. C., Volksen, W., Israel, S. C., Olson, A. P. and Raia, D. C. *Polymer* 1977, **18**, 1058
- 7 Salamone, J. C., Volksen, W., Olson, A. P. and Israel, S. C. *Polymer* 1978, **19**, 1157
- 8 Wielema, T. A. and Engberts, J. B. F.N. *Eur. Polym. J.* 1987, **23**, 947
- 9 Monroy Soto, V. M. and Galin, J. C. *Polymer* 1984, **25**, 254
- 10 Galin, M., Marchal, E., Mathis, A., Meurer, B., Monroy, Y. M. and Galin, J. C. *Polymer* 1987, **28**, 1937
- 11 Knoesel, R., Ehrmann, M. and Galin, J. C. *Polymer* 1993, **34**, 1925
- 12 Konack, C., Rathi, R. C., Kopeckova, P. and Kopecek, J. *Polymer* 1993, **34**, 4767
- 13 McCormick, C. L., Salazar, L. C. *Polymer* 1992, **33**, 4617
- 14 Kathmann, E. E., Davis, D. D. and McCormick, C. L. *Macromolecules* 1994, **27**, 3156
- 15 Zheng, Y., Galin, M. and Galin, J. C. *Polymer* 1988, **29**, 724
- 16 Nakaya, T., Toyoda, H. and Imoto, M. *Polym. J.* 1986, **18**, 881
- 17 Ladenheim, H. and Morawetz, H. *J. Polym. Sci.* 1957, **26**, 251
- 18 Rosenheck, K. and Katchalsky, A. *J. Polym. Sci.* 1958, **32**, 511
- 19 Topchiev, D. A., Mkrtchyan, L. A., Simonyan, R. A., Lachinov, M. B. and Kabanov, R. A. *Polym. Sci. USSR* (Eng. Transl.) 1977, **A19**, 580
- 20 (a) Wielema, T. A. and Engberts, J. B. F. N. *Eur. Polym. J.* 1988, **24**, 647. (b) Wielma, T. A. *PhD Dissertation*, University of Groningen, 1989
- 21 Hsu, Y. G., Hsu, M. J. and Chen, K. M. *Makromol. Chem.* 1991, **192**, 999
- 22 (a) Kathmann, E. E. and McCormick, C. L. *Polym. Prepr. Am. Chem. Soc. Div. Polym. Chem.* 1994, **35**, 641. (b) Kathmann, E. E., White, L. A. and McCormick, C. L. *Polymer* 1997, **38**, 871
- 23 McCormick, C. L. and Salazar, L. C. *J. Polym. Sci., Part A* 1993, **31**, 1099
- 24 McCormick, C. L. and Blackmon, K. P. *Polymer* 1986, **27**, 1971
- 25 Laughlin, R. G. *US Patent 4,287,174* 1981
- 26 Chevalier, Y., Storet, Y., Pourchet, S. and LePerche, P. *Langmuir* 1991, **7**, 848

27 Weers, J. G., Rathman, J. F., Axe, F. U., Crichlow, C. A., Foland, L. D., Scheuing, D. R., Wiersema, R. J. and Zielske, A. G. *Langmuir* 1991, **7**, 854

28 Fineman, M. and Ross, S. *J. Polym. Sci.* 1950, **5**, 259

29 Kelen, T. and Tudos, F. *J. Macromol. Sci. Chem.* 1975, **A9**, 1

30 Tidwell, P. W. and Mortimer, G. A. *J. Polym. Sci.: Part A* 1965, **3**, 369

31 Igarashi, S. *J. Polym. Sci. Polym. Lett. Ed.* 1963, **1**, 359

32 Salamone, J. C., Ahmed, I., Rodriguez, E. L., Quach, L. and Watterson, A. C. *J. Macromol. Sci. Chem. Part A* 1988, **25**, 811

33 Peiffer, D. G. and Lundberg, R. D. *Polymer* 1985, **26**, 1058

34 Laughlin, R. G. In 'Advances in Liquid Crystals' (Ed. G. H. Brown), Vol. 3, Academic Press, New York, 1978, pp. 41 and 99

35 Collins, K. D. and Washabaugh, M. W. *Quat. Rev. Biophys.* 1985, **18**, 323

36 Laughlin, R. G. *Langmuir* 1991, **7**, 842

37 Chevalier, Y. and LePerchec, P. *J. Phys. Chem.* 1990, **94**, 1768

CHAPTER 6: Dilute Polymer Solutions In Extensional Flow

SYNOPSIS

In our previous work¹ involving the extensional flow behavior of polymer solutions using the screen rheometer, it was assumed that a polymer coil to volume fraction, C^* , value of 0.1 would give dilute solution conditions. Because our interpretation and analysis of polymer solution flow behavior in the screen rheometer is strongly based on the assumption of dilute conditions, it was decided to observe polymer solution flow behavior in the screen rheometer at C^* values lower than 0.1 in order to confirm our previous assumption that a C^* value of 0.1 gives dilute polymer solution conditions. In this chapter, three polymers (PEO, PAM, and ATABAM 5-5) were reexamined for solution flow behavior at three dimensionless concentrations ($C^* = 0.025$, $C^* = 0.050$, and $C^* = 0.100$). All solutions were found to be dilute.

An hypothesis was formulated that presumes polymer coils will extend only when the rate of coil extension is greater than the rate of coil recovery from an extensional strain. A mathematical analysis using this hypothesis was used to develop a relationship that predicts the minimum fluid extension rate that produces coil extension. The minimum fluid extension rate was shown to be inversely proportional to the coil's hydrodynamic diameter.

INTRODUCTION

As explained in a previous report¹, a dilute polymer solution is composed of polymer coils surrounded by solvent. Each coil contains a single polymer molecule and a large amount of associated solvent. Each coil can be considered as a sphere having a hydrodynamic diameter, d_h . For high molecular weight polymers in dilute solutions, the coil's hydrodynamic diameter can be approximated from the polymer's molecular weight, M , and its intrinsic viscosity, η_{intr} .

$$d_h = [12/(5\pi N_A)]^{1/3} [M \eta_{intr}]^{1/3} \quad (1) \quad \text{In Equation (1), } N_A \text{ is Avogadro's number.}$$

The intrinsic viscosity can be determined by measuring the first Newtonian shear viscosities of progressively more dilute polymer solutions. A polymer's intrinsic viscosity depends upon solvent, temperature and the presence of other components in the solution such as buffers or electrolytes.

A solution's polymer coil volume content is quantified by using a parameter referred to as the dimensionless concentration, C^* . A polymer solution's dimensionless concentration is equal to the product of the polymer mass concentration in the solution, c , and the intrinsic viscosity of the polymer, η_{intr} .

$$C^* = c \eta_{intr} \quad (2) \quad \text{Note that } C^* \text{ is equal to the volume fraction of polymer coils}$$

within the solution.

Dilute solution conditions exist when individual polymer coils do not interact with one another, and, thus, C^* must be much less than unity. At dilute conditions the increase in polymer solution flow resistance as compared to solvent resistance at the same flow rate is due to the sum of the flow resistances produced by each individual polymer coil in the solution. At dilute conditions, each polymer coil will act independently of all other polymer coils and all coils will respond identically to any given fluid flow condition.

In our previous work¹ involving the extensional flow behavior of polymer solutions using the screen rheometer, it was assumed that a C^* value of 0.1 would give dilute solution conditions. Because our interpretation and analysis of polymer solution flow behavior in the screen rheometer is strongly based on the assumption of dilute conditions, it was decided to observe polymer solution flow behavior in the screen rheometer at C^* values lower than 0.1 in order to confirm our previous assumption that a C^* value of 0.1 gives dilute polymer solution conditions.

EXPERIMENTAL

Three polymers (PEO, PAM, and ATABAM 5-5) were reexamined for solution flow behavior at three dimensionless concentrations ($C^* = 0.025$, $C^* = 0.050$, and $C^* = 0.100$). The polymer properties are shown Table I. The solvent for all polymer solutions was water and all screen rheometer measurements were performed at room temperature conditions. Screen rheometer solvent and solution pressure drop data ($\Delta P_{solution}$ and ΔP_o , respectively) were collected for each fluid at several volumetric flow rates, Q . As previously reported¹ the data can be plotted according to Equation (3) to find the coil viscosity, η_c . Q_{yield} is the flow rate at which the polymer coils extends. At flow rates less than Q_{yield} polymer coils do not extend.

$$\beta (\Delta P_{solution} - \Delta P_o) = \eta_c Q \quad \text{when} \quad Q > Q_{yield} \quad (3)$$

The left side of Equation (3) will be referred to as the Normalized Solution Resistance. The β parameter of Equation (3) is a constant that is determined from screen rheometer geometry and other known experimental conditions.

$$\beta = \frac{\pi D_s^2 d_{wire} f^2}{48 n \phi c \eta_{intr} (1-f)^2} \quad (4)$$

See the nomenclature for an explanation of the other parameters used in Equation (4).

Figures 1, 2, and 3 are plots of the PEO, PAM and ATABAM solutions, respectively, in which the Normalized Solution Resistance is plotted versus the volumetric flow rate. These figures show that the flow rate at which the polymer coils extend, Q_{yield} , is always the same for all three C^* values within a polymer type. Also for all three C^* values within a polymer type, the initial slope of the line which was fit to the data having a flow rate greater than Q_{yield} are equal. The slope of a fit line is equal to the coil viscosity, η_c .

Because each solution of a polymer type has the same Q_{yield} and η_c values regardless of its dimensionless concentration, C^* , all solutions must be dilute. Therefore, the critical assumption that polymer solutions are dilute at a C^* value of 0.1 or less appears to be correct.

RESULTS AND DISCUSSION

Explanation of Coil Extension

As discussed in a previous report¹, the fluid extension strain rate at which a polymer coil extends, $\dot{\epsilon}_{yield}$, can be estimated from screen rheometer geometry and the fluid yield flow rate, Q_{yield} .

$$\dot{\epsilon}_{yield} \approx \frac{16 Q_{yield}}{3 \pi D_s^2 d_{wire}} \frac{1-f}{f} \quad (5)$$

Figure 1: PEO Solutions

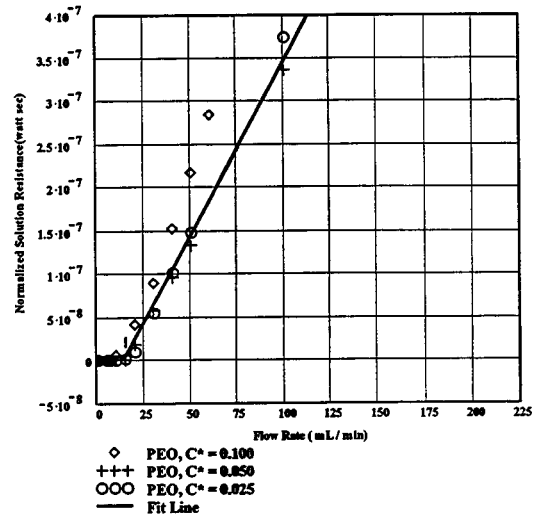


Figure 2: PAM Solutions

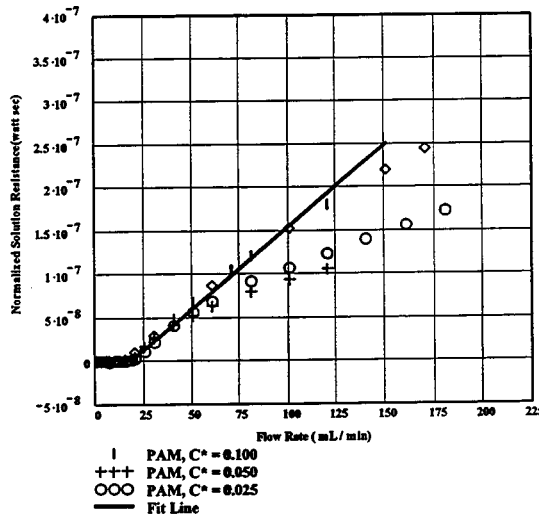
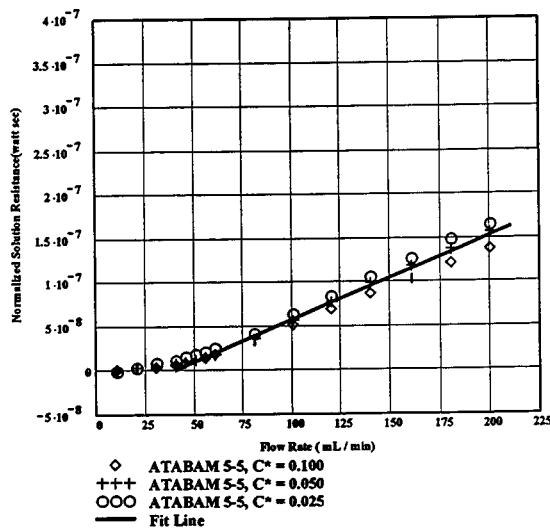


Figure 3: ATABAM Solutions



The fluid extensional strain rate which begins polymer coil extension may be explained by assuming that coil extension starts when the rate of coil extension, R_E , is equal to the rate of coil recovery from an extensional strain, R_C . If $R_E < R_C$, the polymer coil will not extend because any coil extension developed by the fluid flow field will be instantaneously recovered by the random motions of the macromolecule. Thus, significant coil extension only occurs when $R_E \geq R_C$.

Coil extension is the result of a difference in fluid drag forces across the polymer coil². This drag force difference increases as both the fluid extension rate and the size of the polymer coil increase. Therefore, the rate of coil extension, R_E , is expected to be proportional to the product of the fluid extensional strain rate, $\dot{\varepsilon}$, and the

hydrodynamic diameter of the polymer coil. This relationship is expressed by Equation (6)

$$R_E = k_1 d_h \dot{\varepsilon} \quad (6)$$

In Equation (6), k_1 is a proportionality constant and d_h is the polymer coil's hydrodynamic diameter. Equation (1) can be used to determine d_h .

Hassager³ and Durst⁴ have suggested that in dilute solutions the polymer coil recovery rate from a strain deformation would be inversely proportional to the product of the polymer coil's characteristic recovery time, λ_c , and the rate of coil strain deformation, $\dot{\varepsilon}$. Thus, the rate of coil recovery from an extensional strain is

$$R_C = k_2 / (\lambda_c \dot{\varepsilon})^x \quad (7) \quad \text{where } k_2 \text{ is a proportionality constant and } x \text{ is an exponent.}$$

The coil's characteristic recovery time can be equated to the Zimm response time. This time can be estimated from the polymer's molecular weight, M , and its intrinsic viscosity, η_{intr}

$$\lambda_c \approx 25 M \eta_{intr} \mu_o / (6 \pi^2 R T) \quad (8)$$

In Equation (8), μ_o is the solvent shear viscosity, T is the absolute temperature, and R is the gas law constant. Equation (1) can be used to express Equation (8) in terms of the coil hydrodynamic diameter, d_h .

$$\lambda_c \approx 125 \mu_o d_h^3 / (72 \pi k_B T) \quad (9) \quad \text{where } k_B = R / N_A \text{ is the Boltzmann constant.}$$

When R_E is set equal to R_C , an equation is formed which can be solved for the fluid extensional strain rate that first produces polymer coil deformation, $\dot{\varepsilon}_{yield}$.

$$\dot{\varepsilon}_{yield} = k_3 (d_h)^{-\frac{3x+1}{1+x}} \quad (10) \quad \text{where } k_3 \text{ is a grouping of several constants,}$$

$$k_3 = \frac{k_2}{k_1} \left(\frac{72 \pi k_B T}{125 \mu_o} \right)^x$$

Equation (10) can be combined with Equation (5) to find the fluid flow rate that first gives polymer coil extension, Q_{yield} .

$$Q_{yield} = K d_h^b \quad (11) \quad \text{where } K = \frac{3\pi k_2 D_s^2 d_{wire} f}{16 k_1 (1-f)} \left(\frac{72 \pi k_B T}{125 \mu_o} \right)^x \quad \text{and} \quad b = -\frac{3x+1}{1+x}$$

Because all the parameters defining K in Equation (11) were constant in all the polymer solution studied in the screen rheometer, then Equation (11) predicts that for any polymer solution Q_{yield} is only a function of the polymer coil's hydrodynamic diameter. Furthermore Equation (11) suggest that a log-log plot of experimentally measured Q_{yield} values versus corresponding polymer coil hydrodynamic diameters should give a straight line relationship in which the intercept, a, and slope, b, are related to x and K, i.e., $a = \log(K)$ and $b = -(3x+1)/(1+x)$. It is expected from the work of Hassager³ that x should have a value of about 1.0. Thus, the value of b should be approximately -2.0.

Figure 4 displays a plot of experimental fluid yield flow rates versus polymer coil hydrodynamic diameter to the b power. See Table I for polymer properties. The line drawn in Figure 4 is the fit of Equation (11) to the experimental data. Regression of the experimental data gave a best fit value for b of -2.38 and a K value of 6.47×10^8 mL / (min Angstroms^{2.38}). The value for b is slightly larger than that expected from the past work of Hassager³. Nevertheless, it appears that a correlation exists as theory suggests.

Table I : Polymer and Solution Properties

Polymer Type	Molecular Weight M g / mole $\times 10^6$	Monomer Mol. Weight, M g / mole	Hydrodynamic Diameter, d_h Angstroms	Intrinsic Viscosity, η_{intr} dL / g	Yield Flow Rate, Q_{yield} mL / min	Coil Viscosity, η_c dyne sec / cm ²
PEO	0.55	44	727 (756)	5.5 (6.2)	100 (100)	0.12 (0.04)
PEO	2.10	44	1391 (1338)	10.1 (9.0)	36 (34)	1.72 (1.89)
PEO	4.10	44	2131 (1979)	18.6 (14.9)	12 (6.6)	3.27 (3.38)
PAM	1.89	71	1539 (1575)	15.2 (16.3)	10 (14.0)	1.34 (1.00)
ATA BAM	0.65	80	985 (1010)	11.6 (12.5)	47 (41)	0.41 (0.44)

Values in parenthesis are for solutions using 0.514M NaCl solvent. Other solutions used DI Water as the solvent.

During coil extension, stretching of larger volume polymer coils would disrupt more solvent contained within the coil than with smaller coils. This disruption of solvent that is in equilibrium with the polymer requires energy. The more energy required to displace the solvent within the coil, the greater the resistance to flow the coil would experience or the greater the coil extensional viscosity. The work of Hassager³ also suggest that after coil extension its coil viscosity should be related to the polymer coil hydrodynamic volume.

Figure 5 shows a plot of experimental coil viscosities versus polymer coil hydrodynamic volume. The data strongly suggest that the coil viscosity is directly proportional to the hydrodynamic coil volume, V_c . The function is given by

$$\eta_c = k_4 V_c = k_4 \pi d_h^3 / 6 \quad (12)$$

where $k_4 = 7.3 \times 10^{-10}$ poise / Angstrom³.

CONCLUSIONS

As a fluid passes through the channels of a porous media, the fluid velocity is continually accelerating and decelerating. A fluid flowing under these conditions is in an extensional flow field. The fluid forces of an extensional flow field that are applied to a polymer coil is proportional to the average extension rate the fluid experiences in the flow field. The fluid extension rate depends upon the porous media's channel geometry but always increases, regardless of porous media channel geometry, as the fluid flow rate increases.

This study has shown that high molecular weight aqueous polymer solutions experiencing extensional fluid flow fields are dilute when the dimensionless concentration, C^* , is less than or equal to 0.1. At dilute conditions, each polymer coil will act independently of all other polymer coils and all coils will respond identically to the same fluid flow condition.

If polymer coils in dilute solutions extend and compress as they travel in an extensional fluid flow field they significantly increase the fluid's resistance to flow. However, polymer coil extension and compression will occur only if the extension rate or fluid flow rate through the porous media is larger than some critical value. At the critical flow rate the fluid forces applied to a polymer coil are sufficient to extend the coil. Thus, the critical fluid flow rate for a polymer coil extension is dependent upon polymer chemical structure, macromolecular geometry, solvent - polymer interaction and porous media channel geometry. In general, the critical flow rate value increases as the polymer coil size decreases.

When polymer solutions are used to flood an oil reservoir, very low fluid extension rates exist at large distances away from the injection well head. To be effective in decreasing displacing fluid

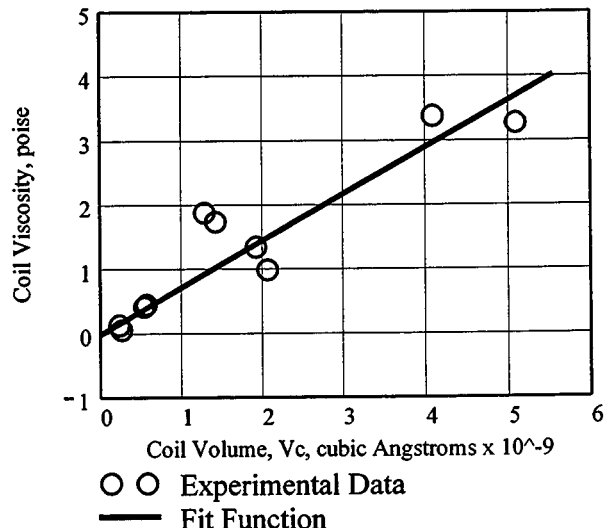


Figure 5. Coil Volume vs. Coil Viscosity

mobility during polymer flooding, polymer coils must extend as they percolate through the porous media. Polymer coil extension lowers displacing fluid mobility and thereby maintains cohesion to the flood front through the reservoir and this increases oil recovery. Thus, an understanding of which fluid flow conditions extend polymer coils is essential to controlling reservoir flooding and improving oil recovery.

In this study a hypothesis was formulated that presumes polymer coils will extend only when the rate of coil extension is greater than the rate of coil recovery from an extensional strain. A mathematical analysis using this hypothesis was used to develop a relationship that predicts the minimum fluid extension rate that produces coil extension. The minimum fluid extension rate was shown to be inversely proportional to the coil's hydrodynamic diameter. Application of this relationship to limited experimental data shows that the data are consistent with the proposed hypothesis.

This finding implies that in typical reservoir flooding where fluid extension rates are very low, polymer coil extension that decreases displacing fluid mobility and improves oil recovery will occur only if the coil hydrodynamic diameter is extremely large. Large coil hydrodynamic diameters are formed with very high molecular weight polymers having large intrinsic viscosities.

References

1. McCormick, C. L. and R. D. Hester, *Responsive Copolymer For Enhanced Petroleum Recovery, Annual Report*, for the Period October 1, 1999 through September 30, 2000, DOE/BC/15111-1
2. Odell, J. A. and A. Keller, *J. Poly. Sci., Poly. Phys.*, B24, 1889, 1986.
3. Hassager, F., *J. Chem. Phys.*, 60, 2111, 1974.
4. Durst, F. and R. Hass, *Rheol. Acta.*, 20, 179, 1981

NOMENCLATURE

Symbol	Description
ATABA M	terpolymer of AMTAC (5 mole %), AMBA(5 mole %) and acrylamide(90 mole %) monomers
b	exponent, see Equation (11)
C *	dimensionless concentration
c	mass concentration of polymer in a solution
D _s	screen diameter, 1.27 cm

d_h	polymer coil hydrodynamic diameter
d_{wire}	screen wire diameter, 0.0020 cm
f	screen fractional free projected area, 0.16
K	constant in Equation (11)
k_B	Boltzmann constant
k_1	proportionality constant in Equation (6)
k_2	proportionality constant in Equation (7)
k_3	grouping of constants, used in Equation (10)
k_4	proportionality constant relating η_c to V_c in Equation (12)
M	viscous or weight average polymer molecular weight
M_0	monomer molecular weight
N_A	Avogadro's number
n	number of screens connected in series
PAM	poly(acrylamide)
PEO	poly(ethylene oxide)
Q	fluid volumetric flow rate
Q_{yield}	volumetric flow rate at which polymer coils start to extend
R	gas law constant
R_c	rate of coil recovery
R_e	rate of coil extension
T	absolute temperature
V_c	polymer coil hydrodynamic diameter
x	exponent used in Equation (7)
ΔP_o	solvent pressure drop across a porous media
$\Delta P_{solution}$	solution pressure drop across a porous media
β	grouping of parameters, see Equation (4)
$\dot{\epsilon}_{fluid}$	fluid extensional strain rate
$\dot{\epsilon}_{yield}$	fluid extensional strain rate required to force polymer coil extension

η_c	polymer coil extensional viscosity
η_{intr}	polymer intrinsic viscosity
λ_c	polymer coil characteristic recovery time or Zimm response time
μ_o	Newtonian solvent shear viscosity
ϕ	porosity of screens, 0.52

CHAPTER 7. Cable Rheometer

SYNOPSIS

Most commercial rheometers are not capable of measuring the very small torques which are produced when very dilute aqueous polymer solutions are subjected to low shear rates that are usually 5 sec^{-1} or less. A Contraves Low Shear Model 30 rheometer is capable of making the viscosity measurements needed to determine polymer intrinsic viscosities. For the past 15 years this model rheometer has been used in our laboratory to obtain intrinsic viscosities. However, recently the instrument has experienced electronic problems and is undergoing repairs. Development of an alternative instrument for making accurate low shear polymer solution viscosity measurements became a necessity. A bob and cone rheometer has been developed in our laboratories for this purpose.

INTRODUCTION

Intrinsic viscosity measurements are used to characterize polymers in dilute solutions. The intrinsic viscosity is the coil volume or solvent associated with each unit mass of polymer dissolved in the solution. This measurement is difficult because of the limitations of low shear and low polymer concentration imposed upon the experimental method used to determine the intrinsic viscosity. The intrinsic viscosity of a polymer in solution, η_{intr} , is defined by Equation (1).

$$\eta_{\text{intr}} = \lim_{c \rightarrow 0} \left(\frac{\lim(\eta) - \eta_s}{\dot{\gamma} \rightarrow 0} \right) \quad (1)$$

The above definition shows that to determine the intrinsic viscosity, the solution shear viscosity, η , must be measured at low shear rate, $\dot{\gamma}$. Also the solution concentration, c , must be a minimum when measuring the solution viscosity. Otherwise, fluid viscosity measurements must be made on very dilute solutions at very low shear rates. Under these conditions the solution viscosity, η , is only slightly greater than the solvent viscosity, η_s .

The steady shear viscosities of most macromolecular solutions are dependent upon the fluid shear rate, temperature and the concentration of polymer in solution. In addition, viscosity is affected by polymer molecular weight, chemical structure and solvent-polymer interactions.

EXPERIMENTAL

Polymer Solution Flow Properties

Most high molecular weight polymer solutions at dilute conditions have a pseudoplastic or shear thinning behavior. As the solutions are subjected to higher fluid shear rates, the apparent viscosity decreases. However at very low shear rates, there is a shear rate region where pseudoplastic fluids begin to behave as Newtonian fluids meaning that the apparent viscosity approaches a constant value. This low shear rate region is referred to as the first Newtonian shear region or "zero" shear region and is recognized as a plateau in a plot of apparent viscosity versus fluid shear rate. See Figure 1. This is the solution viscosity required when determining a polymer's intrinsic viscosity.

Thus, it is important that polymer solution viscosities are measured in the first Newtonian shear region when the data is used to determine intrinsic viscosities. If the solution viscosity is measured in the pseudoplastic region then an extrapolation into the first Newtonian region will be needed to estimate the solution viscosity under low shear rate conditions. As indicated in Figure 1, the extrapolation from the pseudoplastic region into the first Newtonian region is not linear. Extrapolated low shear solution viscosity measurements are not accurate; therefore, fluid viscosity measurements must be made in first Newtonian region of very low shear rates. This measurement is a difficult task and requires the use of a sensitive rheometer.

Low Shear Rheometers

Conventional commercial rheometers are not suitable for dilute polymer solution viscosity measurements because they are unable to measure the small shear stresses at the low shear rates that are produced when measuring fluid viscosities of high molecular weight polymer solutions. In dilute solutions polymer macromolecules are spherical coils. If these large coils are deformed in a fluid shear field, they will be perturbed from their equilibrium spherical shape and their coil volume will decrease. This gives a false, low measurement value of the solution viscosity. As shown by Equation (1), this false solution viscosity measurement would produce an inaccurate intrinsic viscosity. Most commercial rheometers are not capable of measuring the very small torques which are produced when very dilute aqueous polymer solutions are subjected to low shear rates that are usually 5 sec^{-1} or less.

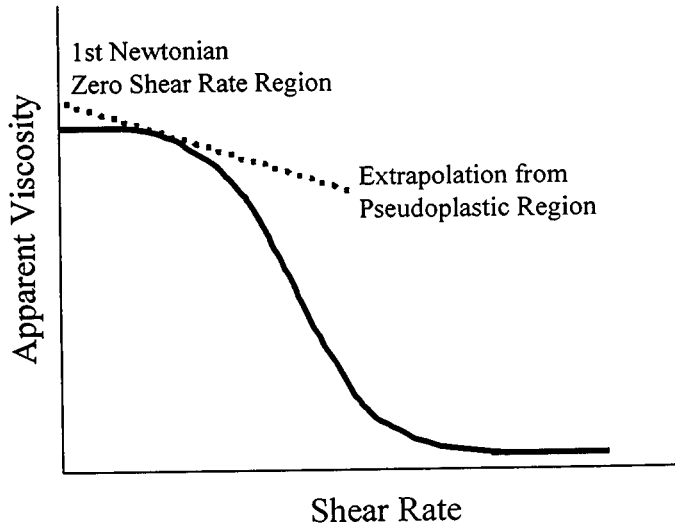


Figure 1. Apparent Viscosity vs. Shear Rate

A Contraves Low Shear Model 30 rheometer is capable of making the viscosity measurements needed to determine polymer intrinsic viscosities. For the past 15 years this model rheometer has been used in our laboratory to measure intrinsic viscosities. However, recently the instrument has experienced electronic problems and is undergoing repairs. Rheometer parts have been back-ordered but there is no guarantee that these parts will ever become available because this instrument has not been manufactured for over 10 years. Because of this, efforts have been made to locate and acquire a used Contraves rheometer. However, these efforts have been fruitless. Therefore, developing an alternative instrument for making accurate low shear polymer solution viscosity measurements is now a necessity.

Cable Rheometer Description

As previously discussed, determination of a dilute polymer solution's "zero shear" viscosities is difficult because of the problems encountered when measuring the small fluid shear stress forces involved with movement of low viscous fluids at low shear rates.

Measurement of these low fluid stress forces can be accomplished by using a cable rheometer.

The cable rheometer designed and fabricated in our laboratory is shown in Figure 2. It consists of a bob concentrically placed in a cup. Fluid is placed within the annular volume located between the cup and bob. The inside cylinder or bob is suspended by a long wire cable. The cup can be rotated at a fixed speed. As the cup rotates, the fluid produces a drag force on the bob surface. This fluid drag force produces a torque on the wire cable. This torque forces the wire to twist at an angle θ . The twist angle developed during rotation of the cup is a function of cup rotational speed, system geometry and the fluid viscosity. The twist angle can be measured by use of a laser pointer attached to a movable compass ring that is concentrically positioned around the rotating cup.

The torque on a wire cable can be determined from strength of material relationships for a circular solid shaft under torsion¹. The torque, T_q , applied to a cable of diameter d and length L , can be determined from Equation (2).

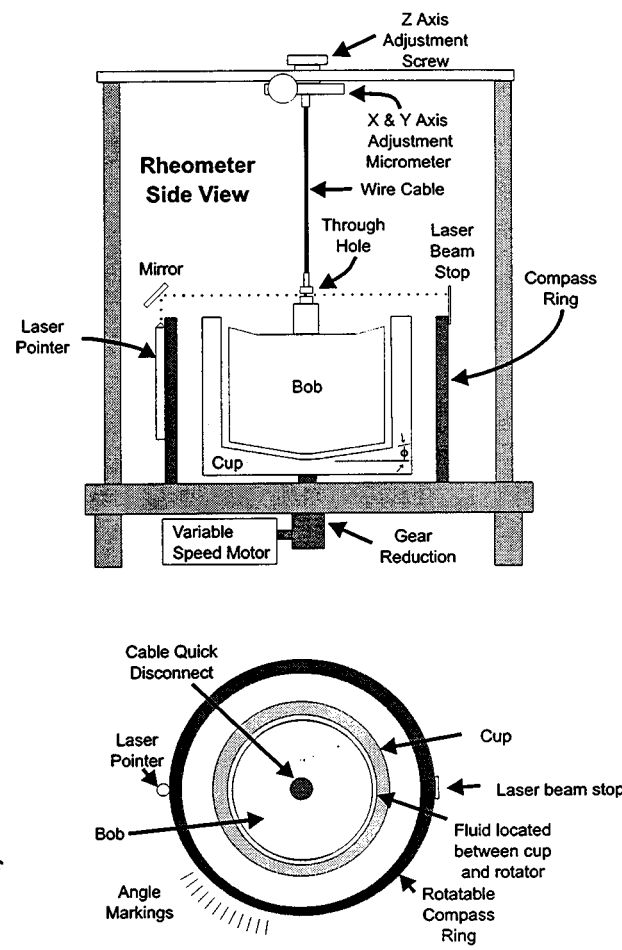


Figure 2. Cable Rheometer

$$Tq = \frac{\pi d^4 G \theta}{32 L} \quad (2)$$

In Equation (2), G is the cable's shearing modulus of elasticity (1.05×10^7 psi for stainless steel) and θ is angle of cable twist, expressed as radians.

If both the rotational speed of the cup, ω , in radians per unit time, and the torque, T_q , applied to the cable are known, then the fluid apparent shear viscosity, η , can be calculated from the following equation^{2,3}.

$$\eta = \frac{Tq (R - r)}{\omega r^3 \left(2\pi H + \frac{r}{4(\cos \phi)^2} \right)} \quad (3)$$

In Equation (3), R is the inside radius of the cup, r is the outside radius of the bob, H is the bob's height and ϕ is the cone angle of the bottom surface of the bob.

Use of Equation (2) to substitute for the torque, Tq , in Equation (3), gives

$$\eta = \left\{ \frac{\pi d^4 G (R - r)}{32 L r^3 \left(2\pi H + \frac{r}{4(\cos \phi)^2} \right)} \right\} \frac{\theta}{\omega} = K \frac{\theta}{\omega} \quad (4)$$

In the above equation, G , d , R , r , H , L and ϕ are constants. Thus, the terms in the set of braces define an instrument constant, K . Therefore, in the cable rheometer fluid viscosities are inversely proportional to the cup rotational speed, ω , and directly proportional to the cable twist angle, θ .

The fluid shear rate, $\dot{\gamma}$, developed by the cable rheometer is dependent upon system geometry and the cup rotational speed². The fluid shear rate is given by Equation (5).

$$\dot{\gamma} = \frac{8 R^2 r^2 \omega}{(R + r)^2 (R^2 - r^2)} \quad (5)$$

The cup speed, ω , in radians per unit time is related to its revolutions per unit time, N .

$$\omega = 2\pi N \quad (6)$$

Use of Equations (4) and (5) enable the cable rheometer to be operated at various cup rotational speeds to develop the data needed to plot a flow curve of apparent viscosity, η , versus fluid shear rate, $\dot{\gamma}$. The flow curve can be used to determine the "zero shear" fluid viscosity.

Rheometer Design Details

Details of the cup and bob are shown in Figure 3. The tapered bottom (see Figure 4) on the bob allows air to escape as the bob is lowered into a test solution. This geometry will insure that there is complete and unvarying fluid-to-bob surface contact. The large bob provides both a radial surface and a bottom surface that gives a large area of fluid in contact with the bob. This large fluid contact area will increase cable torque at any cup rotational speed, thus increasing rheometer sensitivity.

The large fluid gap located between the bob and cup facilitates centering of the bob with the X-Y axis positioning micrometer by eliminating the tendency of the liquid surface tension forces to off center the bob. Also, a fine thread Z-axis adjustment screw is available to allow for precise height adjustment of the bob. See Figure 5.

Perhaps the most significant bob design feature is that mass has been removed from the center of the bob. As shown in Figure 6, the aluminum bob consists of three main pieces; a hollow cylinder, a bottom, and a top. The mass is concentrated in the bottom to aid in centering. The bottom and top are threaded onto the cylinder so that they can easily be removed. The volume of bob's internal cavity was designed such that the assembled bob had a neutral buoyancy in water. The weight of the bob can be adjusted by adding any number of stainless steel washer-like weights that are secured to the inside of the cup by a threaded post. This weight adjustment feature allows exact control of the cable tension by varying the submerged weight of the bob. This improves cable twist response and also aids in damping bob oscillations when the cable tension is set to a optimum value.

Rheometer Operation

Several variables have been investigated in order to determine the best rheometer operating conditions. A cable consisting of 49 strands and having an overall

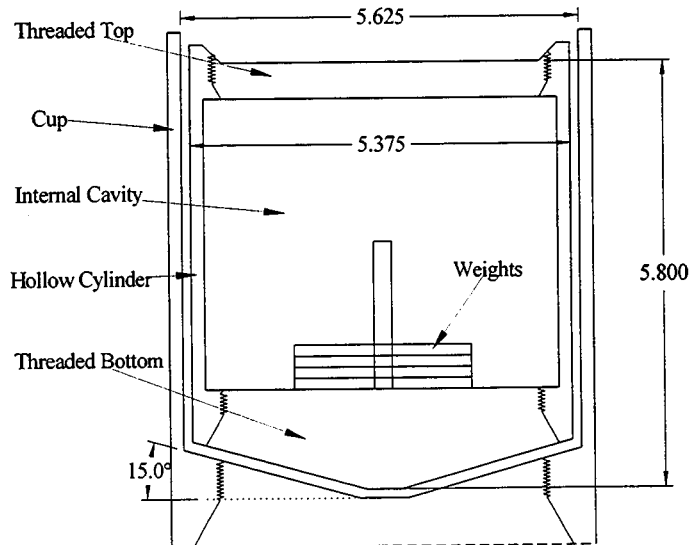


Figure 3 Cup and Bob Details

diameter of 0.024 inches was tested along with a single wire cable having a diameter of 0.007 inches. In each case, the speed of the motor, hence the fluid shear rate, and the weight of the bob, hence tension in the wire, were varied. The data collected during these experiments probing cable rheometer performance under varying conditions has generated the following conclusions.

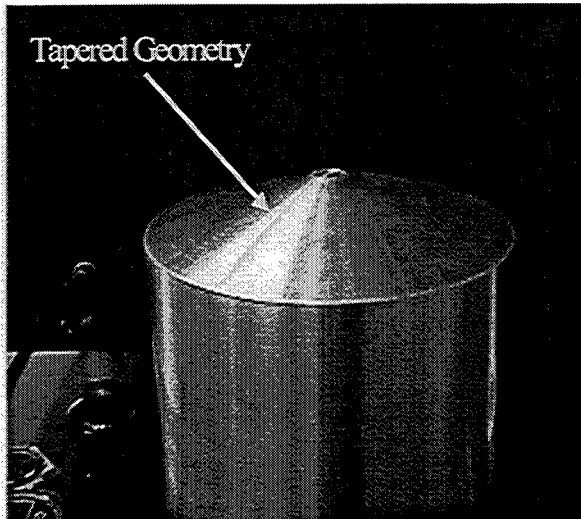


Figure 4. Cone Shaped Bob Bottom

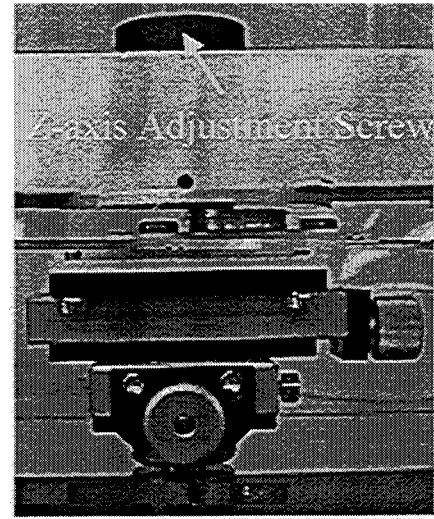


Figure 5. Axis Adjustments

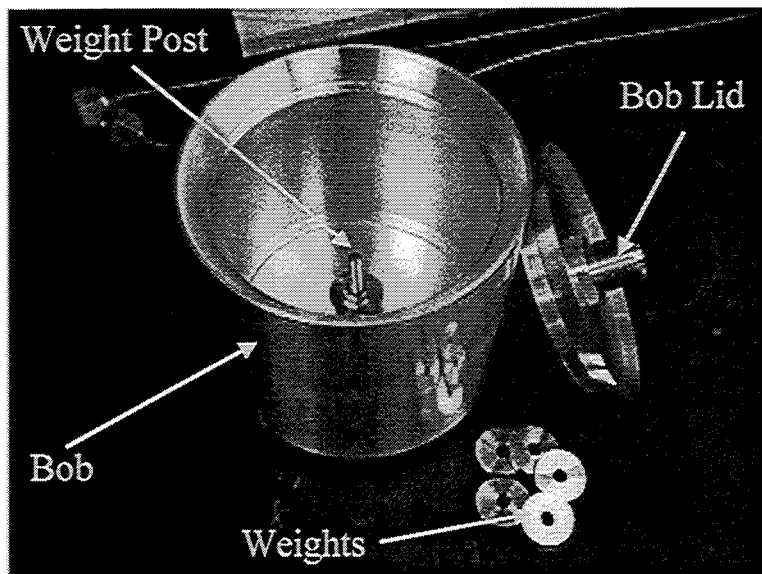


Figure 6. Bob Components

RESULTS AND DISCUSSION

The high torsional modulus of the stranded cable did not allow for adequate cable twist when studying the rheological behavior of aqueous polymer solutions. The

twist angle for water at room conditions was approximately 15 degrees at a shear rate of 2.74 sec^{-1} . The increase in deflection for a dilute polymer solution would not be significantly greater than water. Thus, the stranded cable does not have the sensitivity needed to measure the viscosities of dilute aqueous polymer solutions. Also with this cable large and continuous twist angle oscillations were observed under all conditions. For example, at an average cable twist of 15 degrees, the cable twist angle is actually cycling between 10 to 20 degrees.

In contrast to the stranded cable, the single wire cable gave a twist angle of 45 degrees for water. This increased torque sensitivity enables better viscosity measurements of dilute aqueous polymer solutions. Also unlike the stranded wire cable, the twist angle oscillations associated with the single wire cable were damped with time and therefore enabled a more accurate measurement of the final steady state cable twist angle. A force balance using Newton's second law in a torsional format was used to develop a differential equation that relates twist angle, θ , to the time of rheometer operation. See Appendix A for the derivation. The differential equation solution is plotted together with experimental data in Figure 7. The plot shows that about 10 min of cup rotation is required before the twist angle is stabilized.

Additional factors have also led to the decision that the 0.007 inch diameter single wire cable should be used in subsequent solution viscosity determinations. The single wire consistently gave the same angle of deflection when water was sheared at low shear rates. Figure 8, a plot of cable twist versus cup rotational speed, shows that the twist angle varies linearly with cup angular velocity or the fluid shear rate. This data was used to determine that the rheometer's instrument constant, K , for the single wire cable is $2.30 \times 10^{-8} \text{ psi}$. Finally, the initial oscillations of the bob were much smaller for the single wire cable than for the stranded cable.

The weight of the bob was found not to be an important factor in the accuracy of the twist angle measurements. The twist angle oscillations become slightly larger as weight is added to the bob, but not to a significant extent. Current operation of the instrument is with 108 grams of weight added beyond that required to achieve neutral buoyancy. This results in the single wire cable being under 6200 psi of tension. The maximum yield strength of the stainless steel wire is 88,000 psi which is considerable

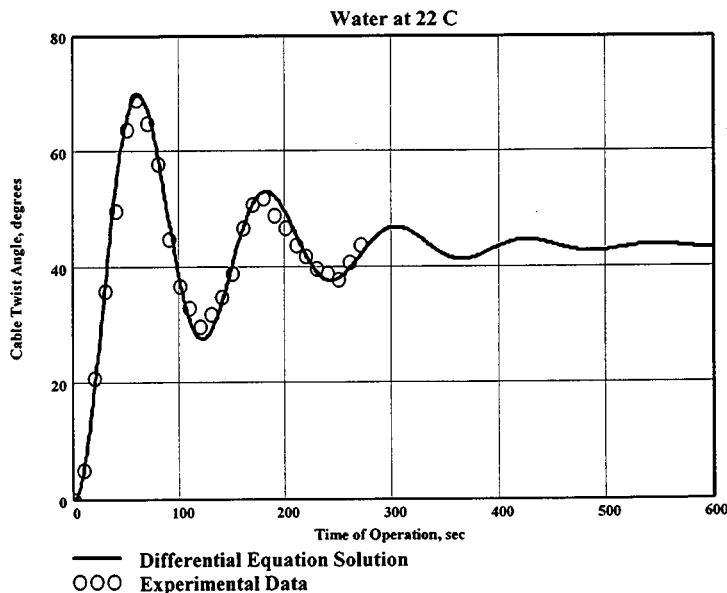


Figure 7 Twist Angle vs. Time of Operation

above the tension experienced during rheometer operation. It was found that low wire tensions results in a tendency for the wire to kink as the twist angle increases.

CONCLUSION

The presently configured cable rheometer has a shear rate range from 1.0 to 2.7 sec⁻¹ and can measure viscosities of most dilute aqueous polymer solutions in the first Newtonian shear rate region. Therefore, intrinsic viscosity values can be determined using the cable rheometer and studies can now be continued on the flow properties of polymer solutions.

References

1. Gere, J. M. and S. P. Timoshenko, *Mechanics of Materials*, 2nd Ed., PWS Publishers, Boston, Mass., p. 134, 1984.
2. Sherman, P., *Industrial Rheology*, Academic Press, N.Y., p. 44, 1970.
3. Macosko, C. W., *Rheology-Principles, Measurement, and Applications*, VCH Publishers, New York, NY, p. 188, 1994.

Appendix A

Twist Angle Variation with Respect to Time

Newton second law in torsional format can be used to describe the motion of the bob or the twist angle, θ , after the cup is instantaneously placed in constant rotation at a speed of ω at time t equal zero. If I is the bob's moment of inertia, k is the elastic modulus of the cable and Tq_{fluid} is the total torque on the bob due to the fluid, then

$$\text{Newton second law gives } I \frac{d^2\theta}{dt^2} = -k\theta + Tq_{fluid}.$$

The total torque on the bob due to the fluid, Tq_{fluid} , has two components, the steady torque due to the constant rotation of the cup, Tq_{cup} , and the unsteady torque due to the variation in the rotation of the bob, Tq_{bob} , i.e., $Tq_{fluid} = Tq_{cup} - Tq_{bob}$. As shown by the equations below, both of these torques also have two components, the torque associated with the bob's side wall surface and the torque associated with the bob's

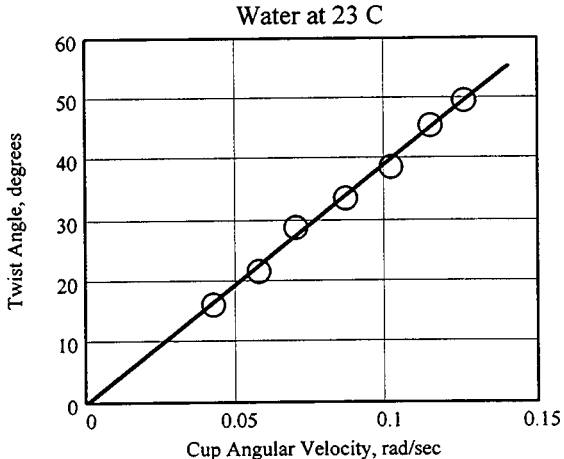


Figure 8 Twist Angle vs. Cup Speed

cone shaped bottom surface.

$$Tq_{cup} = \frac{2\pi\omega r^3 H \eta}{(R-r)} + \frac{\omega r^4 \eta}{4(R-r) \cos^2(\phi)}$$

$$Tq_{bob} = \frac{2\pi r^3 H \eta}{(R-r)} \frac{d\theta}{dt} + \frac{r^4 \eta}{4(R-r) \cos^2(\phi)} \frac{d\theta}{dt}$$

Use of these torques in the torsion equation gives $I \frac{d^2\theta}{dt^2} + a \frac{d\theta}{dt} + k \theta - b = 0$ where the constants a and b are defined by the system geometry and operating conditions.

$$a = \frac{\eta r^3}{(R-r)} \left(2\pi H + \frac{r}{4 \cos^2(\phi)} \right) \quad \text{and} \quad b = a \omega$$

The torsion equation is linear, nonhomogeneous, second order differential equation having real constant coefficients. A solution to this differential equation can be obtained by using the initial conditions that at the start of cup rotation when $t = 0$, $\theta = 0$ and $\frac{d\theta}{dt} = 0$. After a long time of cup rotation steady state conditions will

be obtained and $\frac{d\theta}{dt}$ approaches zero. At this steady state condition $\theta = \frac{b}{k} = \frac{a \omega}{k}$.

This equation rearranges into $\eta = \frac{k(R-r)}{r^3 \left(2\pi H + \frac{r}{4 \cos^2(\phi)} \right)} \frac{\theta}{\omega}$. This equation is an

alternate form of Equation (4). Note that $K = \frac{k(R-r)}{r^3 \left(2\pi H + \frac{r}{4 \cos^2(\phi)} \right)}$.

Nomenclature and Parameter Properties

Description	Symbol	Value	Dimensions
Apparent fluid viscosity	η	variable	psi-sec

Torque	T_q	variable	inch-lb _f
Cup radius	R	2.811	inches
Bob radius	r	2.685	inches
Bob side height	H	5.39	inches
Cup rotational speed	N	variable	rpm
Cable length	L	17.125	inches
Cable modulus	G	1.05×10^7	psi
Twist angle	θ	variable	degrees
Bob cone angle	ϕ	15.0	degrees
Instrument constant	K	2.30×10^{-8}	psi
Shear rate	$\dot{\gamma}$	variable	sec ⁻¹
Cable diameter	d	0.0070	inches
Cable elastic modulus	k	2.0×10^5	kg meter ² / sec ²
Bob moment of inertia	I	5.0×10^{-3}	kg meter ²